Production and characterization of biochar from residual plant matter for the sorption of organic pollutants

Joram Fridtjof Sobanski
Stud Kennz.: UH 066 427/ Matr. Nr.: 01002383

Masterarbeit zur Erlangung des akademischen Grades:
Diplomingenieur (Dipl.-Ing., DI)

Supervisor: Priv.-Doz. Dipl.-Ing. MSc. Dr. Gerhard Soja –
                Austrian Institute of Technology, University of
                Natural Ressources and Life Sciences, Vienna
Co-Supervisor: Priv.-Doz. Mag. Dr. Andrea Watzinger –
                University of Natural Ressources and Life
                Sciences, Vienna
Co-Supervisor: Dipl.-Ing. Dr. Simon Leitner – University of
                Natural Ressources and Life Sciences, Vienna

Institut für Verfahrens- und Energietechnik
Universität für Bodenkultur Wien

Vienna, 13.06.2021

Eidesstaatliche Erklärung

Ich erkläre eidesstattlich, dass ich die Arbeit selbständig angefertigt, keine anderen als die angegebenen Hilfsmittel benutzt und alle aus ungedruckten Quellen, gedruckter Literatur oder aus dem Internet im Wortlaut oder im wesentlichen Inhalt übernommenen Formulierungen und Konzepte gemäß den Richtlinien wissenschaftlicher Arbeiten zitiert, durch Fußnoten gekennzeichnet bzw. mit genauer Quellenangabe kenntlich gemacht habe.

Special thanks to

Abstract

Chlorinated hydrocarbons such as tetrachloroethylene (PCE) are amongst the most widespread organic contaminants in soil and groundwater worldwide. For groundwater remediation biochar has attracted a lot of attention as an alternative for activated carbon. In this work twelve different biochars have been produced from apricot kernels, miscanthus, sunflower seed shells and wood chips at 350 °C, 550 °C and 750 °C (A3-A7, M3-M7, S3-S7, W3-W7, respectively). The goal was to determine the influence of feedstock materials and pyrolytic temperature on the sorptive properties of biochars for PCE. Additionally, the influence of aromaticity and polarity on the adsorption of PCE has been investigated.

In order to examine the basic characteristics of the biochars, a basic characterization was conducted by *Eurofins Umwelt Ost GmbH* laboratory according to EBC standard. Additionally, C and N content of the feedstocks were analysed. To examine the surface chemistry, the biochars were subject to an attenuated total reflectance Fourier-transform mid-infrared spectroscopy (ATR-MIR). Adsorption experiments were conducted to determine the PCE removal efficiency and the adsorption capacity of the biochars and the data was fitted to the Langmuir and Freundlich isotherm model.

The basic characterization showed a significant impact of both feedstock and pyrolytic temperature on the biochars properties. Specific surface area (SSA), C content, and aromaticity increased with higher temperatures whereas O and H content and polarity decreased. High contents of polycyclic aromatic hydrocarbons (PAH) were found in the biochars produced at 750 °C except apricot kernel biochar (AKBC). The ATR-MIR showed a reduction of O and H containing functional groups with a rise in pyrolytic temperature, causing the biochars surfaces to become more hydrophobic at high temperatures.

W7 showed the highest adsorption capacity, followed by M7, S7 and A3 showing that PCE adsorption was highly feedstock and temperature dependent. The high adsorption capacity of W7 was attributed to its high C content, aromaticity, SSA and its low polarity. The strong performance of A3 was attributed to a partitioning process, predominant for biochars produced at lower temperatures.

The results of this work suggest that, based on the nature of the adsorbate, the proper choice of production parameters and feedstock can significantly impact the adsorption behaviour of the adsorbent.

Kurzfassung

Chlorierte Kohlenwasserstoffe wie Tetrachlorethen (PCE) gehören zu den am häufigsten vorkommenden Schadstoffen in Böden und Grundwasserkörpern weltweit. Biokohle erlangt bereits seit längerem viel Aufmerksamkeit als Alternative zu Aktivkohle zur Grundwasserreinigung. In dieser Arbeit wurden insgesamt zwölf Biokohlen aus Marillenkernen, Miscanthus, Sonnenblumenkernschalen und Holzhackschnitzel bei 350 °C, 550 °C und 750 °C hergestellt (A3-A7, M3-M7, S3-S7, W3-W7). Das Ziel war den Einfluss des Ausgangsmaterials sowie der Pyrolysetemperatur auf die Sorptionseigenschaften der Biokohle von PCE zu erheben. Zusätzlich sollte der Einfluss von Aromatizität sowie Polarität auf die Adsorption von PCE erforscht werden.

Um die Eigenschaften der Biokohle zu untersuchen, wurde eine Basis-Charakterisierung nach EBC-Richtlinien von dem Labor *Eurofins Umwelt Ost GmbH* durchgeführt. Zusätzlich wurde C und N Gehalt der Ausgangsstoffe erhoben. Um die Oberflächenchemie der Biokohlen zu untersuchen, wurde eine attenuated total reflectance Fourier-transform mid-infrared spectroscopy (ATR-MIR) durchgeführt. Die Adsorptionskapazität und die PCE Entfernungs-Effektivität wurde durch Adsorptionsexperimente ermittelt und die Daten an das Langmuir und Freundlich Isothermen Modell angepasst.

Die Ergebnisse der Basis-Charakterisierung zeigten einen signifikanten Einfluss des Ausgangsmaterials und der Pyrolysetemperatur auf die Eigenschaften der Biokohle. Mit zunehmender Temperatur erhöhte sich die spezifische Oberfläche, der C Anteil und die Aromatizität wobei der O und H Anteil sowie die Polarität abnahm. Zusätzlich konnte bei allen Biokohlen, welche bei 750 °C produziert wurden, außer die Kohle aus Marillenkernen (AKBC), eine starke Belastung mit polyzyklischen aromatischen Kohlenwasserstoffen (PAK) nachgewiesen werden. Die Ergebnisse der ATR-MIR zeigten eine starke Minderung der O und H enthaltenden funktionellen Gruppen mit einem Anstieg der Pyrolysetemperatur. Dies führte dazu, dass die Biokohlenoberflächen bei höheren Temperaturen deutlich hydrophober wurden.

Die höchste Adsorptionskapazität wurde bei W7 festgestellt, gefolgt von M7, S7 und A3. Die hohe Adsorptionskapazität von W7 wurde durch den hohen Kohlenstoffgehalt, die hohe Aromatizität sowie spezifische Oberfläche und die niedrige Polarität erklärt. Die hohe Adsorptionskapazität von A3 ist höchstwahrscheinlich auf einen Partitionierungsprozess, welcher dominant ist bei Biokohlen, die bei niedrigen Temperaturen produziert wurden, zurückzuführen.

Aus den Ergebnissen dieser Arbeit lässt sich ableiten, dass, je nach Natur des jeweiligen Adsorptivs, sowohl Ausgangsmaterial als auch Pyrolysetemperatur einen erheblichen Einfluss auf das Verhalten des Adsorbens haben kann und entsprechen berücksichtig werden müssen.

Abbreviations

AKBC	apricot kernel biochar
a.u.	arbitrary units
ATR-MIR	attenuated total reflectance Fourier-transform mid-infrared spectroscopy
HTT	highest treatment temperature
MCBC	miscanthus biochar
PAH	polycyclic aromatic hydrocarbons
PAK	polyzyklische aromatische Kohlenwasserstoffe
PV	total pore volume
SSA	specific surface area
SSBC	sunflower seed shells biochar
VOC	volatile organic compound
WCBC	wood chips biochar

Table of content

1. Introduction

1.1 Problem and objective

Chlorinated hydrocarbons such as tetrachloroethylene (PCE) are among the most detected contaminants in soils and groundwater worldwide (Schreiter at al., 2018). Through its frequent use in the dry cleaning and textile industry in the 1970s and 1980s, PCE contaminated liquid waste ended up at waste treatment facilities from where it contaminated air, water, and soil (ATSDR, 2014). Also in Austria, PCE is among the most detected contaminants in contaminated sites (Philippitsch et al., 2012). Since PCE is carcinogenic, hazardous to the environment and has a strong aquatic toxicity (WHO, 2006), proper contamination management is vital.

Activated carbon has proven as a reliable material for the adsorption of PCE. However, its cost-prohibitive nature and difficulties with regeneration have led to the search for more cost effective and environmentally friendly alternatives (Foo & Hameed, 2009). Regarding groundwater remediation, biochar has attracted a lot of attention as an alternative to activated carbon (Kim et al., 2019; Ahmad et al., 2014; Schreiter et al., 2018). Biochar is defined as "a solid material obtained from the thermochemical conversion of biomass in an oxygen-limited environment" (IBI, 2012). Biochars high porosity and its recalcitrance make it not only effective in contamination management but also an attractive substance for the improvement of soil quality and carbon sequestration (Lehmann & Joseph, 2015).

CHARBAK is a KPC funded project of the University of Natural Resources and Applied Life Sciences Vienna and the Austrian Institute of Technology. The goal of the project is the design of physical-biological biochar filters for groundwater remediation with a focus on biofilm development. Embedded in this project, this thesis focuses on the production of the biochar filter material and seeks to determine the biochars with the best PCE adsorption behaviour. Extensive research has been done on the characterization of biochars and how its properties enhance the adsorption of organic contaminants. Generally, a high degree of aromaticity, porosity and a high specific surface area have been reported to improve PCE adsorption whereas it tends to decrease with polarity (Ahmad et al., 2014; Schreiter et al., 2018; Kim et al., 2019). However, sorption mechanisms for organic compounds are complex due to the heterogenous nature of biochar. A combined partitioning-adsorption process is often predominant (Schreiter et al., 2018). The question this thesis seeks to answer is what influence the pyrolysis temperature and the feedstock material have on the adsorption behaviour of biochar towards tetrachloroethylene.

In order to answer that, twelve different biochars have been produced from four different feedstocks at three different temperature levels. One of the goals of the project CHARBAK is the utilization of local and resource-saving by-products from forestry and agriculture. Therefore, miscanthus, wood chips, apricot kernels and sunflower seed shells were used as a feedstock material. To examine the influence of the pyrolytic temperature on PCE adsorption, the feedstocks were pyrolyzed at 350 °C, 550 °C and 750 °C. To compare the biochars in respect to their elemental composition, specific surface area (SSA) and other parameters, they were subject to a basic characterization according to EBC-Standard by *Eurofins Umwelt Ost GmbH*. Additionally, C and N content of the feedstock was determined. To analyse functional groups, both the feedstock and the biochars were subject to an ATR-MIR analysis. Adsorption

experiments were conducted to determine the adsorption capacities of the biochars, and the data was fitted to the Langmuir and Freundlich isotherm model.

Based on an extensive literature review, two hypothesises were formed:

I: The PCE sorption capacity of the produced biochars increases with a rise in pyrolysis temperature.

II: The PCE sorption capacity of biochars increases with a rise in aromaticity and a decline in polarity.

To test these hypothesises, this work delivers a comprehensive overview of the relevant parameters regarding the adsorption of organic contaminants with biochar. In the first chapter an insight into the origin and history of biochar as well as the production process and its physiochemical properties is given. Then, the various adsorption mechanisms of biochar are discussed and the targeted compound, PCE, and the project CHARBAK are described in more detail. In the second chapter, the materials and methods of this thesis, from the production of the biochars to the characterization and the adsorption experiments, are displayed. The results of the characterization and the adsorption experiments are presented in chapter 3. In chapter 4, these results are discussed in respect to the research question. Ultimately, the conclusion in chapter 5 seeks to evaluate the hypothesises described above and deliver a final discussion of the research question as well as recommendations for further research on the topic.

1.2   Biochar – history and definitions

Biochar has been known for its qualities as a soil amendment for improved soil fertility and sustainability for centuries. In fact, the origin of biochar lies in the ancient Amerindian populations of the Amazon region. Amazonian Dark Earths, locally known as Terra Preta de Indio, were soils created through slash-and-char techniques several hundreds to even a few thousands of years ago. Besides its use in soil improvement, biochar found to be applicable in waste management, energy production, mitigation of climate change and for the prevention and mitigation of water pollution (Lehmann & Joseph, 2015).

The International Biochar Initiative defines biochar as „a solid material obtained from the thermochemical conversion of biomass in an oxygen-limited environment." (IBI, 2012). According to Lehman & Joseph (2015) it is the "product of heating biomass in the absence of or with limited air to above 250 °C". This process, the heating of biomass und oxygen-limited conditions, is called charring or pyrolysis. A more descriptive definition is given by Shackley et al. (2012). They define biochar as "the porous carbonaceous solid produced by the thermochemical conversion of organic materials in an oxygen depleted atmosphere that has physicochemical properties suitable for safe and long-term storage of carbon in the environment". This definition gives credit to the climate change mitigation potential of biochar. Sohi et al. (2009) define biochar as "a fine-grained and porous substance, similar in its appearance to charcoal produced by natural burning".

In literature, there are various terms for carbonaceous materials. Therefore, a classification of the most widely used terms is helpful. The following list aims to provide a better differentiation between the various terms and the different products obtained from incomplete combustion processes.

Char: The material generated by incomplete combustion processes that occur in natural and man-made fires (Lehmann & Joseph, 2015). A good example is char created from forest fires (Sohi et al., 2009).

Charcoal: Produced by thermochemical conversion from biomass mostly for energy generation but also rarely as soil amendment or control of odour (Lehmann & Joseph, 2015; Okimori et al., 2003). Typical temperatures in kilns are between 450-500 °C with a significantly lower yield than industrial pyrolysis and all heat as well as gaseous and liquid co-products being lost during the combustion process (Sohi et al., 2009).

Biochar: The solid product of pyrolysis, designed to be used for environmental management (Lehmann & Joseph, 2015).

Hydrochar: The solid product of hydrothermal carbonization (HTC) or liquefication. It differs from biochar due to its production process and properties (higher H/C ratios, lower aromaticity, little or no fused aromatic ring structures) (Schimmelpfennig & Glaser, 2012., Libra et al., 2011).

Activated carbon: A carbonaceous material produced from thermochemical conversion that has undergone activation from steam or additions of chemicals. It is characterised by its high porosity and surface area and mostly used in filtration or separation processes such as water filtration or adsorption of gas, liquid or solid contaminants (Lehmann & Joseph, 2015). Typically, activated carbon is produced at high temperature (above 500 °C) and under long heating time (over 10 hours) (Sohi et al., 2009).

Black carbon: a general term for diverse forms of refractory organic matter from incomplete combustion, that will not be used further in this work (Sohi et al. 2009).

In general, the high porosity and the recalcitrance of biochar make it an attractive substance for the improvement of soil quality and carbon sequestration as well as decontamination.

In the following chapter, the principles of biochar production will be examined to provide a basis for further discussion of the results of this work.

1.3 Biochar – production

1.3.1 Feedstock

There are various factors in the production process that can influence the biochars chemical, biological and physical properties. One factor, that has a big impact, is the choice of biomass. A wide variety of feedstock, which has increased exponentially over the last decade, can be used to produce biochars which leads to different biochar qualities and quantities (Ippolito et al., 2015). Common biomass used for biochar production are woody crops like wood chips from pine, herbaceous crops like switchgrass or miscanthus, agricultural residues like corn stover, rice straw or nut shells. Also waste biomass like distillers' grain or paper sludge and even aquatic species like algae are common (Lehmann & Joseph, 2015).

Biochar is only one of the products of pyrolysis. Besides the solid and carbon-rich residue, a combustible synthesis gas ("syngas") and oil ("bio-oil") are formed, which can be put to further use by producing power or heat. The ratio between biochar formation and energy production can be influenced by adapting production parameters during the pyrolysis process and by the choice of feedstock. It is, however, notable that the maximisation of biochar yield always comes at the expense of energy production (Sohi et al., 2009).

Important feedstock parameters are the elemental ratios of carbon (C), oxygen (O) and hydrogen (H) as well as the proportions of hemi-cellulose, cellulose and lignin, which determine the ratio of volatile and stabilised carbon in pyrolyze products (Sohi et al., 2009). When pyrolyzed at moderate temperatures around 500 °C feedstocks with a high lignin content produce the highest biochar yields (Fushimi et al., 2003; Demirbas, 2006). Using biomass that has not been grown for the sole purpose of feedstock for pyrolysis, but rather residues from crop production or waste management, can prolong the life cycle of said systems and make the biochar production process more efficient (Lehmann & Joseph, 2015). Hence, in this work, by-products from agriculture and forestry are utilized.

1.3.2 Temperature

Pyrolysis parameters can also differ in their highest treatment temperature (HTT), duration and heating rate (Sohi et al., 2009). Especially the HTT has a substantial impact on important biochar properties. A rise in pyrolysis temperature typically leads to a rise in carbon content, aromaticity, porosity, ash content, specific surface, micro porosity and pH and to a decline in H content, O content and polarity of the biochar, respectively (Ahmad et al. 2014; Chen et al., 2011). Typically, for biochar production, HTT lies between 250°C and 700°C (Lehmann & Joseph, 2015).

1.3.3 Production process

Literature distinguishes between different production processes. During **slow pyrolysis**, biomass is slowly heated in the absence of oxygen at low to medium temperatures ranging from 450 to 650 °C. This kind of process leads to a somewhat equal yield of biochar, bio-oil and syngas. A technique, that leads to a much higher yield of bio-oil is the **fast pyrolysis**. Rapid biomass heating, low resistance time (time taken, for the feedstock to reach peak temperature) leads to an enhanced overall conversion efficiency. Another process called **intermediate pyrolysis** describes a hybrid technology with low to moderate temperatures and a long residence time. It was designed to produce bio-oil with a very low tar content for a potential use as motor fuel. **Gasification** describes the process of converting carbonaceous material into monoxide and hydrogen in a high temperature reaction, with limited oxygen supply at high pressures. This technique is often used as for waste disposal and its main product is the gas mixture (Sohi et al., 2009). Table 1 summarizes the different pyrolysis processes with their respective product yields.

Table 1: Pyrolysis processes with their respective product yield (IAE, 2007; cited from Sohi et al., 2009).

Pyrolysis process	Liquid (bio-oil) [%]	Solid (biochar) [%]	Gas (syngas) [%]
Fast pyrolysis Moderate temperature (~500 °C) Short hot vapour residence time (< 2 s)	75 (25 water)	12	13
Intermediate Pyrolysis Low-moderate temperature, Moderate hot vapour residence time	50 (50 water)	25	25

Slow Pyrolysis Low-moderate temperature, Long residence time	30 (70 water)	35	35
Gasification High temperature (> 800 °C) Long vapour residence time	5 tar (5 water)	10	85

It becomes clear, that depending on the planned application of the biochar, the process parameters can be optimized to obtain favourable results. The production of biochar optimized for adsorption of organic pollutants, implies a trade-off between yield and pore volume considering the pyrolysis temperature.

1.3.4 EBC

The Biochar Science Network has introduced guidelines for obtaining a biochar certificate (European Biochar Certificate). The certificate ensures the sustainable production of biochar and a transparent and measurable quality for biochar users. The guidelines include detailed rules on production as well as quality criteria for biochar. Table 2 list some of the limits for elemental composition and organic contaminants in respect to the four EBC classes. Since the biochars produced in the course of this thesis did not exceed any of the heavy metal limits proposed by the EBC-Guidelines, they are not listed in table 2.

The different classes refer to different means of use for the produced biochars and to a different level of requirements proposed by various EU-regulations regarding biochar. According to EBC (2020), Biochars that meet EBC-Feed Class I requirements may be used as animal feed or feed additive and meet all requirements of the EU feed regulation. "Biochars certified with EBC-Agro and EBC-AgroOrganic meet all requirements of the new, though as of 2020 not yet adopted, EU fertilizer regulations". Biochars that fall under the EBC-Material Class, can be used in industrial materials such as "building materials, plastics, electronics, or textiles without risk to the environment and users." (EBC, 2020). For the production of filter material for ground water remediation, EBC-Material Class IV is sufficient.

Table 2: elemental analysis and organic contaminants limit according EBC guidelines.

EBC – Class	EBC-Feed Class I	EBC-AgroBio Class II	EBC-Agro Class III	EBC-Material Class IV
H/C$_{org}$	< 0.7	< 0.7	< 0.7	< 0.7
O/C$_{org}$	< 0.4	< 0.4	< 0.4	< 0.4
16 EPA PAH [mg/kg DM]	4 ± 2	4 ± 2	6.0 + 2.2	30

1.4 Biochar - physiochemical properties

The factors, that influence the physicochemical characteristics of biochar are feedstock choice, pyrolysis temperature and pyrolysis type. The following chapter seeks to give

an overview over the most important characteristics of both physical and chemical properties and the processes, that influence them.

1.4.1 Physical properties

Various studies have shown that feedstock choice, pyrolysis type and pyrolysis temperature have a significant influence on SSA and total pore volume (PV) as well as pore distribution (Keiluweit et al., 2010; Ahmad et al., 2014; Schreiter et al., 2018). Especially the micropores (< 50 nm diameter) contribute most to SSA (Downie et al., 2009). Ippolito et al. (2020) have evaluated over 5400 peer-reviewed journal articles and over 50,800 individual data points in their meta-data analysis review and found, that fast pyrolysis, as described in chapter 1.2, had a positive influence on SSA, compared to slow pyrolysis.

Concerning the feedstock, wood-based biochars showed greater SSA and PV as compared to other feedstock choices. This can be linked to the reduction of relatively large wood-based cell structures to smaller pores, resulting in an overall increase of SSA and therefore also PV (Weber and Quicker 2018; Downie et al. 2009, cited from Ippolito et al., 2020). Biochar produced from manures or biosolids showed relatively low SSA. This is likely due to deformation, structural cracking or micropore blockage and less distinct porous structures on the feedstock as compared to wood-based biochars (Ahmad et al. 2014; Lian et al. 2011).

With an increase of HTT, SSA increases as well. This is caused by a shrinking of the solid matrix, causing large pores to become smaller and shrinking the overall SSA (Weber & Quicker, 2018 cited from Ippolito et al., 2020). SSA has been reported to have a strong influence on sorption/retention of nutrients and contaminants while PV is assumed to affect water availability and soil aeration (Ajayi and Horn 2016; Qambrani et al. 2017).

1.4.2 Chemical properties

The chemical composition of biochar is highly heterogeneous and generally consists of fixed carbon, volatile matter (e.g. tars), mineral matter (ash) and moisture (Sohi et al., 2009; Antal & Gronli, 2003). However, chemical properties of the organic C structure of biochars differ fundamentally from those of the material that the biochar was produced from (Lehmann & Joseph, 2015). With an increase in pyrolysis temperature, plant biomass undergoes a transformation from randomly ordered, amorphous aromatic structures into fused aromatic ring structures. This is followed by a progressive condensation of smaller aromatic units into larger, more structured, conjugated graphene sheets (Amonette & Joseph, 2009; Keiluweit et al., 2010; Verhejen et al., 2010; Chen et al. 2011).

Regarding the elemental composition, besides the major biomass constituents like C, H and O, biochar derived from plants contains nutrients like N, P, K, S, Ca, Mg, Al, Na, and Cu (Amonette & Joseph, 2009; Singh et al., 2010). An increase in pyrolysis temperature usually leads to an increase in total C, K and Mg content. Slow pyrolysis, as described in chapter 1.3.3, generally produces biochars with a higher N, S, available P, Ca, and Mg content. Generally, pyrolysis type has less influence on total macroelements compared to feedstock choice and temperature (Ippolito et al. 2020)

At HTT below 250 °C the primary changes in biomass that occur are dehydration and slight depolymerization of cellulose with little mass loss observed. At temperatures ranging from 250-350 °C a complete depolymerization of cellulose occurs and with that a significant loss of mass due to volatilization. An amorphous C matrix develops. Above

350 °C polyaromatic graphene sheets begin to develop and above HTTs of 600 °C carbonization sets in. At this point, most of the remaining non-C atoms are gone (Amonette & Joseph, 2009).

A great portion of the mineral content from feedstock is also found in biochars. There it is concentrated, due to loss of C, H and O during pyrolysis. SiO_2, KCl, $CaCO_3$, $CaSO_4$, hydroxyapatite and various nitrates, oxides and hydroxides of Ca, Mg, Al, Ti, Zn and Fe are the main minerals found in biochar (Amonette & Joseph, 2009).

The surface chemistry of biochar is very heterogeneous and varies with both hydrophilic and hydrophobic as well as acidic and basic properties. Their manifestation is strongly feedstock and process dependent (Amonette & Joseph, 2009). During pyrolysis numerous functional groups (e.g. hydroxyl -OH, amino-NH_2, ketone -OR, ester -(C=O) OR, nitro -NO_2, aldehyde -(C=O)H, carboxyl -(C=O)OH), occurring predominantly on the outer surface of the graphene sheets and surfaces of pores, are formed (Van Zwieten et al., 2009 cited from Verheijen et al., 2010). Amonette and Joseph (2009) state, that the relative concentration of each of the functional groups depends heavily upon the initial composition of the biomass as well as pyrolysis process parameters like reaction temperature, gas composition surrounding the char at final reaction temperature, heating rate and any kind of post-treatment.

Through their surface charge and the availability of π electrons, functional groups influence the sorption behaviour of biochar. For oxide surfaces, the charge of the functional group may vary depending on the pH of the solution (hence the surface is amphoteric) and some organic sorbates, like phenols or anilines also show amphoteric behaviour (Amonette & Joseph, 2009).

Generally, pH shows little variation between biochars and usually exceeds seven (Keiluweit et al., 2010). However, Lehman (2015) states, that biochar can be produced at any range between 4-12. Various studies report a positive correlation between alkalinity and HTT (e.g. Ippolito et al., 2015; Weber & Quicker, 2018). This can be linked to a loss of acidic functional groups and the formation of Ca- Mg-, Na-, and K-bearing oxides, hydroxide, and carbonate mineral phases (Ippolito et al. 2020).

The following chapter will share some fundamental definitions of adsorption and discuss the sorption mechanisms of biochar in further detail since it is important to comprehend for the later discussion of the results of this work.

1.5 Adsorption

One of the most important functions of biochar application in environmental management is, besides their use as soil amendment, their ability to adsorb pollutants from the surrounding environment. The immobilization of contaminants by adsorption is a commonly applied technique in soil and water remediation (Schreiter et al., 2018). Before discussing the specific mechanisms involved in the adsorption process, the following chapter seeks to share some key definitions and concepts.

1.5.1 Definitions

Adsorption can be defined as the "change in concentration of a given substance at the interface as compared with the neighbouring phases" (Dabrowski, 2001). Ruthven (1984) defines adsorption as a process that occurs when a gas or liquid solute accumulates on the surface of a solid or a liquid, forming a molecular, ionic, or atomic film. This surface accumulation is what differentiates adsorption from absorption. **Absorption** is a physical or chemical process in which a substance will diffuse into a solid or

a liquid, not just attaching to the surface. Dabrowski (2001) defines it as the "penetration by the adsorbed molecules into the bulk solid phase". This work however focuses on the adsorption of organic pollutants to biochar and for further discussion it is important to define some key terms in adsorption theory.

As stated above, adsorption describes the process of a substance concentrating on the surface of a solid or a liquid. **Desorption** describes the converse process, so the detachment of a substance from the surface. The substance in the adsorbed state is commonly referred to as **adsorbate** or **adsorptive**. The substance the adsorbate adsorbs to is called the **adsorbent** (Dabrowski, 2001).

There are two different kinds of adsorption processes that differ due to the nature of bonding between adsorbate and adsorbent. During **physical adsorption** (**physisorption**), the adsorbate binds to the adsorbent through Van-der-Waal forces. This bond is reversible, and it does not alter the chemical composition of the substances involved. **Chemical adsorption** (**chemisorption**), however, forms strong irreversible chemical bonds which lead to the formation of a surface compound (Králik, 2014).

1.5.2 Adsorption Isotherms

A concept for the quantitative evaluation of adsorption behaviour and the adsorbents capability is the **adsorption isotherm**. Dabrowski (2001) defines it as the "equilibrium relation between the quantity of the adsorbed material and the pressure or concentration in the bulk fluid phase at constant temperature". Isotherms describe how the adsorbate reacts with the adsorbent material. They are used for the optimization of the adsorption mechanism pathways, the expression of the surface properties and the adsorption capacities of the adsorbents (Foo & Hameed, 2009). There are various isotherm models, which describe the adsorption process based on different assumptions, some of which are discussed in the following.

1.5.2.1   Freundlich isotherm

The Freundlich isotherm can be used for the experimental determination of the adsorption capacity (Ayoob, 2008). It is applicable for heterogonous adsorbent surfaces and can be applied to describe multilayer adsorption (in contrast to the Langmuir isotherm, as discussed next), with an uneven distribution of adsorption heat and adsorption site affinities. The Freundlich isotherm is, inter alia, applied when dealing with heterogenous adsorbents for organic compounds (Foo & Hameed, 2009). Figure 1 (b) shows a typical Freundlich isotherm.

It can be described by:

$$Q_e \ = \ K_{Fr} C_e^{\frac{1}{n}}$$

where Q_e [mg/g] is the amount of sorbate adsorbed at equilibrium per unit weight of adsorbent, K_f is the Freundlich constant [l/g] indicating adsorption capacity and 1/n is a constant representing adsorption intensity or surface heterogeneity. When *1/n* gets closer to zero it implies the adsorbents surface becoming more heterogenous. A *1/n* value above 1 implies cooperative adsorption whereas 1/n below 1 implies chemisorption (Foo & Hameed, 2009).

1.5.2.2   Langmuir isotherm

The Langmuir isotherm was originally developed for solid-gas adsorption but can be applied for any interface. Often used for higher concentrations of adsorbate, it provides a possibility to describe non-linear relations between Q_e and C_e. It is based on the assumptions, that all sites on the adsorbent surface have equal affinity for the adsorbate, adsorption can only occur at a finite number of sites, interactions among adsorbate molecules are negligible and that the adsorption proceeds with the formation of only one layer of adsorbate on the adsorbent surface (monolayer adsorption) (Ayoob, 2008; Foo & Hameed, 2009; Kralik, 2014). Figure 1 (a) shows a Langmuir isotherm. It is characterized by a plateau which occurs due to the saturation of the adsorbent, where all sites are occupied by adsorbate molecules and no further adsorption can take place (Foo & Hameed, 2009).

It can be described by:

$$Q_e = \frac{K_L q_{max} C_e}{1 + K_L C_e}$$

Equation 2: Langmuir isotherm (Foo & Hameed, 2009)

where Q_e [mg/g] is the amount of sorbate adsorbed at equilibrium per unit weight of adsorbent, C_e [mg/l] is the equilibrium solute concentration, K_L and q_{max} [mg/g] are the Langmuir constants related to maximum monolayer coverage capacities and binding energy. (Ayoob & Gupta, 2008; Foo & Hameed, 2009).
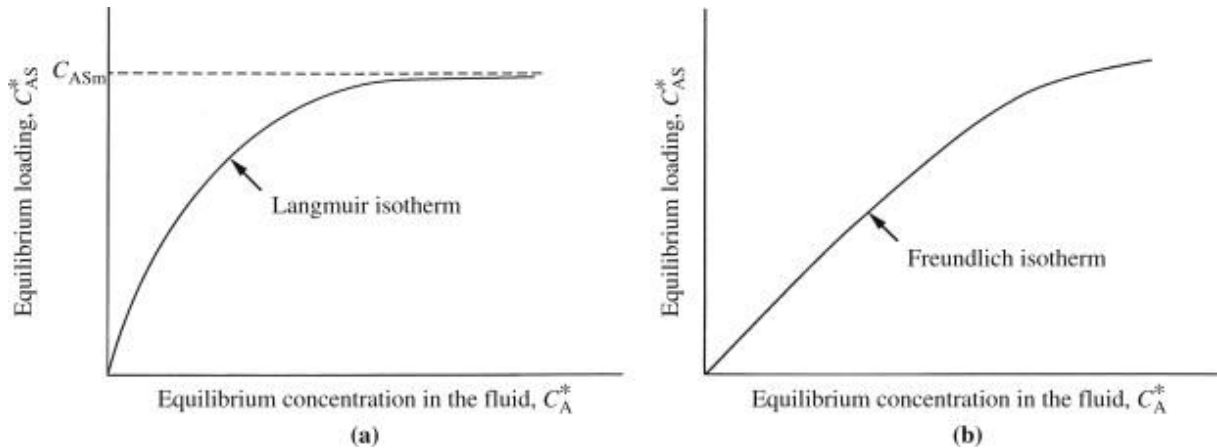
Figure 1: Adsorption isotherms, (a) Langmuir isotherm, (b) Freundlich isotherm (Doran, 2013).

In order to understand the processes involved in the sorption of organic pollutants onto biochar, one has to not only comprehend the adsorption process in general but also the manifold surface interactions and adsorption mechanisms that characterize biochar as an adsorbent. The following chapter seeks to display these mechanisms.

1.5.3 Adsorption mechanisms of biochar

Due to the heterogeneous nature of biochar, sorption mechanisms are complex and often follow a combined partitioning-adsorption process (Chen et al., 2008, 2017; Chen and Chen, 2009; Chiou et al., 2015; cited by Schreiter et al., 2018). Since biochar has a relatively structured carbon matrix with a high degree of porosity, it can act as a surface sorbent, similar to activated carbon (Chen et al., 2011). Additionally, biochar contains a non-carbonized fraction that can interact with contaminants, like O-containing carboxyl, hydroxyl and phenolic surface functional groups (Ahmad et al. 2014). The adsorption process, however, does not just depend on the properties of the adsorbent

but also on the nature of the adsorbate. Organic and inorganic contaminants have different adsorption mechanisms. Therefore, they shall be discussed separately.

1.5.3.1 Adsorption of organic contaminants

For organic contaminants, pore filling, partitioning, hydrophobic and π-π electron donor-acceptor interactions are the main adsorption mechanisms (Chen et al., 2017). Figure 2 from Ahmad et al. (2014) summarizes and visualizes these mechanisms.

Figure 2: Mechanisms of the interactions of biochar with organic contaminants (Ahmad et al., 2014).

Generally, sorption of organic contaminants onto biochar occurs due to its porosity and its high surface area (Ahmad et al. 2014). The positive correlation of SSA and PV with pyrolysis temperature leads to the suggestion, that sorption of organic pollutants is more effective for biochar produced at higher temperatures. This aligns with the results of various studies, however there are some exceptions regarding polarity of both adsorbate and adsorbent (e.g. Sun et al., 2011). Ahmad et al. (2014) report, that biochars produced at >400 °C are more effective for the sorption of organic contaminants. Adsorption mainly takes place in the well carbonized, aromatic structure, which are dominant for biochars with high HTT between 400-700 °C, whereas partitioning can occur in the non-carbonized phase, predominant at low pyrolysis temperatures (100-300 °C) (Ahmad et al., 2014, Schreiter et al., 2018).

At pyrolysis temperatures over 500 °C biochar surfaces become less polar and more aromatic, due to the loss of O- and H-containing functional groups. Various studies have shown an increase in sorption capacity with an increase in aromaticity (and an increase in HTT) for organic contaminants (Chen et al., 2008; Uchimiya et al., 2010; Ahmad et al., 2012). Ahmad et al. (2012) reported an increase for the sorption of trichloroethylene onto biochar produced from soybean stover and peanut shells at 700 °C compared to 300 °C and Uchimiya et al. (2010) reported similar results for the sorption capacity of deisopropylatrazine with biochar derived from broiler litter at 700 °C.

The functional groups of biochar also have a strong influence on the sorption behaviour due to their influence on polarity. Depending on the nature of the sorbate, it can be advantageous to use biochar produced at lower temperatures with a higher content of H- and O-containing functional groups or at higher temperatures, where the absence

of functional groups leads to non-polar attraction of the contaminants to the hydrophobic sites (Ahmad et al., 2014).

Another important adsorption mechanism is electrostatic attraction/repulsion between organic contaminants and biochar. The surfaces of biochar are usually negatively charged. This can facilitate electrostatic attraction towards positively charged cationic organic compounds (Ahmad et al., 2014). Keiluweit et al. (2010) reported an abundance of electron withdrawing functional groups in highly polar biochars, produced at 400 °C. Biochars produced at high temperatures contain both electron rich and electron poor functional groups which allows them to interact with both electron donors and electron acceptors (Sun et al., 2012).

Additional to SSA, PV, functional groups and electrostatic attraction/repulsion the solution chemistry like pH and ionic strength also affects the sorption of organic compounds onto biochar. Xu et al. (2011) report a sharp increase of the sorption capacity for biochars derived from crop residue at 350 °C for methyl violet from pH 7.7 to 8.7 which is explained by the increase of electrostatic attraction due to the dissociation of phenolic -OH groups. Since biochar contains variable charged surfaces, an increase in pH on these surfaces results in an increase of the net negative charge, which, as stated above, can increase attraction towards positively charged cationic organic compounds. The ionic strength of a solution can also increase the adsorption of organic contaminants onto biochar. This is, however, pH dependent (Ahmad et al. 2014).

Overall, it can be said, that biochars produced at higher temperatures show a higher adsorption efficiency for non-polar organic pollutants due to high SSA and PV as well as hydrophobic binding sites. Since, however, adsorption capacity of biochars is very sorbate dependent and can vary due to polarity, pH or ionic strength, it is important to have the properties of the targeted pollutant in mind, when producing biochar for the adsorption of organic contaminants.

1.5.3.2   *Adsorption of inorganic contaminants*

Since this work focuses on the adsorption of PCE, an organic compound, the sorption mechanisms for inorganic contaminants will not be discussed in greater detail but only summarized shortly in this chapter.

Inorganic pollutants in the environment originate mostly from anthropogenic sources. The most prominent groups of inorganic contaminants are metals, which, unlike organic contaminants, are non-biodegradable. Their bioavailability poses a threat to living organisms (Ahmad et al., 2014).

There are four different sorption mechanisms for metals onto biochar, which are displayed in figure 3. There is ion exchange between target metal and exchangeable metal in biochar, electrostatic attraction of anionic metal, precipitation of target metal and electrostatic attraction of cationic metal. Unlike for organic contaminants, biochar produced at low temperature is more efficient for inorganic contaminants. This is due to the presence of more O-containing functional groups and the greater release of cations at lower HTT (Ahmad et al., 2014).
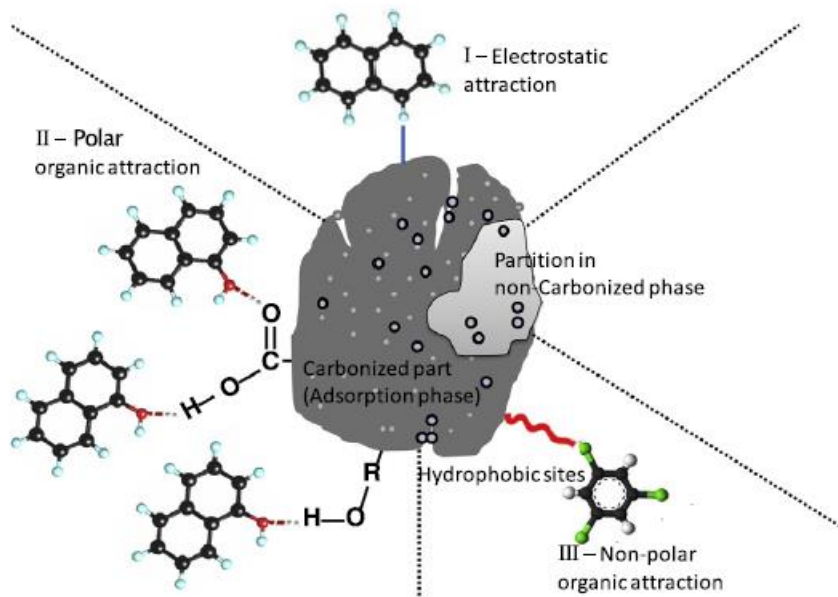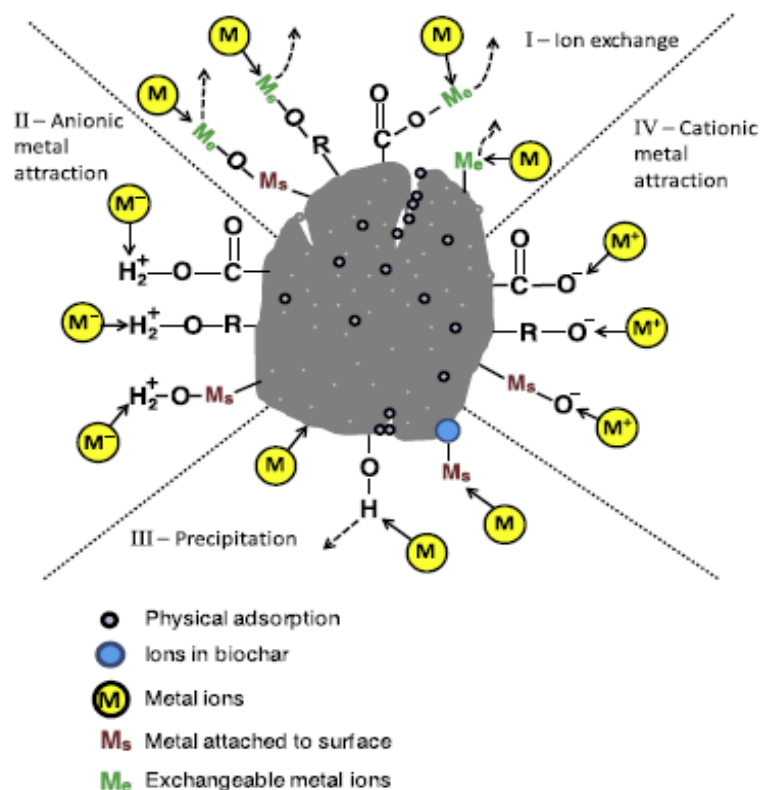
Figure 3: Mechanisms of the interactions of biochar with inorganic contaminants (Ahmad et al., 2014).

Just like for organic contaminants, sorption properties are very sorbent specific so cationic and anionic metals have different affinities for biochars especially compared to organic contaminants. Not all biochars are equally effective for the sorption of contaminants and should be analysed thoroughly before application (Ahmad et al., 2014).

The following chapter will take a closer look at the targeted contaminant of this thesis, PCE.
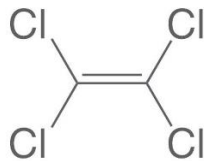
1.6   Tetrachloroethylene

Chlorinated hydrocarbons such as PCE are amongst the most detected contaminants in soil and groundwater (Schreiter at al., 2018). PCE became known by its name "the dry-cleaning fluid" because of its use as a solvent in dry cleaning and is found frequently in contaminated ground water bodies. Besides its use in the dry-cleaning industry, it was often used for metal degreasing, the textile industry, in the production of chemicals and is even found in some consumer products. Other names for PCE are perchloroethylene, tetrachloroethene or perchlor (ATSDR, 2014). In Austria, PCE is also among the most detected contaminants in contaminated sites (Philippitsch et al., 2012).

PCE is a clear, non-flammable, colourless liquid with a density of 1.622 g/cm³ and a solubility in water of 160 mg/l at room temperature. Its properties are listed in table 3. It has a characteristic etheric odour that can be recognized when in the air at levels as low as 1 ppm.

Table 3: properties of PCE.

Substance	PCE

Sum formula	C_2Cl_4
Density [g/cm³]	1.62
Solubility in water at 20 °C [mg/l]	160
Structural formula	

The usual pathway for the contaminant into the environment is through waste disposal sites. Industries that use PCE produce liquid waste contaminated with the compound which then ends up at waste treatment facilities where it can contaminate both air, water, and soil (ATSDR, 2014). Tetrachloroethene volatilizes readily from soil and surface water and undergoes degradation in the air. Its half-life in air is approximately 3-5 months. In water PCE is resistant to abiotic and aerobic degradation and is only degradable under anaerobic conditions (WHO, 2006).

PCE is carcinogenic and hazardous to the environment and has a strong aquatic toxicity (WHO, 2006). Chronic uptake can lead to liver and kidney damage and is believed to be teratogenic (IARC, 2014).

1.7 CHARBAK

This thesis is part of the project CHARBAK, which is a KPC funded project under the supervision of Dr. Andrea Watzinger. Both the University of Natural Resources and Applied Life Sciences Vienna and the Austrian Institute of Technology are involved. The goal of the project is the design of physical-biological biochar filters for groundwater remediation with a focus on biofilm development. The primary focus is on the controlled establishment of ideal conditions for retention and biodegradation of contaminants in the biochar filter. The target compounds comprise of chlorinated hydrocarbons (tetrachloroethene and its degradation products) as well as polycyclic aromatic hydrocarbons (PAH) with the example of naphthalene.

Through a combination of physical (sorption) and biochemical (bacterial conversion of contaminants) processes the cleaning costs for filters are ought to be reduced by increasing their service life. Another aim is the generation of a climate neutral, cheap, and reusable filter material as an alternative to common activated charcoal. Finally, the utilization of local and resource-saving feedstock for the production of the biochar is a key requirement. Hence, by-products from forestry and agricultural by-products shall be used.

The process of development involves the initial production and characterization of biochars adsorbing the target compounds and being colonized by compound degrading biofilms. Tracer experiments combined with monitoring of the organic compounds and isotope analysis will be conducted to distinguish between sorption and degradation processes in laboratory batch and column experiments.

This thesis, however, focuses on the production and characterization of the biochar and includes first sorption experiments with PCE.

2. Material and Methods

2.1 Biochar production

The biochar was produced with a PYREKA Lab plant from *PYREG GmbH* with a screw reactor and continuous input. Figure 4 shows a process diagram of the PYREKA lab plant. Figure 5 displays the plant itself and in figure 6 the feeder, screw reactor, discharge container and burning chamber are shown.
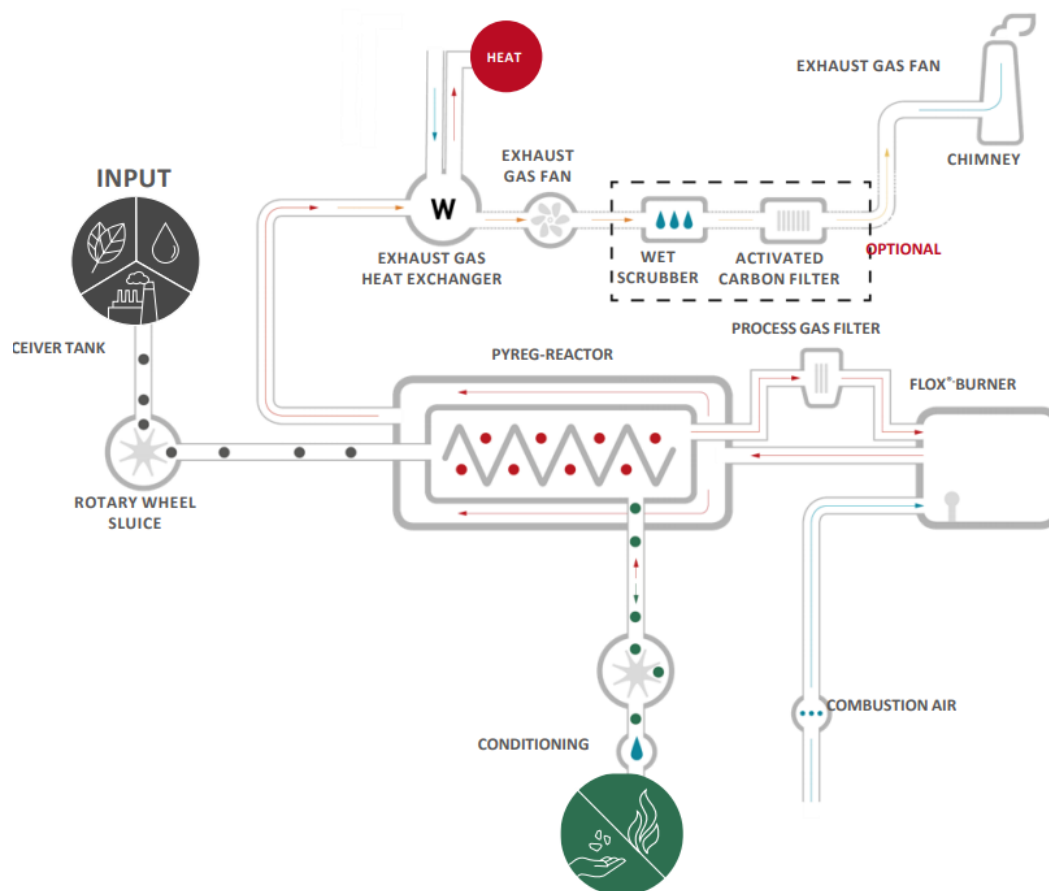
Figure 4: Process diagram PYREKA lab plant (Pyreg, 2021).

Figure 5: PYREKA lab plant (Pyreg, 2016)

Figure 6: PYREKA feeder and screw reactor, discharge container and burning chamber (personal archives, 2020)

As feedstock apricot kernels, wood chips from soft wood, miscanthus sinensis and sunflower seeds were used. The apricot kernels were obtained From *Verein Wachauer Marille*. The miscanthus from a farmer in Tullnerfeld, lower Austria. Sunflower seeds shells were received from *Öhlmühle Bunge,* Bruck an der Leitha and the wood chips

were taken from stocks at AIT Tulln. All materials were air dried at ambient temperature for over a week. Everything but the sunflower seed shells were chopped and subsequently hand sieved to < 2 cm.

The feedstock was pyrolyzed at three different temperature levels: 350, 550 and 750 °C. In order to compare the produced biochars to an industrial reference material, activated carbon was used in the first adsorption experiment (Hydraffin A 8x30 from *Donau Carbon GmbH)*. As the results of the biochar characterization will show in chapter 3.3, the biochars with the highest sorption capacities had a very high PAH content. Therefore, during the project, three more biochars were produced; two at 650 °C from wood chips (W6) and sunflower seed shells to see if the PAH content would be lower at that temperature and one at 350 °C from apricot kernels. Although these biochars were not subject to any basic characterization, W6 was included in the 4th adsorption experiment since it was believed to have promising properties for the later course of the project.

2.2   Biochar characterization

Basic physicochemical properties of the biochars were examined by Labor *Eurofins Umwelt Ost GmbH* according to EBC standard. The included parameters and the analytical method applied are listed in table 4. A selection of the results of the analysis are presented in chapter 3.3. The entire report is found in the appendix.

Table 4: Parameters and analytical methods from eurofins biochar characterization.

Parameter	Analytical method
Sample preparation	DIN 51701-3
Water content	DIN 51718
Ash content (550 °C)	Analog DIN 51719
Carbon, hydrogen	DIN 51732
Nitrogen	DIN 51732
Sulphur	DIN 51724-3
Oxygen (calculated)	DIN 51733
Carbonate-CO_2	DIN 51726
Corg (calculation from Ctot and C-carbonate)	Calculation
H/C and O/C	Calculation
Trace metals b, Cd, Cu, Ni, Hg, Zn, Cr, B, Mn in microwave digestion	EN ISO 17294-2 /DIN 22022-4/-1
Main elements main elements P, Mg, Ca, K, Na, Fe, Si, S in melting digestion	EN ISO 11885 /DIN 51729-11

PAK (EPA)	EN 16181 (extraction with toluene)
pH-value	DIN ISO 10390 (CaCl$_2$)
bulk density	Based on VDLUFA Bd. I A 13.2.1
conductivity (salt content)	BGK, Kap. III. C2
surface area analysis according to BET (incl. pure density)	DIN ISO 9277

2.3 Feedstock analysis

Elemental analysis of the feedstock was conducted with a Thermo Scientific™ FLASH 2000 CHNS/O Analyzer. Prior to the analysis, the feedstock was dried at 60 °C for 2 hours and ground in a ball mill (MIXER MILL MM 200 by Retsch) at 15 Hz for 2 minutes.

2.4 ATR-MIR

ATR-MIR was conducted in order to analyse functional groups of the biochars. It was carried out with a 4 cm^{-1} resolution measuring the absorbance from 4000 to 400 cm^{-1} (32 scans per sample; Tensor 27 SN 1683; Bruker, Austria). Prior to analysis, the biochar samples were ground manually with an agate mortar. Each sample was measured five times at different locations, vector normalised and averaged using OPUS (version 6.5) software. The data was visualized with Microsoft Excel.

The ranges of 4000-3656 cm^{-1} and 2494-1819 cm^{-1} were excluded due to distortion from the CO$_2$ band around 2350 cm^{-1} and the ATR crystal. The assigned bands are displayed in chapter 3.4.

2.5 Adsorption experiments

In total, four adsorption experiments were conducted and one preliminary experiment, to become acquainted with the method and the contaminant. This preliminary experiment is not further discussed in this work. The samples from the adsorption experiment were analysed via GC/MS-C/IRMS with purge and trap auto sampling.

Purge and trap autosampler (VSP4000; IMT GmbH, Vohenstrauss, Germany) were equipped with a membrane water trap, an assay volume of 10 ml and a vial (23 × 79 mm) volume of 20 ml. Purge temperature was 60 °C; trap cooling (LN2), − 50 °C; Purge flow (He) 1200 hPa; purge time 20 min; desorption temperature 200 °C; desorption time 7 min; transfer temperature, 200 °C. Desorbed analytes were then directly injected into a gas chromatograph (Trace GC; Thermo Fisher) equipped with a GS-Gas-Pro column (Agilent; 30 m; 0.32 mm ID). The temperature program was 40 °C for 2,5 min; 40 °C min^{-1} to 140 °C, hold for 2 min; 20 °C. min^{-1} to 240 °C, hold for 5 min. Analytes were split after leaving the GC column. One part (1/10) was analysed by a mass spectrometer (MS) (ISQ; Thermo Fisher) and the second part (9/10) was converted to CO2 in a combustion unit (GC-Isolink, Thermo Fisher; heating zone, 1000 °C) which was analysed by an IRMS (DeltaV, Thermo Fisher; analysed masses: 44, 45, 46) (Leitner et al., 2017). The IRMS was used for the identification of the compound whereas the MS was used for quantification.

In order to quantify the MS results, a calibration standard was prepared with 1 µl PCE, cis-DCE and TCE in 63 ml of MQ water to obtain a concentration of 27 mg/l PCE.

Limit of detection and quantification for the MS were calculated according to ICH (1996) and were 0.11 µg/l and 0.36 µg/l, respectively. Following formulas were used:

$$LOD = 3S_\alpha/b$$

Equation 3: Limit of detection (Shrivastava & Gupta, 2011)

LOD   Limit of detection

S_α   Standard deviation of the response

b   slope of the calibration curve

$$LOQ = 10S_\alpha/b$$

Equation 4: Limit of quantification (Shrivastava & Gupta, 2011)

LOQ   Limit of quantification

2.5.1 Calculations

Equilibrium concentrations (C_e in mg/l) were measured. Since the control groups of the isotherm experiments without adsorbent showed a substantial reduction in concentration (up to 11,06 mg/l after 120 h), C_e was corrected using following formula:

$$Ce = y + a + b$$

Equation 5: Equilibrium concentration

C_e   solute concentration at equilibrium without PCE loss [mg/l]

y   solute concentration at equilibrium including PCE loss [mg/l]

a   PCE loss measured in control groups [mg/l]

b   amount of PCE taken for measurement in GC vial [mg/l]

The equilibrium adsorption capacity Q_e [mg/l] was then calculated using following formula:

$$Qe = V (C0 - Ce) / m$$

Equation 6: Adsorption capacity

Q_e   Adsorption equilibrium capacity [mg/g]

V *liquid volume of stock solution [l]*

C$_0$ *initial solute concentration [mg/l]*

m *mass of adsorbent [mg]*

The % PCE removal was calculated using following formula:

$$\% \, PCE \, removal \; = \frac{C0 - Ce}{C0} * 100$$

2.5.2 1st adsorption experiment

A first adsorption experiment was conducted in order to determine the adsorption capacity of the different biochars produced. The experiment was carried out in duplicates. A stock solution with 2350 ml of deionized water and 145 µl PCE (≥ 99 %, Sigma-Aldrich) was produced in a 2 l DURAN® Schott bottle to receive a concentration of 100 mg/l.

For the experiment 100 mg of biochar was added to 20 serum bottles (120 ml). Samples were weighed with a Sartorius ENTRIS 623-1S Milligram Balance. The weighing is found in the appendix. They were filled with the stock solution up to the top to minimize headspace and two controls without biochar were included to monitor possible PCE volatilization or adsorption to the glass. The bottles were then sealed with crimp caps and PTFE septa. The experiment was carried out in duplicates. The bottles were placed into an overhead shaker (GFL 3040 - Overhead Shaker) at 6 rpm for three days. Samples were taken at 0 h, 6 h, 24 h, 48 h, and 72 h. Figure 7 shows the serum bottles before filling.
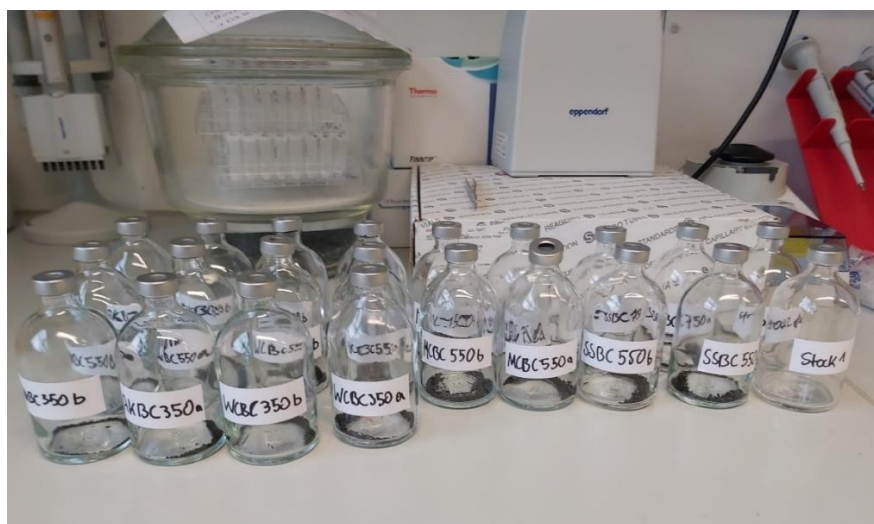
Figure 7: 120 ml serum bottles with crimp caps and PTFE septa before filling.

2.5.3 2nd adsorption experiment

In this experiment, the goal was to monitor the behaviour of the adsorbent when increasing the adsorbent dose. In order to compare the adsorption capacity to an industrial reference material, activated carbon was included in this experiment. Eleven headspace vials (60 ml) with 100 mg and 200 mg of adsorbent and one control group were filled with a PCE stock solution with a set concentration of 150 mg/l to the top to prevent headspace. Samples were weighed with a Sartorius ENTRIS 623-1S Milligram

Balance. The weighing is found in the appendix. The vials were sealed with mininert caps and placed in in an overhead shaker (Heidolph Reax 2) at 30 rpm for 168 hours. Samples were taken at 0 h, 5 h, 24 h, 48 h and 168 h. Figure 8 displays the experimental setup.

Figure 8: 60 ml headspace vials with mininert caps and varied adsorbent dose (100, 200 mg).

2.5.4 3rd adsorption experiment

Based on the results of the first two experiments, the isotherm experiment was designed to include the best performing biochar from each feedstock. Therefore W7, M7, S7 and A3 were included. The experiment was carried out in duplicates. A stock solution was prepared in a 10 l DURAN® Wide neck bottle with 10,5 l of deionised water and 649 µl of PCE to obtain a concentration of 100 mg/l PCE.

30 Schott bottles (250 ml) with DURAN® screw caps with aperture and DURAN® PTFE coated GL 45 silicone septa for piercing were filled with five different amounts of adsorbent; 100-300 mg; 50 mg steps in between; adsorbent concentrations of 30-100 mg/l. Samples were weighed with a Sartorius ENTRIS 623-1S Milligram Balance. The weighing is found in the appendix. They were filled with PCE stock solution to the top in order to minimize headspace with a Drechsel-type bottle head without a filter disk.

Since there was not enough stock solution to conduct the whole experiment with 250 ml flasks, 10 serum bottles (120 ml) with crimp seals and PTFE septa were used for the A3. The bottles were placed into an overhead shaker (GFL 3040 - Overhead Shaker) at 6 rpm for 120 h. Samples were taken after 0h, 96h and 120h.

2.5.5 4th adsorption experiment

Since the results of the 1st Isotherm experiment showed variations of up to 20 mg/l in the initial solute concentrations and gave rise to suspicion, that other factors in the setup of the isotherm experiment were not optimal, another isotherm experiment was conducted with a different setup. As mentioned in chapter 2.1, due to the excessive PAH content of the biochars produced at 750 °C, two more biochars were produced at 650 °C in the course of the project. Since W6 was believed to obtain favourable results regarding their adsorption capacity and PAH content, it was used in this experiment as an adsorbent, although no basic characterization of the biochar was conducted at the time of this thesis.

In the prior experiments, the stock solution was prepared by introducing the PCE with a 10 ml Eppendorf pipette into the Schott bottle with H_2O. Since the use of pipettes can lead to a loss of PCE due to volatilization (EPA, 1992), for this experiment 250 μl glass syringes were used to inject the PCE directly into a Schott bottle (5 l) closed with a DURAN® screw cap with aperture and a DURAN® PTFE coated GL 45 silicone septa for piercing. This resulted in the targeted initial solute concentration of 100 mg/l being achieved with just minor variations of 6.5 mg/l.

Since for a thorough isotherm analysis, the adsorbent concentration range of the prior isotherm experiment (30-100 mg/l) was believed to be too low, in this experiment the concentration was increased to 50-400 mg/l; eight steps of 50 mg/l in between. The experiment was carried out in duplicates. In order to increase homogeneity between the duplicates, the samples were weighed with a more precise scale (Sepor Micro Balance Models MC 5) with a readability of 1 μg. The weighing is found in the appendix.

16 serum bottles (120 ml) were filled with the adsorbent and closed with crimp caps and PTFE coated septa. Additionally, two control groups were added, one filled right before the filling of the biochar bottles, the second one after they were filled, in order to monitor any losses of PCE during the filling process. The stock solution was again filled into the serum bottles with a Drechsel-type bottle head without a filter disk.

During the prior experiments, the biochars tended to float on top during the filling of the serum bottles with stock solution. Therefore, this time the biochar was wetted with 1 ml of deionized water 2 h before the filling process in order to reduce the floating issue. This, however, did not have a major impact and the problem was still present.

The bottles were placed into an overhead shaker (GFL 3040 - Overhead Shaker) at 6 rpm for 96 h. Samples were taken after 0h and 96h. Figure 9 shows the setup of the experiment after filling.

Figure 9: 120 ml serum bottles with crimp caps and PTFE septa after filling.

3. Results

3.1 Biochar production

The yield of the biochar production is presented in table 5. It should be noted that during the pyrolysis process of W3, M3 and S3 the targeted HTT was exceeded due to malfunctioning of the oven. For W3 temperatures up to 385 °C were observed, for M3 up to 520 °C and for S3 530 °C. During the process of this thesis, the reason for that problem could not be determined, which resulted in exclusions of these biochars in the later experiments, since they were believed to have to similar properties to the respective 550 °C biochars.

Table 5: results of biochar production.

Biochar	Input mass [kg]	Biochar yield mass [kg]	Yield [%]
A3	3.45	1.21	35.19
A5	3.45	0.74	21.51
A7	3.45	0.58	16.75
W3	3	0.84	28.13
W5	2.35	0.4	17.11
W7	2.35	0.32	13.57
M3	3	0.61	20.2
M5	3	0.56	18.6

M7	3	0.41	13.77
S3	3	0.79	26.33
S5	3	0.68	22.67
S7	3	0.57	18.87

As seen in table 5, with an increase in HTT for all the biochars a substantial decrease of biochar yield could be observed. The biochar derived from apricot kernels seemed to have the highest yield compared to the other input materials. However, as mentioned above, during the production of the 350 °C biochar from wood chips, miscanthus and sunflower seed shells the temperature exceeded the targeted temperature and can therefore not be compared. At 550 °C sunflower seed biochar (SSBC) showed the highest yield with 22.67 % followed by AKBC, miscanthus biochar (MCBC) and wood-chips biochar (WCBC). At 750 °C, this trend did not change and again SSBC had the highest yield with 18.87 % followed by AKBC, MCBC and WCBC.

Figures 10 to 13 show feedstock next to its respective biochars at 550 °C. Since the biochar did not look different at lower or higher temperatures only pictures of BC550 are displayed.

Figure 10: AKBC produced at 550 °C.

Figure 11: MCBC produced at 550 °C.

Figure 12: SSBC produced at 550 °C.

Figure 13: WCBC produced at 550 °C.

3.2 Characterization feedstock

In table 6 the total C and N content of the different feedstock materials are shown. Apricot kernels show both the highest C content with 51,75 % followed by wood chips, sunflower seeds and miscanthus. For nitrogen, again apricot kernels have the highest content with 1,48% followed by sunflower seeds, wood chips and miscanthus.

Table 6: Elemental content of feedstock.

Feedstock	C	N
	[%]	[%]
Apricot kernels	51.75	1.48
Wood chips	48.66	0.31
Miscanthus	46.68	0.16
Sunflower seeds	47.44	0.66

3.3 Characterization biochar

Table 7 shows a selection of the results of the *eurofins* biochar characterization. The complete report is found in the appendix. M3 was not included in the analysis since the actual HTT was 520 °C. Additionally, the texture of the biochar already suggested that it would not be suitable for the further requirements of the project CHARBAK, since it was too fragile compared to the other biochars.

With an increase in HTT a significant rise in surface area is observable. M7 shows the highest surface area with 453.32 m²/g followed by W7 with 423,54 m²/g, A7 with 362,62 m²/g and S7 with 361.83 m²/g. The surface area of A3 was below the limit of detection, according to *eurfofins*.

Ash content is highest for S7 with 12.6 wt% and M7 with 10.9 wt% and increases gradually with pyrolysis temperature. WCBC shows a relatively low ash content compared to the other feedstocks. The pH is slightly alkaline and increasing with HTT ranging from 7.3 to 10.9. Only WCBC and SSBC deviate from that trend with both W3 and S3 having a higher pH than the biochars produced at 550 °C. pH is highest for SSBC followed by MCBC, WCBC and AKBC.

PAH content is particularly high for all 750 °C biochars except AKBC with 0.7 mg/kg. With 48.4 mg/kg it is highest for S7 followed by W7 with 32.4 mg/kg and M7 with 26.2 mg/kg, respectively.

Table 7: BET surface area, ash content, pH value and PAH content of the biochar.

Biochar	Surface area [m²/g]	Ash [wt%]	pH	PAH [mg/kg]
A3	n.n.	3.6	7.3	0.1
A5	178.17	4.9	8.1	2.1
A7	362.62	6.4	8.9	0.7
W3	5.16	1.9	8.9	0.7
W5	263.8	2.3	8.3	5.6
W7	423.54	3.0	9.3	32.4
M5	215.62	8.6	9.2	4.8
M7	453.32	10.9	9.4	26.2
S3	7.54	8.6	10.0	7.4
S5	82.97	10.6	9.1	2.0
S7	361.83	12.6	10.9	48.4

Table 8 shows the elemental composition and the molar ratios of the biochars. C content is increasing together with HTT and ranges from 73.8 % for A3 to 94.7 % for W7. Both SSBC and MCBC showed lower C content, compared to WCBC and AKBC. Compared to the feedstocks C and N content (listed in table 6), C is increasing through pyrolysis and is further increasing with pyrolysis temperature. N is increasing for AKBC through pyrolysis but reducing with pyrolysis temperature (1.83 wt% at 350 °C to 1.47 wt% at 750 °C). For the wood chips N content is 0.31% and is first decreasing by pyrolysis (0.22 wt% at 350 °C) and then increasing to 0.77 wt% at 750 °C. For MCBC N is increasing through pyrolysis and further increasing with pyrolysis temperature. For SSBC N is increasing through pyrolysis but decreasing with pyrolysis temperature. H, O and N content is reducing with HTT continuously, S content is increasing and is especially high for MCBC and SSBC compared to WCBC and AKBC. H content is

ranging between 0.9 and 4 wt%. O is ranging between 17.9 wt% for W3 and 3 wt% for A7. During the heating from 350 °C to 550 °C substantial O losses occurred compared to heating from 550 °C to 750 °C.

The H/C ratio, an indicator for aromaticity, decreases with an increased pyrolysis temperature indicating that the biochar becomes more aromatic with HTT. With 0.13 it is identical for all 750 °C biochars except A7 where it is slightly higher with 0.15. Generally, aromaticity seems to not be very feedstock dependent at temperatures >500 °C since it does not vary much across the different feedstocks.

The O/C ratio is an indicator for polarity and decreases with HTT indicating that the biochars are becoming less polar. W7 has the lowest O/C ratio with 0.01 followed by A7, M7 and S7.

The activated carbon used in the first adsorption experiment was not subject to the biochar characterization from *eurofins*. From the manufacturer *Donau Carbon* the bulk density is given with 360 ± 30 kg/m^3, the pH is between 8-11 and the ash content is 12 %. The surface area BET is 1250 m^2/g and therefore nearly three times as high as for the biochar with the highest surface, M7.

Table 8: elemental composition (water free) and molar ratio of the biochar.

Biochar	C [wt%]	Corg [wt%]	H [wt%]	O [wt%]	N [wt%]	S [wt%]	H/C	O/C
A3	73.8	73.6	4.8	16.1	1.83	0.05	0.78	0.164
A5	82.9	82.6	2.8	8	1.63	0.04	0.4	0.072
A7	88.5	88.2	1.1	3	1.47	0.06	0.15	0.025
W3	76.5	76.5	3.9	17.9	0.22	0.03	0.6	0.176
W5	89.8	89.6	2.8	5.1	0.55	< 0.03	0.37	0.043
W7	94.7	94.3	1.1	1.2	0.77	0.04	0.13	0.01
M5	84.6	84.2	2.3	4.5	0.54	0.18	0.32	0.04
M7	84.3	83.9	0.9	3.4	0.75	0.24	0.13	0.03
S3	76.3	75.9	3.4	11.7	1.51	0.26	0.52	0.115
S5	83.0	82.8	2.1	4.7	1.21	0.21	0.30	0.043
S7	83.1	82.2	0.9	4.1	1.17	0.28	0.13	0.037

3.4 ATR-MIR

In order to analyse the functional groups of the biochars ATR-MIR was conducted. The following figures show the ATR-MIR spectra of the biochars produced as well as the respective feedstocks. The biochar produced from miscanthus and sunflower seed shells at 350 °C were not measured due to the exceeded temperatures during production. Each detected peak is indicated, and the respective wavelength [cm-1] and func-

tional group are labelled above. The assigned bands of the various peaks are listed in table 9.

Aprikot kernel biochar ATR-MIR
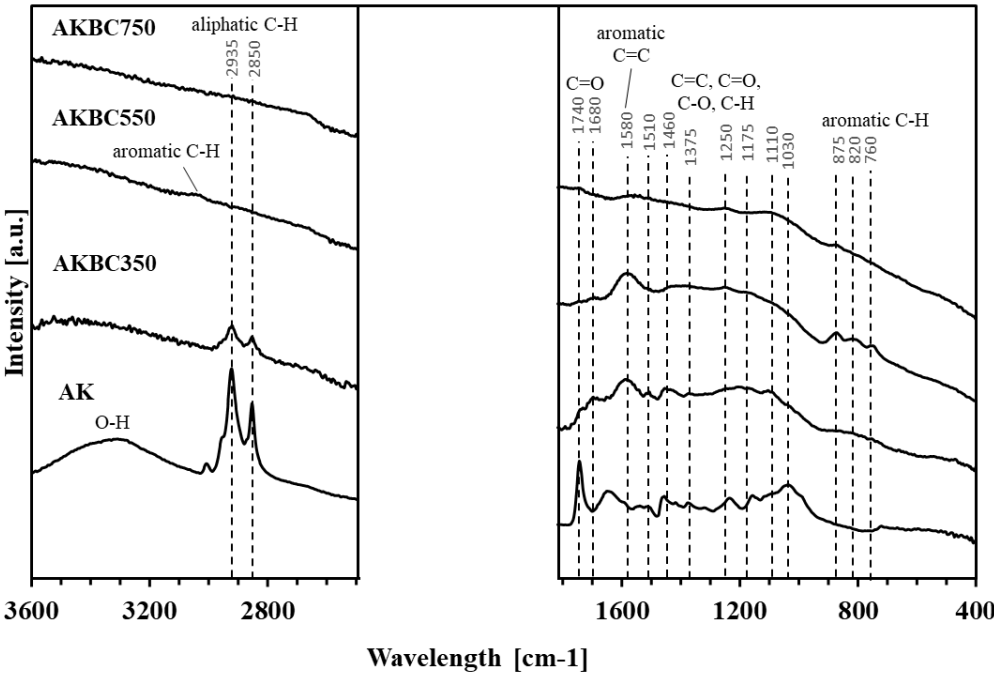
Figure 14: ATR-MIR spectra for biochar produced from apricot kernels at 350 °C, 550 °C, and 750 °C and the respective feedstock.

Wood chips biochar ATR-MIR
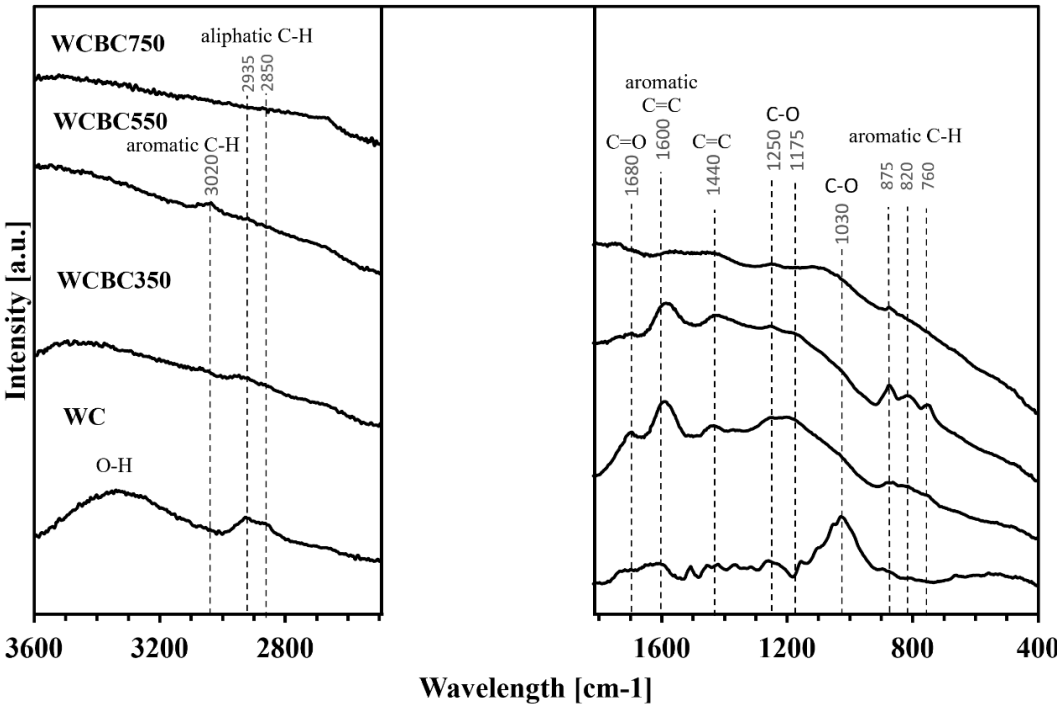
Figure 15: ATR-MIR spectra for biochar produced from wood chips at 350 °C, 550 °C, and 750 °C and the respective feedstock.

Miscanthus biochar ATR-MIR
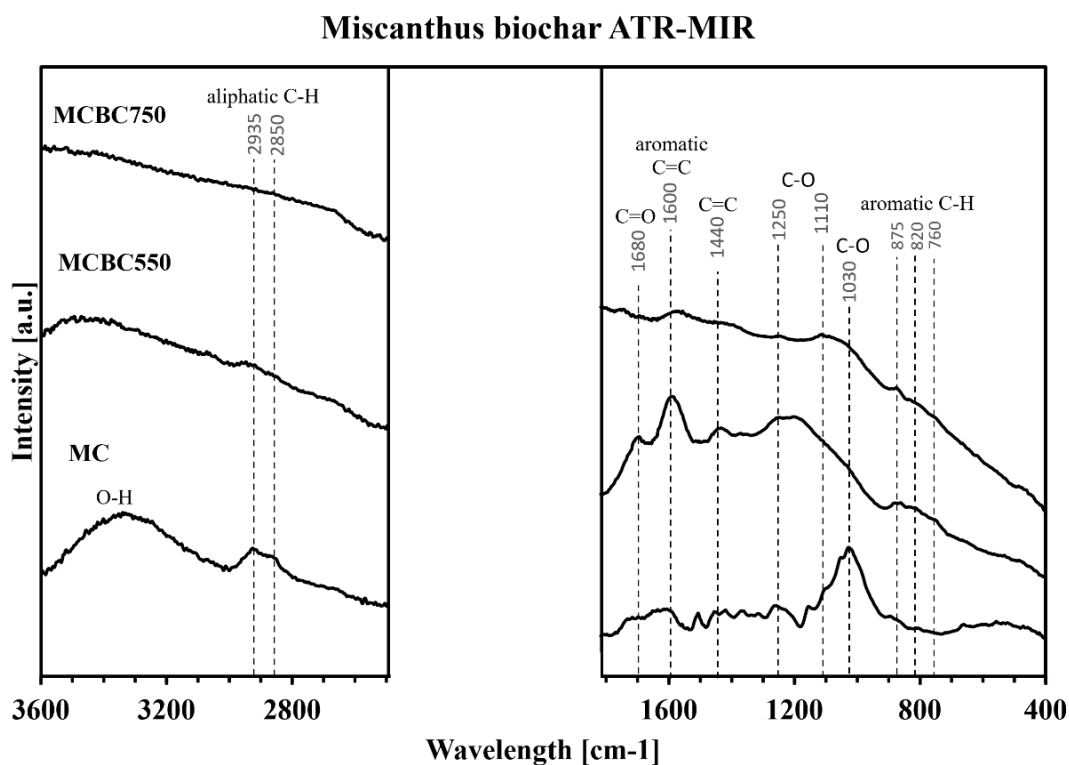
Figure 16: ATR-MIR spectra for biochar produced from miscanthus at 550 °C and 750 °C and the respective feedstock.

Sunflower seed shells biochar ATR-MIR
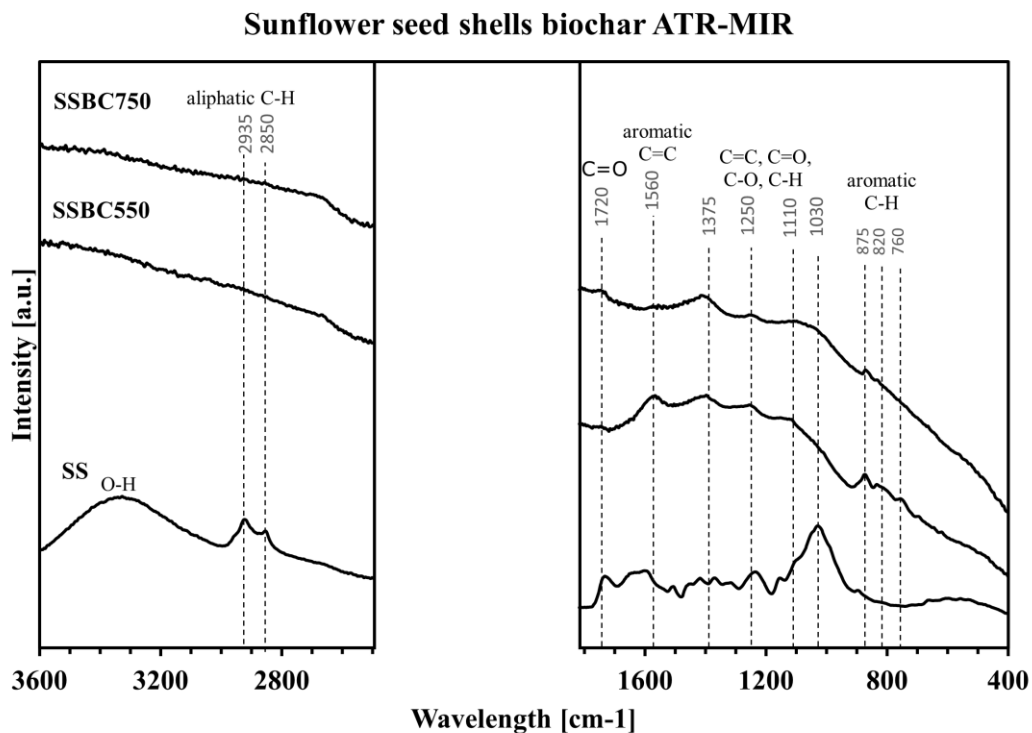
Figure 17: ATR-MIR spectra for biochar produced from sunflower seed shells at 550 °C and 750 °C and the respective feedstock.

At 3200-3500 cm^{-1} all four feedstocks show a characteristic O-H stretching of contained water molecules which are still detectable at 350 °C but at reduced intensity (Keiluweit et al., 2010; Pretsch et al., 2009). At a HTT of 550 °C these bands are completely diminished.

AK show a strong peak at 2930 and 2850 cm^{-1} due to aliphatic C-H stretching which decreases slightly at 350 °C (Chen et al., 2008; Keiluweit et al., 2010). WC show the same peak but significantly reduced. At 350 °C it is barely detectable. Aliphatic C-H vibrations are also detectable for SS and MC but not for the respective biochars at 550 °C which aligns with the findings of Chen et al. (2008), where the aliphatic C-H of bio-char produced from orange peels decreases significantly from 250 °C to 350 °C and is eliminated at 400 °C. The intensive peak of the feedstocks at around 1030 cm^{-1} due to C-O stretching in cellulose and hemicellulose is completely disappeared at 350 °C.

At 350 C°, AKBC, MCBC and WCBC show small peaks starting at 1740 and a clear peak at 1680 which is reduced when heating to 550 °C for AK and WC and not detectable for MC. This is due to C=O stretching of carboxyl groups as well as aldehydes, ketones and esters disappearing at temperatures over 500 °C (Chen et al., 2008; Keiluweit et al. 2010). All four biochars at 350 °C and 550 °C show an intensive peak between 1600 and 1560 cm^{-1} which is due to C=C and C=O stretching of aromatic C which diminishes when heating to 750 °C. At 550 °C all four biochars show signs of increased aromaticity also have clear peaks at 885, 815 and 750 cm^{-1} which is caused by aromatic C-H out-of-plane deformations (Haberhauer et al., 1998; Keiluweit et al., 2010).

Table 9: ATR-MIR bands assigned to biochars produced from apricot kernels, wood chips, miscanthus and sunflower seed shells as well as their respective feedstocks.

Wave number [cm-1]	Assigned bands and functionality
3200-3500	O-H stretching of water and H-bonded hydroxyl (-OH) groups [5, 12, 13, 15]
3020	C-H stretching from substituted aromatic carbon [8, 14]
2935	Aliphatic C-H stretching [3, 5]
2850	Aliphatic C-H stretching [3, 5]
1740-1680	C=O stretching of carboxyl groups as well as aldehydes, ketones and esters [3, 5, 6, 11]
1600-1560	C=C stretching of aromatic components, C=O stretching [1, 3, 4, 5]
1510	C=C stretching of aromatic skeletal vibrations, indicative of lignin [1, 4, 9]
1440-1460	C=C stretching from aromatic C, indicative of lignin C-O stretching of carbonates [1, 4, 9]
1375	Phenolic O-H bending [5, 9]
1250	C-O stretching of aryl esters [3, 9, 2, 15]
1175	C-O stretching ester groups in cellulose and hemicellulose [10, 7]
1110, 1030	C-O stretching in cellulose and hemicellulose [4, 5, 12]

| 885, 815, 750 | Aromatic C-H out-of-plane deformations [1, 4, 5] |

[1]Bustin and Guo, 1999; [2]Chen et al., 2005; [3]Chen et al., 2008; [4]Haberhauer et al., 1998; [5]Keiluweit et al., 2010; [6]Koch et al., 1998; [7]Labbe et al., 2006; [8]Lin-Vien et al., 1991; [9]López-Pasquali and Herrera, 1997; [10]Pastorova et al., 1994; [11]Pradhan and Sandle, 1999; [12]Pretsch et al., 2009; [13]Sarmah et al., 2010; [14]Sharma et al., 2004; [15]Smith and Chughtai, 1995.

Based on the ATR-MIR analysis, the biochars produced at 750 °C show the most promising results in respect to the adsorption capacity for PCE. The diminishment of H and O containing functional groups, that can be witnessed with a rise in pyrolytic temperature, indicates a high degree of aromatization and a high C content as well as a low polarity. This should increase the adsorption of PCE. When comparing the spectra in respect to each feedstock at 750 °C, no concise prediction can be made since the spectra all align at higher temperatures. At 550 °C the aromatic C-H peak between 875 and 760 of AKBC and WCBC is slightly more distinct. The peak at 1030, which is characteristic for C-O stretching in cellulose and hemicellulose, is less distinct for AK compared to the other three feedstocks. Since the AK included the seed material, not just the shells as for SS, the cellulose content was likely to be lower compared to the other feedstocks.

3.5 Adsorption experiments

3.5.1 1st adsorption experiment
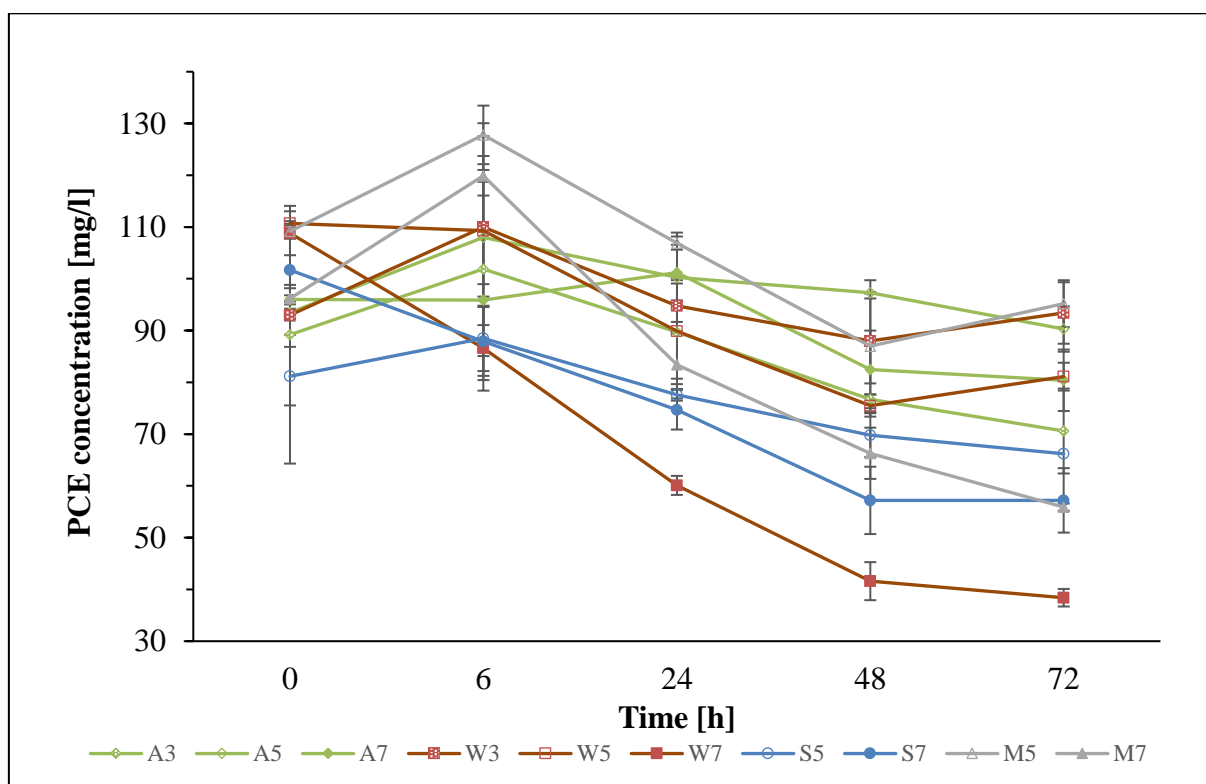
Figure 18: change in PCE concentration [mg/l] over time for 100 mg of adsorbent at a PCE concentration of ~100 mg/l. Error bars represent the standard deviation.

The results of this preliminary adsorption experiment show, that for all the biochars except AKBC, a rise in pyrolysis temperature led to a higher PCE removal efficiency. Figure 18 shows the change in PCE concentration over time for 100 mg of biochar. The rise in concentration at 6 h can be attributed to inhomogeneous mixing of the PCE with water. For most of the biochars, equilibrium was reached after 48 h. However, W7, M7, A3 and A5 showed a decrease of ~10 mg/l from 48 h to 72 h. Therefore, in the

following experiment, another sample point after 168 h was included, to ensure that equilibrium was reached.

Table 10 displays the % PCE removal and the adsorption capacity Q_e [mg/g] of the biochars. With 64.71 %, W7 showed the highest PCE removal efficiency of all the biochars followed by S7 (43.76 %) and M7 (41.89 %). For the biochars produced at 550 °C the PCE removal efficiency was half. The best performing was W5 with 31.8 % followed by M5 (20.33 %), S5 (18.47 %) and A5 (3.42 %). W3 only removed 5 % of the PCE. The only biochar acting completely different was AKBC. Here, with 20.85 %, A3 had the highest PCE removal followed by A7, with 16.25 % and A5, which had the lowest removal efficiency of all the biochars. This contrary behaviour will be discussed further in chapter 4.2.

With 82,68 mg/g, W7 showed the highest Q_e, followed by S7 (52.31 mg/g) and M7 (47.69 mg/g). The biochars produced at 550 °C had a substantially lower Q_e, with W5 being the highest (34.84 mg/g) and A5 being the lowest with 3.78 mg/g.

Table 10: % PCE removal and adsorption capacity Q_e [mg/g] of the 1st adsorption experiment.

Biochar	% PCE removal	Q_e [mg/g]
A3	20.85	21.87
A5	3.42	3.78
A7	16.25	18.35
W3	5.38	5.85
W5	31.8	34.84
W7	64.71	82.68
S5	18.47	17.72
S7	43.76	52.31
M5	20.33	26.21
M7	41.89	47.69

Based on the adsorption capacity determined through this experiment, the isotherm experiment was designed. Before that, another adsorption experiment was conducted in order to determine the influence of an increased biochar dose on the PCE removal efficiency and the adsorption capacity.

3.5.2 2nd adsorption experiment
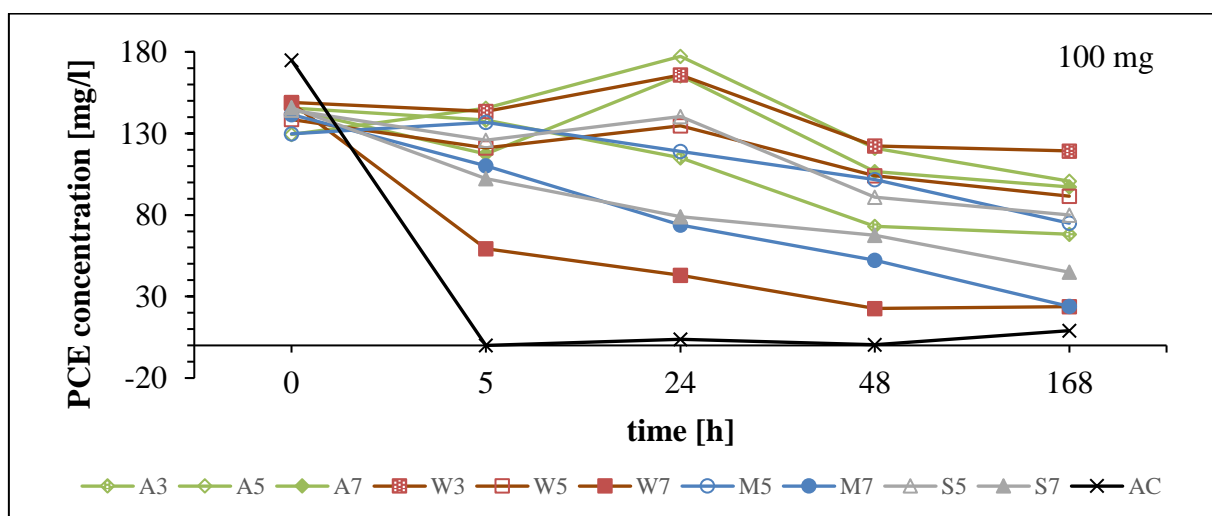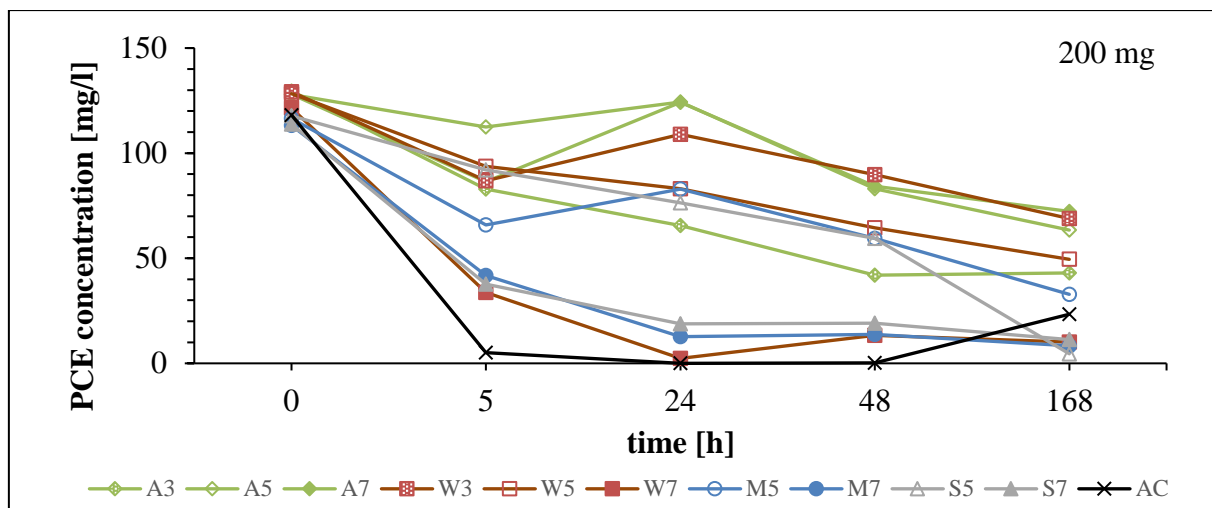
Figure 19: change in PCE concentration [mg/l] over time [h] for 100 mg (top) and 200 mg (bottom) of adsorbent.

In this experiment, the adsorption capacity of the biochar was monitored and compared to an industrial reference material - activated carbon. Figure 19 shows the PCE concentration over time in mg/l. Since the first adsorption experiment showed that for some biochars equilibrium was not reached after 48 h, this time another measurement after 168 h was included to ensure equilibration. As figure 19 shows, the activated carbon adsorbed all the PCE after 5h. For A3 and W7 no further decrease in concentration from 48 to 168 h could be monitored. All other biochars, however, seemed to not have reached equilibrium after 48 h. Since no control groups were included in this experiment, it is not possible to credit this drop in concentration to purely adsorption. The other adsorption experiments showed losses due to volatilization of the PCE and therefore no definite conclusion can be drawn from this.

When ranking the biochars regarding % PCE removal however, a clear trend can be observed. Table 11 shows the % PCE removal as well as the Q_e of the second adsorption experiment in respect to the adsorbent dose. Increasing the amount of biochar increases the total % PCE removal but decreases the Q_e for all the biochars and the activated carbon except W3. With a % PCE removal of > 99 % the activated carbon did not reach its adsorption capacity during this experiment so no Q_e could be calculated. Regarding the biochars, for 100 mg W7 and M7 showed the highest % PCE removal as well as the highest Q_e, followed by S7, A3, S5, M5, A7, A5 and W3. For 200 mg biochar, S5 showed the highest % PCE removal and Q_e, followed by M7, S7, M5, A3, W5, A5, W3 and A7. However, since the high % PCE removal of S5 at 200 mg was not observed at 100 mg and the experiment was not carried out in duplicates, a handling mistake or volatilization cannot be ruled out here. Again, AKBC behaves very differently compared to the other biochars.

Table 11: Adsorbent dose [mg], % PCE removal and adsorption capacity Q_e [mg/g] of the second adsorption experiment.

Adsorbent	Dose [mg]	% PCE removal	Q_e [mg/g]
A3	100	53.16	49.66
	200	66.81	27.52

A5	100	22.13	18.32
	200	50.42	20.56
A7	100	32.87	30.52
	200	43.54	17.69
W3	100	19.94	18.88
	200	46.68	19.15
W5	100	33.94	29.99
	200	61.44	25.14
W7	100	84.05	79.78
	200	91.62	35.2
M5	100	42.21	34.94
	200	71.82	26.51
M7	100	83.13	74.78
	200	92.63	33.37
S5	100	44.56	40.94
	200	96.14	35.92
S7	100	69.2	63.89
	200	90.07	32.61
AC	100	99.72	
	200	99.8	

3.5.3 3rd adsorption experiment
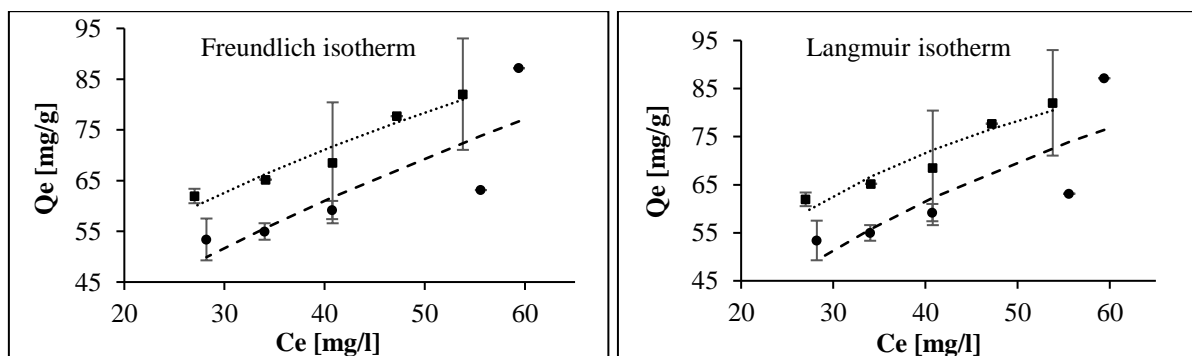
Figure 20: Freundlich isotherm (left) and Langmuir isotherm (right) of PCE adsorption for W7 (■) and M7 (●). The experiment was carried out with a PCE concentration of 80 mg/l and 120h of equilibrium time.

For the third adsorption experiment, increasing amounts of biochar were added to a PCE stock solution with a concentration of 80 mg/l in order to determine the adsorption isotherms. As an adsorbent, the best performing biochars of each feedstock were used; W7, M7, S7 and A3. During the filling of the bottles, the stock solution was exposed, which might have led to strong variations in the initial solute concentration (± 10 mg/l). To obtain interpretable results, samples with a deviation from the set concentration of more than 10 mg/l were excluded from the evaluation. For M7 and W7 this led to interpretable isotherms, which are shown in figure 20. S7 and A3 also had strong variations in the equilibrium concentration. The adsorption data obtained from these biochars was not usable, the isotherms could not be fitted and is therefore not further discussed here. The isotherms for these biochars as well as the respective coefficients are found in the appendix.

For W7 and M7, interpretable results were obtained although a broader range of adsorbent concentration would have been needed, to determine whether the adsorption process was following a Freundlich or a Langmuir isotherm. Figure 20 shows the adsorption isotherms for W7 and M7. Table 12 lists the Freundlich and the Langmuir coefficients for W7 and M7. With a nearly identical R^2 for both Langmuir and Freundlich isotherm, no definite conclusion can be drawn here. Maximum adsorption capacity q_{max} was highest for M7 with 152.11 and 125.18 for W7, respectively.

Table 12: Freundlich constant K_F [mg/g], Freundlich exponent n and R^2 for the Freundlich isotherm as well as Langmuir constant K_L [l/g], maximum adsorption capacity q_{max} [mg/g] and R^2 for the Langmuir isotherm for W7 and M7.

Adsorbent	K_F [l/g]	1/n	R^2
W7	14.15	0.37	0.94
M7	7.28	0.58	0.68

Adsorbent	K_L [l/g]	q_{max} [mg/g]	R^2
W7	0.045	125.18	0.91
M7	0.017	152.11	0.66

Figure 21 shows the % PCE removal over a range of biochar concentration for the different biochars. Although no isotherms could be plotted for S7 and A3, it is still possible to compare the overall removal efficiency of the materials. Just like in the other experiments, W7 and M7 performed the best, with W7 having a slightly higher removal efficiency than M7 (69.4 % and 65.5 %, respectively).

For A3 the adsorbent concentration used was higher than for W7, M7 and S7, which is the reason for it being plotted into an additional graph. Although the total amounts of biochar used in the experiment were identical for all the biochars (100, 150, 200, 250 and 300 mg), the volume of stock solution was lower, as explained in chapter 2.5.4. Due to variations in initial solute concentrations for A3 and S7, one sample had to be excluded from the data.
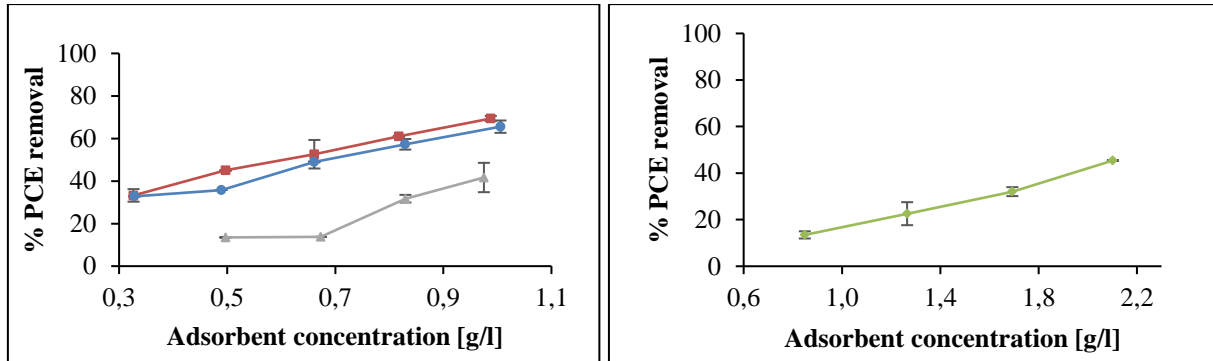
Figure 21: % PCE removal over a range of biochar concentrations for W7(■), M7(●) and S7 (▲) and A3 (♦) with a PCE concentration of 80 mg/l.

3.5.4 4th adsorption experiment
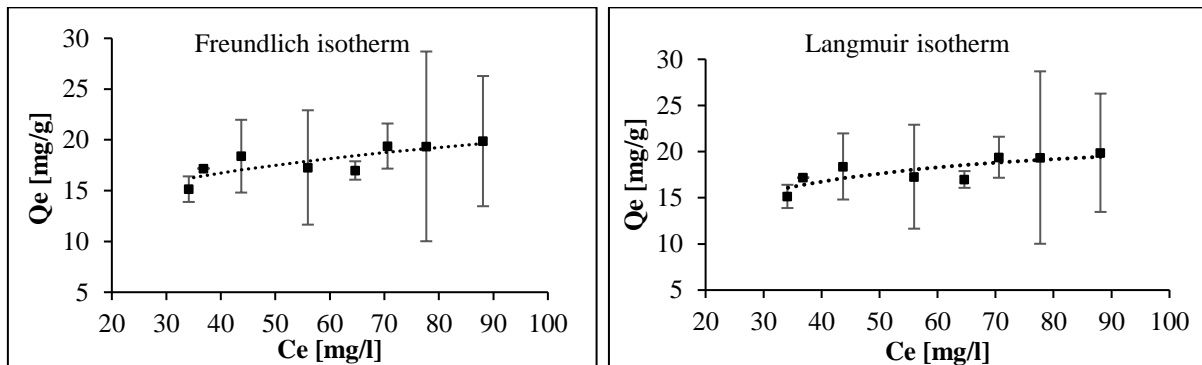
Figure 22: Freundlich isotherm (left) and Langmuir isotherm (right) of PCE adsorption for W6. The experiment was carried out with a PCE concentration of 100 mg/l and 96h of equilibrium time.

The results of the 4th adsorption experiment are displayed in figure 22. As in the prior experiment it can be seen that the adsorption capacity for the adsorbent was not fully reached with a concentration of 400 mg/l and could have been increased even more. With a Q_e of ~ 20 mg/g the adsorption capacity is significantly below W7 (~ 80 mg/g). Table 13 lists the Freundlich and Langmuir coefficients. With an R^2 of not more than 0.63, neither the Freundlich nor the Langmuir isotherm could fully describe the adsorption process. The q_{max} of 22.4 mg/g, however, is clearly lower than for the biochars from the prior experiment, W7 and M7. In order to fit the isotherm properly, the maximum adsorption capacity for the biochar would have to be determined through a different kind of adsorption experiment than the preliminary adsorption experiments used in this approach. The flaws of the experimental setup will be discussed further in chapter 4.3.

Table 13: Freundlich constant K_F [mg/g], Freundlich exponent n and R^2 for the Freundlich isotherm as well as Langmuir constant K_L [l/g], maximum adsorption capacity qmax [mg/g] and R^2 for the Langmuir isotherm for W6.

Adsorbent	K_F [l/g]	1/n	R^2
W6	7.92	4.93	0.63

Adsorbent	K_L [l/g]	q_{max} [mg/g]	R^2
W6	0.074	22.4	0.62

In figure 23, the % PCE removal of W6 over a range of biochar concentration is displayed. At 4 g/l only 64% of the PCE is adsorbed which shows that the concentration could have been increased to at least 6 g/l to achieve better isotherm data. However, for this experiment the initial concentrations were much more stable and the set concentration of 100 mg/l was achieved, compared to the prior isotherm experiment. This shows that the adaptations done in the filling procedures and the preparation of the stock solution had a positive impact on the results. Figure 23 shows a steady increase of % PCE removal when increasing the adsorbent concentration.
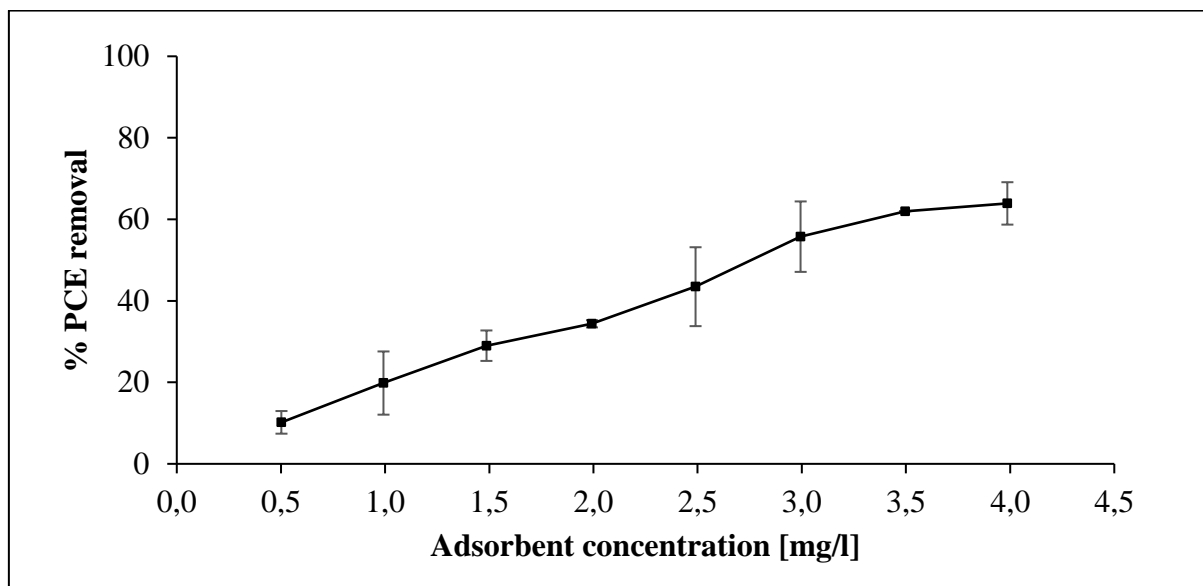
Figure 23: % PCE removal over a range of biochar concentration for W6 at a PCE concentration of 100 mg/l and 96 h equilibrium time.

However, there was still a variation of up to 10 mg/l in the equilibrium concentrations between duplicates. This could be explained by some of the biochar particles not being filled with the stock solution and will be further discussed in chapter 4.2.

4. Discussion

The research question of this thesis was: what influence does the pyrolysis temperature and the feedstock material have on the adsorption behaviour of biochar for tetrachloroethylene? The two hypothesises were, that the PCE sorption capacity of the produced biochars increases with a rise in pyrolysis temperature and that the PCE sorption of the biochars increases with a rise in aromaticity and a decline in polarity. In order to answer the research question and evaluate the hypothesises, the biochar and the respective feedstock were analysed. This chapter will discuss the results of this characterization in respect to the adsorptive properties of the biochars and evaluate the results from the adsorption experiment while comparing it to the results of the published literature. Since the isotherm experiments could not deliver meaningful results for all the biochars, the experimental setup, its flaws and possible improvements and adaptations for further experiments will be discussed as well.

4.1   Biochar characterization

One goal of this thesis was to determine the best biochars for the further use as a filter material for ground water remediation and PCE adsorption. However, factors like the

PAH content must be kept in mind when choosing between the different biochars, since, according to the limits of EBC-Material Class IV, a threshold of 30 mg/kg PAH content cannot be exceeded for the biochars to be applicable for commercial use (EBC, 2020). Therefore, a careful consideration between properties that influence adsorption like surface area, carbon content, aromaticity and polarity as well as commercial factors like the yield and the limits, proposed by the EBC guidelines, has to be done in order to choose which biochar to proceed with for further use. Table 14 summarises the yield, the SSA, C and PAH content as well as molar ratios H/C and O/C from the basic characterization of the biochar.

Table 14: biochar yield [%], surface area [m²/g], C content [wt%], H/C and O/C ratio and PAH content [mg/kg] of the produced biochars.

Biochar	Yield [%]	Surface area [m^2/g]	C [wt%]	H/C	O/C	PAH [mg/kg]
A3	35.19	n.n.	73.8	0.78	0.164	0.1
A5	21.51	178.17	82.9	0.4	0.072	2.1
A7	16.75	362.62	88.5	0.15	0.025	0.7
W3	28.13	5.16	76.5	0.6	0.176	0.7
W5	17.11	263.8	89.8	0.37	0.043	5.6
W7	13.57	423.54	94.7	0.13	0.01	32.4
M5	18.6	215.62	84.6	0.32	0.04	4.8
M7	13.77	453.32	84.3	0.13	0.03	26.2
S3	26.33	7.54	76.3	0.52	0.115	7.4
S5	22.67	82.97	83	0.3	0.043	2
S7	18.87	361.83	83.1	0.13	0.037	48.4

With 48.4 mg/kg, PAH content was especially high for S7 and therefore well above the EBC limit of 30 mg/kg for material class IV. W7 was also above the limit with 32.4 mg/kg and M7 was very close, with 26.2 mg/kg. Surprisingly, with 0.7 mg/kg A7 had the second lowest PAH content, right after A3 with 0.1 mg/kg. All the other biochars were well within the EBC limit and are therefore suitable for further commercial use except A3. With an H/C ratio of 0.78 it exceeds the EBC limit of 0.7 (EBC, 2020). At higher pyrolysis temperatures PAH formation occurs mainly as gas phase pyrosynthesis. At lower temperatures, the primary formation processes are mainly solid phase reactions like carbonization, aromatization and the reduction of feedstock (Bucheli et al., 2015). Since the PAH content of the biochars < 750 °C is relatively low, the gas phase formation must have been the dominant process. Kloss et al. (2012) report similarly high PAH content for biochar produced from straw at 525 °C (33.7 mg/kg) and spruce at 400 °C (30.7 mg/kg) which indicates a different PAH formation process. Bucheli et al. (2015) discuss the proportion of high to low molecular weight PAH and propose it being dependent on pyrolysis temperature. "(…) light PAHs are generated first and at lower temperatures and they will fuse into heavier ones at higher tempera-

tures. Moreover, heavier PAHs will condensate and associate with biochar first and to a larger extent as lighter ones, which are more volatile and may gas off from the system more easily." However, high molecular weight PAH like naphthalene only contributed to around 20 % of the total PAH for S7 and W7 (the table with the exact PAH distribution is found in the attachments from *eurofins*), which is below the 40 % average found by Bucheli et al. (2015). It could be observed that naphthalene, pyrene and phenanthrene increased strongly with pyrolysis temperature.

As discussed in chapter 3.2, the biochar yield was highly HTT dependent. With an increase in HTT the biochar yield decreased substantially for more than 50 %. The type of feedstock also had an impact on the yield. A3 had the highest yield with 35 %, higher than the other biochars produced at 350 °C. At 550 °C SSBC and AKBC had the highest yield with around 22 % and at 750 °C SSBC had the highest yield with around 19 %. In their Work "Biochar as a sorbent for contaminant management in soil and water: A review" Ahmad et al. (2014) evaluate biochar characteristics for a wide variety of biochars from different feedstocks and at different temperatures. Biochars derived from crop residue or wood generally have a lower yield compared to biochars from e.g., solid wastes or animal litter. In general, a high lignin content in the feedstock leads to a high biochar yield (Sohi et al., 2010). Keiluweit et al. (2010) also report higher yields for grass derived biochar compared to wood derived.

Surface area, however, increased from around 5 m²/g for biochars at 350 °C to up to 450 m²/g for MCBC750. Chen et al. (2008) explain this through the removal of H and O carrying functional groups of main aliphatic alkyl-CH_2, ester C=O, aromatic-CO and phenolic -OH groups. An increase in surface areas at high pyrolysis temperature is caused by the removal of volatile material which leads to an increased micropore volume (Ahmad et al., 2012). This is consistent with other findings in literature. Chun et al. (2005) report similar SSA of 438 m²/g for biochars produced from wheat at 700 °C. Schreiter et al. (2018) report a SSA of 341 m²/g for biochar derived from wood chips at 450 °C. Ahmad et al. (2012) report similar SSA for biochar produced at 300 °C and 700 °C derived from peanut shells and soybean stover (3-5 m²/g for 300 °C and 420-448 m²/g for 700 °C). Siggins et al. (2020) reported SSA for biochar derived from oak at a pyrolysis temperature of 600 °C of 216 m²/g.

SSA was also highly dependent on the feedstock. Both MCBC and WCBC showed higher SSA than SSBC and AKBC. Studies reviewed from Ahmad et al. (2014) show higher surface areas for biochars derived from crop residues and wood biomass compared to animal litter or solid waste. Siggins et al. (2020) reported a higher SSA for oak derived biochar than for spruce as well as a higher SSA for biochar derived from herbal pomace (374 m²) all being produced at 650 °C. When looking at the adsorption capacity of the biochars from the adsorption experiments, it also correlated with the SSA for the most part. The two biochars with the highest adsorption capacity were W7 and M7, which both have a substantially higher SSA than the other.

Carbon content increased with higher pyrolysis temperature for AKBC and WCBC ranging from 73.8 % and 76.5 % at 350 °C to 82.9 % and 89.8 % at 550 °C up to 88.5 % and 94.7 %, respectively. For SSBC C content increased from 76.3 % to 83 % from 350 °C to 550 °C but for both SSBC and MCBC it did not increase from 550 °C to 750 °C, for MCBC it even decreased by 0.3%.

As already shown in the results in chapter 3.3, the H/C ratios are decreasing with pyrolysis temperature for all biochars, suggesting that the biochars are becoming more aromatic with a rise in HTT. H/C ratios are ranging between 0.78 for A3 and 0.13 for

W7, M7 and S7 indicating that the biochars at 750 °C are already highly carbonized and show an aromatic structure (Chen et al., 2008). These findings align with previously reported studies. Kloss et al. (2012) also report a decrease of H/C ratios for biochar derived from poplar and spruce with ratios between 0.4 and 0.46 at an HTT of 525 °C which is comparable to the biochars produced during this project at 550 °C, with H/C ranging from 0.4 (A5) to 0.3 (S5). Keiluweit et al. (2010) also reported a steady reduction of H/C for biochar derived from grass and wood with HTT ranging from 100 °C to 700 °C and H/C ranging from 1.81 to 0.2. The highest loss of H was found when increasing pyrolysis temperature from 300 to 400 °C (Keiluweit et al., 2012). Chen et al. (2008) also report a reduction of H/C with a rise in HTT for biochars produced from pine needles. With a decline in H/C, and thus a rise in aromaticity, a higher adsorption capacity has been reported. Adsorption of organic contaminants generally increases with aromaticity of C materials (Ahmad et al., 2012). In their sorption experiments for tetrachloroethylene with biochar derived from peanut shells and soybean stover, Ahmad et al. (2012) reported a higher adsorption capacity for the biochars produced at 700 °C compared to 300 °C and explained this with the high aromaticity and the low polarity of said biochars. Sun et al. (2011) however reported high adsorption capacities for biochars produced at 400 °C with high polarities for the sorption of norflurazon and fluoridone. These contrary findings can be explained by the nature of the sorbates. Trichloroethylene, just like tetrachloroethylene, are non-polar compounds which like to access the hydrophobic sites on biochar surfaces (as displayed in chapter 1.4.3) in the absence of H-bonding between water and O-containing functional groups. Norflurazon and fluridone, however, are polar compounds. They are adsorbed by H-bonding between the compounds and the O-containing moieties, thus explaining the results from Sun et al. (2011, cited by Ahmad et al., 2014).

Pyrolysis temperature also had a strong influence on the polarity of the biochars. At 350 °C, AKBC, WCBC and SSBC had an O/C ratio of 0.164, 0.176 and 0.115, respectively. At 750 °C it decreased significantly to around 0.03 for AKBC, MCBC and SSBC indicating that the surface of the biochar becomes less hydrophilic with an increase of pyrolytic temperature (Chen et al., 2008). With 0.01 W7 had the lowest O/C ratio of all biochars. The reduction of O at higher temperatures, displayed in chapter 3.3, resulted in the removal of acidic functional groups which caused the biochars to become more basic. Ahmad et al. (2014) also reported an increase of aromaticity and a decrease in polarity for biochars produced at 700 °C "due to the formation of aromatic structures by a higher degree of carbonization and the removal of polar surface functional groups" (Ahmad et al. 2014). For PCE being a nonpolar compound, a decrease in polarity and an increase in aromaticity should lead to a higher adsorption capacity for the biochars. The results from the adsorption experiments displayed in chapter 3.5 align with this. W7, with the lowest O/C ration of 0.01 and H/C ratio of 0.13 as well as the highest C content of 94.7 % consistently showed the highest % PCE removal and with around 80 mg/g the highest Q_e. Generally, biochars produced at higher temperatures are reported to be more effective for the sorption of organic pollutants due to the higher SSA and micropore development (Ahmad et al., 2014). This can be partially verified by the results from the adsorption experiments.

4.2   Adsorptive behaviour

The results of the adsorption experiments were displayed in chapter 3.5. The % PCE removal positively correlated with SSA and C content and negatively correlated with

H/C and O/C ratio. Table 15 ranks the biochars from the 1st adsorption experiment with 100 mg of biochar based on their % PCE removal and Q_e from highest to lowest.

Table 15: biochars ranked by % PCE removal and Q_e [mg/g] from highest to lowest from the 1st adsorption experiment with 100 mg of biochar and a PCE concentration of ~100 mg/l.

Biochar	% PCE removal	Biochar	Q_e [mg/g]
W7	64,71	W7	82,68
S7	43,76	S7	52,31
M7	41,89	M7	47,69
W5	31,8	W5	34,84
A3	20,85	M5	26,21
M5	20,33	A3	21,87
S5	18,47	A7	18,35
A7	16,25	S5	17,72
W3	5,38	W3	5,85
A5	3,42	A5	3,78

With a % PCE removal of 64.7 % and a Q_e of 82.68 mg/g W7 consistently showed the best adsorption behaviour for PCE, followed by S7 and M7. A7 was performing significantly worse than the other biochars produced at 750 °C with a Q_e of 18.35 mg/g and a % PCE removal of 16.25 %. These results align with the 2nd adsorption experiment except for S7 having a slightly lower PCE removal efficiency than M7. The biochars produced at 550 °C perform significantly worse than the 750 °C biochars with W5 having the highest Q_e (34.83 mg/g) followed by M5 (26.21 mg/g) and S5 (17.72 mg/g). The biochar with the lowest % PCE removal and Q_e was A5 (3.42 % and 3.78 mg/g). These results are consistent with the 2nd adsorption experiment. As expected from the characterization, W3 showed a low % PCE removal of 5.38 % and a low Q_e of 5.85 mg/g.

The only group of biochars behaving entirely different from the others and therefore against the trend that was expected (adsorption increasing with higher SSA and C content and with lower H/C and O/C ratio) was AKBC. With a % PCE removal of 20.85 % and a Q_e of 21.87 mg/g, A3 was the best performing biochar within its group, followed by A7 and A5. These results were also consistent with the 2nd adsorption experiment. In order to rule out any mistake during production or sieving, during the project another AKBC was produced at 350°C and tested in an experiment not further discussed in this thesis. It showed comparable results to the biochar used in the experiments displayed here. When comparing their elemental composition, everything indicates that the A7 and the A5 should have a better PCE removal efficiency than A3. A3 is more polar (O/C ratio 0.164), less aromatic (H/C ratio 0.78) and has a lower C content (73.8 %) as well as a lower SSA than A5 and A7. The ATR-MIR spectra would also suggest A7 to have a much higher adsorption capacity than A3, since it shows much less H and O containing functional groups.

There have been reports of biochars produced at lower temperatures performing better than at higher. In their study with peat moss-derived biochars for the sorption of VOCs in groundwater, Kim et al. (2019) report a higher removal efficiency for biochars produced at 500 °C compared to 700 °C. This is explained with the collapsing of micropore walls at such high temperatures which leads to the blocking of sorption sites.

As stated before, Sun et al. (2011) have produced biochars at 400 °C for the sorption of norflurazon and fluoridone which are polar compounds and are absorbed by H-

bonding to the O-containing functional groups of the biochars. PCE, however, is a non-polar substance and usually likes to access the hydrophobic sites of the biochar surfaces (Ahmad et al., 2014). Findings from Chun et al. (2005) also showed a higher uptake of benzene (nonpolar) and nitrobenzene (has both polar and nonpolar characteristics) for biochars produced at 300 °C compared to 700 °C. They explained this by a "concomitant solute partition, since without this effect the uptake with these two chars [300 and 400 °C] would have been lower because of the hydrophilic nature of their polar functional groups on the surfaces. A somewhat larger partition effect for nitrobenzene with the chars is expected, because nitrobenzene, due to its polar nature, should partition more effectively than benzene into the organic phase of the chars."

The predominant adsorption effect, which is proposed here, is partitioning. As stated in chapter 1.5.3, for the adsorption of organic contaminants, pore filling, partitioning, hydrophobic and π-π electron donor-acceptor interactions are the main adsorption mechanisms (Chen et al., 2017). And although the positive correlation of SSA and PV with pyrolysis temperature leads to the suggestion, that sorption of organic pollutants is more effective for biochar produced at higher temperatures, partitioning can occur in the non-carbonized phase, predominant at low pyrolysis temperatures (100-300 °C) (Ahmad et al., 2014, Schreiter et al., 2018).

An explanation for the higher adsorption capacity of A3 compared to A7 and A5 can therefore be that adsorption was following a partitioning process in the non-carbonized phase of the biochar. The adsorption mechanisms for PCE to A5 and A7 probably followed a combined adsorption-partitioning process. Non-polar organic attraction to the hydrophobic sites of the well carbonized phase of the biochar and electrostatic attraction are predominant for biochars produced at higher temperatures (Schreiter et al., 2018). For A3 partitioning was stronger than the other adsorption mechanisms. Chen et al. (2009) also witnessed a higher sorption capability of biochar derived from orange peels produced at 200 °C compared to 600 °C and even 700 °C for a high equilibrium concentration of naphthalene and 1-naphthol. This was attributed to multiple sorption mechanisms involved; Partitioning and surface coverage for naphthalene and partitioning, surface coverage and specific interaction for 1-naphthol (Chen et al., 2009). Generally, it can be said, that due to the heterogenous nature of biochars, a variety of sorption mechanism can occur. The differences in the predominant sorption mechanisms have a significant impact on the sorption capabilities of the adsorbent and although for PCE it mostly correlates positively with pyrolytic temperature, SSA and aromaticity and negatively with polarity, research has shown exceptions for some cases (Chun et al., 2005; Chen et al., 2009; Sun et al., 2011; Kim et al., 2019). From the isotherm experiment it would have been possible to obtain an indication which sorption mechanism was predominant for the AKBC. Unfortunately, as discussed in the previous chapter, due to flaws in the experimental setup, the data obtained from the isotherm experiment for A3 could not give valid information about this.

Even though the isotherms could not be fitted for all the biochars produced, as displayed in chapter 3.5.3, it was possible to fit them for W7 and M7. Table 16 summarizes the Freundlich coefficients from the 3rd adsorption experiment. For both biochars the Freundlich isotherm was the best fit with an R^2 of 0.94 and 0.68, respectively. The higher K_F value for W7 reflects the higher adsorption capacity compared to M7 (Ahmad et al., 2012).

Table 16: Freundlich constant K_F [mg/g], Freundlich exponent 1/n and R^2 for W7 and M7.

Adsorbent	K_F [l/g]	1/n	R^2

W7	14.15	0.37	0.94
M7	7.28	0.58	0.68

Freundlich isotherm coefficients 1/n were <1 for both biochars, reflecting nonlinearity. It was closer to 1 for M7 than for W7, thus showing a more linear isotherm and resulting in higher K_F values for W7. At low pyrolysis temperatures, hydrophobic partitioning plays a bigger role for the sorption of PCE to biochar whereas at higher temperatures adsorption is predominant (Kim et al., 2019). As stated in chapter 1.4.3 it mainly takes place in the well carbonized, aromatic structure, which are dominant for biochars with high HTT between 400-700 °C, whereas partitioning can occur in the non-carbonized phase, predominant at low pyrolysis temperatures. Therefore, the predominant adsorption mechanism for W7 and M7 is most likely not a partitioning process. The highly carbonized (C content for W7 94,7 % and 84,3 % for M7) and aromatic (H/C ratio 0,13) structure of the biochars suggest that PCE adsorbed to the non-polar, organic and hydrophobic sites of the well carbonized phase of the biochar. Schreiter et al. (2018) and Ma et al. (2011) state that the C=C double bond in TCE and PCE is capable of p-p interactions with the aromatic parts of the biochar. Ahmad et al. (2014) proposes this as a mechanism for TCE adsorption for highly carbonized, high temperature biochar (H/C 0,15). This p-p interaction between PCE and the aromatic, well carbonized biochar is also proposed for W7 and M7.

4.3 Experimental setup

In chapter 2.5 the setup of the various adsorption experiments has already been displayed and partially discussed. However, since especially the isotherm experiments failed to deliver valid data for most of the biochars, this chapter seeks to discuss the flaws of the experimental design and to make recommendations on how the setup can be improved for future experiments.

One major problem, that occurred all through the different adsorption experiments, was the preparation of the stock solution. Although the amount of PCE needed to obtain a certain concentration was calculated correctly and the results from the standards of the IRMS measurements suggested that the syringe handling during sampling was not an issue, the targeted concentration was consistently lower for the first three experiments. One of the possible problems was the use of a pipette to transfer the PCE into the stock solution bottle. As mentioned in chapter 2.5.5, the EPA (1992) suggests using glass syringes for the preparation of the stock solution in order to minimize exposure for volatile organic compounds (VOC). For the 4th adsorption experiment, this was adapted and the PCE was injected directly with a 250 µl glass syringe into a Schott bottle (5 l). This resulted in a stable initial PCE concentration of 100 mg/l. For further experiments, the use of a pipette for the production of the stock solution should be avoided.

Another problem that was observed during the 3rd adsorption experiment was the variation in the volume of stock solution used within one experiment. In a preliminary isotherm experiment not further discussed in this thesis, for smaller amounts of biochar, serum bottles (120 ml) were used and for higher amounts Schott bottles (250 ml and 500 ml). The goal of this was initially to use less stock solution, since the number of samples was so high, that the amount of stock solution needed would have been substantial. However, this setup resulted in inconsistent adsorbent concentrations which had a negative impact on the isotherms. Based on these results, the 3rd adsorption

experiment was planned, and the setup was changed accordingly with only one type of volume being used for one biochar. However, since the experiment was supposed to include the best performing biochar from each feedstock, for one biochar (AKBC) the volume of stock solution had to be reduced (120 ml instead of 250 ml), since the total amount of stock solution available would have not been sufficient (as discussed in chapter 2.5.4). The biochar amount was left unchanged, which resulted in a much higher adsorbent concentration of the AKBC (0.85-2.55 g/l) compared to the other biochars (0.3-1 g/l) which makes a comparison difficult. For the 4th adsorption experiment this was adapted and a homogenous stock volume with gradually increasing amounts of biochar was used.

Since PCE is a volatile substance, during the filling process volatilization was also a problem. During the first two adsorption experiments, the serum bottles (120 ml) were filled with a 10 ml pipette, which left a lot of time for the PCE to volatilize. This resulted in a high deviation of the initial PCE concentration. To minimize this problem, other studies have opted towards using a methanol PCE solution. Schreiter et al. (2018) have prepared PCE stock solutions with methanol and injected the solution directly into headspace vials (50 ml) filled with an aqueous solution and the adsorbent. The same was done by Kim et al. (2019) when testing the effectiveness of peat moss-derived biochars for the sorption of VOC`s. They used HPLC grade methanol to produce a PCE stock solution. The biochar was placed in an amber glass vial (40 ml) which was then filled with deionized water. The vials where then spiked directly with the stock solution (Kim et al., 2019). This approach guarantees minimal exposure of the volatile compound. However, the addition of another toxic substance, which would also not be present in the field, was not considered reasonable for the experiments of this project.

Figure 24 displays the initial PCE concentration of the 3rd (left) and 4th (right) adsorption experiment measured right after the filling of the vials. It becomes clear that during the filling process a substantial amount of PCE is lost due to volatilization and that the initial concentration stabilized in the 4th adsorption experiment compared to the 3rd.
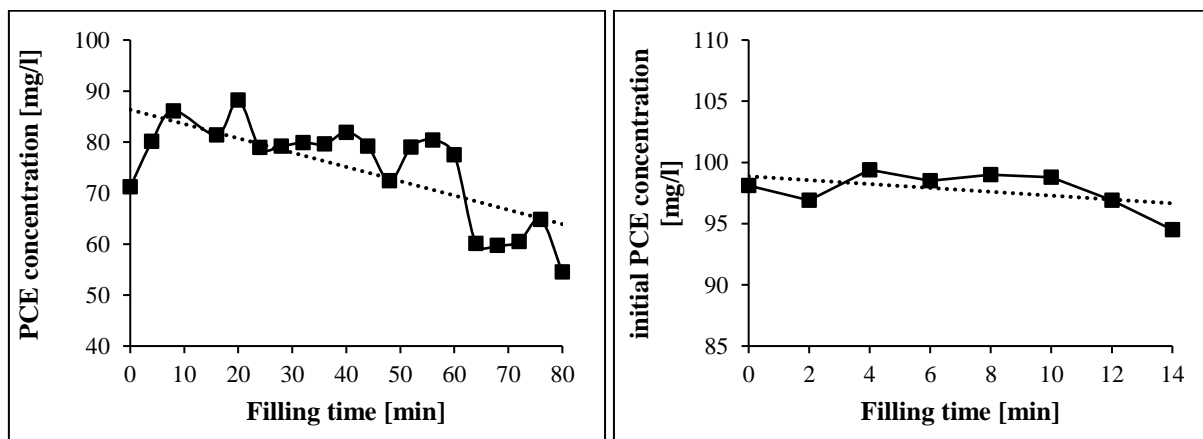
Figure 24: initial PCE concentrations [mg/l] of the 3rd adsorption experiment (left) and the 4th adsorption experiment (right) during the filling process [min].

Since the fluctuations of the initial concentrations in the 1st and 2nd adsorption experiment seemed to have been caused by the filling process with pipettes, for the 3rd and the 4th adsorption experiment the vials were filled using a Drechsel-type bottle head which already helped stabilizing the initial concentration. The decreased amounts of samples in the 4th experiment also helped with the filling process, since a smaller Schott bottle (5 l) could be used for the stock solution. This made the filling process much easier to handle, therefore quicker and less prone to errors. In order to obtain

even more accurate results and to completely rule out any volatilization, the direct injection of the PCE-solution into the closed bottles is recommended. However, the process is very time consuming and therefore not applicable for a large number of samples.

Figure 25: Biochar particles floating on top after 96 h.

As displayed in chapter 3.5. there were variations not only in the initial concentration but also in the equilibrium concentrations between duplicates. Figure 25 shows a possible explanation for this variation. It displays a serum flask (120 ml) from the 4th adsorption experiment equipped in an overhead shaker. It is clearly visible, that some biochar particles are floating on top, while the majority is settled at the bottom. This could mean that the biochar pores are not filled with the stock solution which could lead to inconsistent equilibrium concentrations in-between samples, since the portion of unfilled biochar particles is not homogeneous.

In order to prevent this problem, wet sieving could be applied to filter the floating particles out and thus obtain a more homogenous result. Schreiter et al. (2018) ground their biochar to a fine powder before further experiments, however, this would have a significant impact on the sorption capacity of the biochars and would not have reflected the conditions, the biochar is used later in the field.

5. Conclusion

The question, this thesis tried to answer, was, what influence the pyrolysis temperature and the feedstock material have on the adsorption behaviour of the produced biochars for tetrachloroethylene. The following hypothesises were formed at the beginning of this work:

I: The PCE sorption capacity of the produced biochars increases with a rise in pyrolysis temperature.

II: The PCE sorption of biochars increases with a rise in aromaticity and a decline in polarity.

Both hypothesises were partially verified. In three of four cases an increase in pyrolysis temperature led to an increase in PCE adsorption with AKBC being the only exception. The best performing biochars were the ones produced at 750 °C followed by 550 °C

and 350 °C. AKBC most likely behaved contrary because it was following a partitioning mechanism. An increase in pyrolysis temperature led to a higher SSA, an increased C content, an increase in aromaticity and a decrease in polarity which is consistent with other studies. H and O containing functional groups decreased with a rise of pyrolysis temperature, increasing the hydrophobicity, aromaticity and decreasing the polarity of the biochars produced. The biochar with the highest adsorption capacity, W7, had the lowest H/C (0.13) and O/C ratio (0.01) and therefore the highest degree of aromatization and the lowest polarity amongst the biochars produced.

The choice of feedstock also had an influence on the adsorption behaviour of the biochars. Woodchips consistently showed a higher PCE adsorption followed by miscanthus, sunflower seed shells and apricot kernels. The choice of feedstock influences the later characteristics of the biochars. Although being subject to the same pyrolysis process, WCBC showed a higher C content and a lower polarity than the other biochars. Schreiter et al. (2018) conclude, that biochars with a high polarity (like AKBC) favour partitioning while biochars with a high degree of micro pores favour pore-filling mechanisms. In order to further investigate the adsorption processes that influence the PCE adsorption of the biochars produced, the total pore volume and the pore size distribution should be examined.

Since the isotherm experiments could not deliver conclusive results, they could be repeated with an improved setup. Using a wider range of adsorbent concentration, minimizing contaminant exposure through the sole use of glass syringes for the preparation of the stock solution and the batch bottle set up and conducting a wet sieving of the biochars prior to the experiment, in order to filter out biochar particles with air captured inside, should significantly increase the quality of the data obtained.

Nonetheless, this work could deliver an answer on the research question and partially verify the hypothesises proposed. For the project CHARBAK, due to the high PAH content of the best performing biochars, further experiments should be conducted with the best performing biochars that meet the EBC restrictions. S5 and A3 showed promising results and could be subject to further investigations regarding their adsorptive behaviour. As mentioned before, during the project additional biochars were produced at a new temperature level of 650 °C in order to determine if the adsorption capacity would increase without the transgression of the PAH limit proposed by EBC. As the 4th adsorption experiment showed, adsorption capacity for W6 was significantly lower than for W7. A basic characterization could deliver more insights on the sorptive properties of the material.

Both pyrolysis temperature and choice of feedstock play a critical role in the production of biochar for the sorption of organic pollutants and should be considered carefully. Based on the nature of the adsorbate, the proper choice of production parameters and feedstock can significantly impact the adsorption behaviour of the adsorbent.

6. References

Ahmad, M., Sang Soo, L., Xiaomin, D., Dinesh, M., Jwa-Kyung, S., Jae E, Y., Yong Sik, O. 2012. Effects of pyrolysis temperature on soybean stover- and peanut shell-derived biochar properties and TCE adsorption in water. Bioresource Technology 118: 536-544.

Ahmad, M., Anushka, U. R., Jung, E. L., Ming, Z., Nanthi, B., Dinesh, M., Meththika, V., Sang, S. L., Yong, S. O. 2014. Biochar as a sorbent for contaminant management in soil and water: A review. Chemosphere 99: 19–33.

Ajayi, A.E. and Horn, R. 2016. Modification of chemical and hydrophysical properties of two texturally differentiated soils due to varying magnitudes of added biochar. Soil. Till. Res. 164: 34–44.

Antal Jr, M.J. and Grönli, M. 2003. The art, science, and technology of charcoal production. Industrial and Engineering Chemistry Research 42(8): 1619-1640.

ATSDR. 2014. Public Health Statement Tetrachloroethylene. Department of Healthand Human Services, Public Health Service, Atlanta, GA.

Ayoob, S., Gupta, A.K. 2008. Insights into isotherm making in the sorptive removal of fluoride from drinking water. Journal of Hazardous Materials 152: 976-985.

Bucheli, D.T., Hilber, I., Schmidt, H. 2015. Polycyclic aromatic hydrocarbons and polychlorinated aromatic compounds in biochar. In: Biochar for Environmental Management - Science, Technology and Implementation. Earthscan. London. Chapter 21.

Bustin, R., Guo, Y. 1999. Abrupt changes (jumps) in reflectance values and chemical compositions of artificial charcoals and inertinite in coals. Int. J. Coal Geol. 38(3-4): 237-260.

Chen, B.; Johnson, E.; Chefetz, B.; Zhu, L.; Xing, B. 2005. Sorption of polar and non-polar aromatic organic contaminants by plant cuticular materials: Role of polarity and accessibility. Environ. Sci. Technol. 39(16): 6138-6146.

Chen, B., Zhou, D., Zhu, L. 2008. Transitional adsorption and partition of nonpolar and polar aromatic contaminants by biochars of pine needles with different pyrolytic temperatures. Environ. Sci. Technol. 42(14): 5137-5143.

Chen, B., Chen, Z. 2009. Sorption of naphthalene and 1-naphthol by biochars of orange peels with different pyrolytic temperatures. Chemosphere 76: 127-133.

Chun, Y., Sheng, G., Chiou, C.T., Xing, B. 2005. Composition and Sorptive Properties of Crop Residue-Derived Chars. Environ. Sci. Technol. 38: 4649-4655.

Dabrowski, A. 2001. Adsorption – from theory to practice. Advances in Colloid and Interface Science 93 (1-3): 135-224.

Demirbas, A. 2004. Effects of temperature and particle size on bio-char yield from pyrolysis of agricultural residues. Journal of Analytical and Applied Pyrolysis 72: 243-248.

Doran, M.P. 2013. Bioprocess Engineering Principles (Second Edition). Academic Press.

Downie, A., Crosky, A., Munroe, P. 2009. Physical properties of biochar. In: Lehmann, J., Joseph, S. (Eds.)., Biochar for environmental management: Science and technology, Earthscan, London, 13-32.

European Biochar Foundation (EBC), 2012. European Biochar Certificate - Guidelines for a Sustainable Production of Biochar. Arbaz, Switzerland. Version 9.2E of 2nd December 2020.

Foo, K.Y., Hameed, B.H. 2009. Insights into the modelling of adsorption isotherm systems. Chemical Engineering Journal 156: 2-10.

Fushimi, C., Araki, K., Yamaguchi, Y., Tsutsumi, A. 2003. Effect of heating rate on steam gasification of biomass 2. Thermogravimetric-mass spectrometric (TG-MS) analysis of gas evolution. Industrial & Engineering Chemistry Research 42.: 3929-3936.

Haberhauer, G.; Rafferty, B.; Strebl, F.; Gerzabek, M. 1998. Comparison of the composition of forest soil litter derived from three different sites at various decompositional stages using FTIR spectroscopy. Geoderma 83 (3-4): 331-342.

IARC, 2014. Trichloroethylene, Tetrachloroethylene, and Some Other Chlorinated Agents, Monograph IARC Monographs on the Evaluation of Carcinogenic Risks to Humans 106.

IBI. 2012. Standardized product definition and product testing guidelines for biochar that is used in soil. International Biochar Initiative.

International Conference on Harmonization (ICH) of Technical Requirements for the Registration of Pharmaceuticals for Human Use, Validation of analytical procedures: Text and Methodology. ICH-Q2B, Geneva; 1996.

Ippolito, J.A., Spokas, K.A., Novak, J.M., Lentz, R.D., Cantrell, K.B. 2015. Biochar elemental composition and factors influencing nutrient retention. In: Biochar for Environmental Management - Science, Technology and Implementation. Earthscan. London.

Ippolito, J.A., Cui, L., Kammann, C. et al. 2020 Feedstock choice, pyrolysis temperature and type influence biochar characteristics: a comprehensive meta-data analysis review. Biochar 2: 421–438.

Keiluweit, M., Nico, S. P., Johnson, M. G., Kleber, M. 2010. Dynamic Molecular Structure of Plant Biomass-Derived Black Carbon (Biochar). Environ. Sci. Tecchnol. 44: 1247-1253.

Kim, J., Lee, SS., Khim, J. 2019. Peat moss-derived biochars as effective sorbents for VOCs' removal in groundwater. Environ Geochem Health 41 (4): 1637-1646.

Kloss, S., Zehetner, F., Dellantonio, A., Hamid, R., Ottner, F., Liedtke, V., Schwanninger, M., Gerzabek, M.H., Soja, G. 2012. Characterization of slow pyrolysis biochars: effects of feedstocks and pyrolysis temperature on biochar properties. J Environ Qual. 41(4): 990-1000.

Koch, A.; Krzton, A.; Finqueneisel, G.; Heintz, O.; Weber, J.; Zimny, T. 1998. A study of carbonaceous char oxidation in air by semi-quantitative FTIR spectroscopy. Fuel 77(6): 563-569.

Králik, M., 2014. Adsorption, chemisorption, and catalysis. Chemical Papers 68 (12): 1625-1638.

Labbe, N., Harper, D., Rials, T. 2006. Chemical structure of wood charcoal by infrared spectroscopy and multivariate analysis. J. Agric. Food Chem. 54(10): Pages 3492-3497.

Lehmann, J., Joseph, S. 2015. Biochar for environmental management. Science, Technology and Implementation. 2nd Edition. Science and Technology. Earthscan. London.

Leitner, S., Berger, H., Gorfer, M., Reichenauer, T.G., Watzinger, A. 2017. Isotopic effects of PCE induced by organohalide-respiring bacteria. Environ Sci Pollut Res. 24: 24803-2418

Lian, F., Huang, F., Chen, W., Xing, B., Zhu, L. 2011. Sorption of apolar and polar organic contaminants by waste tire rubber and its chars in single-and bi-solute systems. Environ Pollut. 159: 850–857.

Libra, J., Ro, S.K., Kammann, C., Funke, A. 2011. Hydrothermal carbonization of biomass residuals: A comparative review of the chemistry, processes and applications of wet and dry pyrolysis. Biofuels 2 (1): 71-106.

Lin-Vien, D., Colthup, N. B., Fateley, W. G., Grassell, J. G. 1991. The handbook of infrared and raman characteristic frequencies of organic molecules. Academic Press, Inc.: San Diego, CA.

López-Pasquali, C. E.; Herrera, H. 1997. Pyrolysis of lignin and IR analysis of residues. Thermochim. Acta 293 (1-2): 39-467.

Ma, X., Anand, D., Zhang, X., Talapatra, S. 2011. Adsorption and desorption of chlorinated compounds from pristine and thermally treated multiwalled carbon nanotubes. J. Phys. Chem. 115: 4552-4557.

Okimori, Y., Ogawa, M., Takahashi, F. 2003. Potential of CO2 emission reductions by carbonizing biomass waste from industrial tree plantation in south Sumatra, Indonesia. Mitigation and adaptation strategies for global change 8: 261-280.

Pastorova, I., Botto, R. E., Arisz, P., Boon, J. 1994. Cellulose char structure - a combined analytical PY-GC-MS, FTIR, and NMR-study. Carbohydr. Res. 262 (1): 27-47.

Philippitsch, R. et al. 2012. Wassergüte in Österreich. Jahresbericht 2012.

Pradhan, B., Sandle, N. 1999. Effect of different oxidizing agent treatments on the surface properties of activated carbons. Carbon 37 (8): 1323-1332.

Pretsch, E., Bühlmann, P., Badertscher, M. 2009. Structure Determination of Organic Compounds. Springer-Verlag: Berlin.

Qambrani, N.A., Rahman, M.M., Won, S., Shim, S., Ra, C. 2017. Biochar properties and eco-friendly applications for climate change mitigation, waste management and wastewater treatment: a review. Renew Sustain Energy Rev. 79: 255–273.

Roy, W.R., Krapac, I.G., Chou, S.F.K., Griffin, R.A. 1992. Technical Resource Document: Batch-Type procedures for estimating soil adsorption of chemicals. United States Environmental Protection Agency. USA: Washington.

Ruthven, D.M., 1984. Principles of adsorption & adsorption processes. Hoboken, NJ, USA: Wiley.

Sarmah, A. P., Srinivasan, R., Smernik, M., Manley-Harris, M., Antal, A., Downie, L. van Zwieten. 2010. Retention capacity of biochar-amended New Zealand dairy farm soil for an estrogenic steroid hormone and its primary metabolite. Aust. J. Soil Res. 48: 648–658.

Schimmelpfennig, S., Glaser, B. 2012. One Step Forward toward Characterization: Some Important Material Properties to Distinguish Biochars. Journal of Environmental Quality 41 (4): 1001-1013.

Schreiter, I.J., Schmidt, W., Schüth, C. 2018. Sorption mechanisms of chlorinated hydrocarbons on biochar produced from different feedstocks: Conclusions from single- and bi-solute experiments. Chemosphere 203: 34-43.

Sharma, R., Wooten, J., Baliga, V., Lin, X., Chan, W., Hajaligol, M. 2004. Characterization of chars from pyrolysis of lignin. Fuel 83: 1469–1482.

Shrivastava, A., Gupta, V.B. 2011. Methods for the determination of limit of detection and limit of quantitation of the analytical methods. Chron. Young Sci. 2: 21-5.

Siggins, A., Abram, F., Healy, M.G. 2020. Pyrolyzed waste materials show potential for remediation of trichloroethylene-contaminated water. Journal of Hazardous Materials 390: 121909

Singh, B., Singh, B.P., Cowie, A.L. 2010. Characterisation and evaluation of biochars for their application as a soil amendment. Soil Res. 48: 516–525.

Shackley, S., Carter, S., Knowles, T., Middelink, E., Haefele, S., Sohi, S., Cross, A., Haszeldine, S. 2012. Sustainable gasification-biochar systems? A case-study of rice-husk gasification in Cambodia, Part 1: Context, chemical properties, environmental and health and safety issues. Energy Policy 42: 49–58.

Smith, D. M.; Chughtai, A. R. 1995. The surface-structure and reactivity of black carbon. Colloid Surface A. 105 (1): 47-77.

Sohi, S.P., Lopez-Capel, E., Krull, E., Bol, R. 2009. Biochar, climate change and soil: a review to guide future research. CSIRO Land and Water Science Report 05/09.

Sohi, S.P., Krull, E., Lopez-Capel, E., Bol, R., 2010. A review of biochar and its use and function in soil. In: Sparks, D.L. (Ed.), Advances in Agronomy. Academic Press, Burlington: 47–82.

Sun, K., Keiluweit, M., Kleber, M., Pan, Z., Xing, B. 2011. Sorption of fluorinated herbicides to plant biomass-derived biochars as a function of molecular structure. Biaresour. Technol. 102: 9897–9903.

Uchimiya, M., Wartelle, L.H., Lima, I.M., Klasson, K.T. 2010. Sorption of deisopropylatrazine on broiler litter biochars. J. Agric. Food Chem. 58: 12350–12356

Van Zwieten, L., Singh, B.P., Joseph, S., Kimber, S., Cowie, A., Chan, K.Y., 2009. Biochar for environmental management: An introduction. Science and Technology. Earthscan. London.

Verheijen, F., Jeffery, S., Bastos, A.C. 2010. Biochar application to soils: A critical scientific review of effects on soil properties, processes and functions. Publications Office.

Weber K., Quicker P. 2018. Properties of biochar. Fuel 217: 240–261.

WHO. 2006. Concise International Chemical Assessment Document 68: TETRACHLOROETHENE. Geneva

Xu, R.K., Xiao, S.C., Yuan, J.H., Zhao, A.Z. 2011. Adsorption of methyl violet from aqueous solutions by the biochars derived from crop residues. Bioresour. Technol. 102: 10293–10298.

7. Figures

8. Tables

9. Equations

10. Appendix

10.1 Weighing

10.1.1 1st adsorption experiment

Sample	Adsorbent [mg]	Flasks empty [mg]	Flask filled [mg]	Stock content [ml]
AKBC350 a	100	96.37	209.11	117.31
AKBC350 b	100	93.13	211.03	117.89
AKBC550 a	100	93.47	210.93	117.46
AKBC550 b	100	95.76	214.69	118.93
AKBC750 a	100	98.54	216.13	117.59
AKBC750 b	100	93.30	210.90	117.61
WCBC350 a	100	99.86	215.97	116.12
WCBC350 b	100	93.34	211.10	117.76
WCBC550 a	100	99.28	215.96	116.68
WCBC550 b	100	91.81	210.54	118.73
WCBC750 a	100	99.18	216.15	116.97
WCBC750 b	100	92.95	210.85	117.90
MCBC550 a	100	99.10	216.71	117.61
MCBC550 b	100	95.16	213.84	118.68
MCBC750 a	100	93.22	210.74	117.52
MCBC750 b	100	93.55	211.12	117.56
SSBS550 a	100	93.56	210.89	117.33
SSBC550 b	100	92.20	211.00	118.80
SSBC750 a	100	91.77	211.24	119.47
SSBC750 b	100	93.16	210.36	117.19
Blank Stock 1		91.89	211.02	119.14
Blank Stock 2		93.28	211.11	117.83

10.1.2 2nd adsorption experiment

Sample	Adsorbent [mg]	Flasks empty [mg]	Flask filled [mg]	Stock content [ml]
A3	100	42.67	106.84	64.18
A5	100	42.86	106.80	63.94
A7	100	42.74	106.88	64.15
W3	100	42.72	106.29	63.58
W5	100	42.85	106.65	63.79
W7	100	42.76	106.60	63.85
M5	100	42.57	106.39	63.82
M7	100	42.66	106.19	63.53
S5	100	42.19	105.86	63.67
S7	100	42.49	105.81	63.32
AC	100	42.36	106.61	64.25
Control		42.29	105.90	63.62
A3	200	42.73	106.32	63.59
A5	200	42.59	106.34	63.75
A7	200	42.63	106.09	63.46
W3	200	42.64	106.16	63.52
W5	200	42.73	106.50	63.77
W7	200	43.05	106.34	63.29
M5	200	42.29	105.66	63.38
M7	200	42.72	106.37	63.65
S5	200	42.57	106.06	63.48
S7	200	43.20	106.83	63.63
AC	200	42.38	105.92	63.54

10.1.3 3rd adsorption experiment

Sample	Adsorbent [mg]	Flasks empty [mg]	Flask filled [mg]	Stock content [ml]
w7 0.1 a	100	265	575.76	310.76

w7 0.1 b	100	250.10	551.56	301.47
w7 0.15 a	150	253.87	549.87	296
w7 0.15 b	150	265.59	573.48	307.89
w7 0.2 a	200	251.19	549.48	298.29
w7 0.2 b	200	256.48	563.08	306.60
w7 0.25 a	250	267.80	572.30	304.50
w7 0.25 b	250	265.36	572.41	307.05
w7 0.3 a	300	252.45	554.95	302.50
w7 0.3 b	300	267.10	572.03	304.94
m7 0.1 a	100	253.35	549.85	296.49
m7 0.1 b	100	258.02	562.60	304.58
m7 0.15 a	150	264.28	570.88	306.61
m7 0.15 b	150	255.54	559.88	304.34
m7 0.2 a	200	254.86	555.79	300.93
m7 0.2 b	200	261.07	564.97	303.91
m7 0.25 a	250	260.20	562.21	302.01
m7 0.25 b	250	260.72	561.42	300.70
m7 0.3 a	300	260.26	560.02	299.77
m7 0.3 b	300	254.29	551.14	296.86
s7 0.1 a	100	263.54	571.03	307.49
s7 0.1 b	100	266.30	572.88	306.58
s7 0.15 a	150	254.55	552.11	297.56
s7 0.15 b	150	253.99	560.23	306.24
s7 0.2 a	200	252.51	549.97	297.46
s7 0.2 b	200	255.05	551.83	296.78
s7 0.25 a	250	251.24	554.90	303.66
s7 0.25 b	250	255.08	554.02	298.94
s7 0.3 a	300	247.25	559.15	311.90
s7 0.3 b	300	252.93	556.55	303.62
a3 0.1 a	100	99.18	216.04	116.86

a3 0.1 b	100	92.16	210.95	118.79
a3 0.15 a	150	91.82	211.20	119.38
a3 0.15 b	150	93.52	211.26	117.75
a3 0.2 a	200	91.82	210.81	118.99
a3 0.2 b	200	98.61	215.90	117.29
a3 0.25 a	250	92.12	211.05	118.92
a3 0.25 b	250	93.73	211.22	117.50
a3 0.3 a	300	99.66	216.65	116.99
a3 0.3 b	300	92.88	210.29	117.41
Control 1		93.05	210.79	117.74
Control 2		93	210.59	117.59

10.1.4 4th adsorption experiment

Sample	Adsorbent [mg]	Flasks empty [mg]	Flask filled [mg]	Stock content [ml]
w6 0.5 a	59.00	92.74	210	117.26
w6 0.5 b	59.09	93.29	211	117.72
w6 0.1 a	117.00	93.18	211	117.82
w6 0.1 b	117.11	92.90	211	118.10
w6 0.15a	175.34	92.78	211	118.22
w6 0.15b	175.41	93.23	211	117.77
w6 0.2 a	234.23	93.03	211	117.97
w6 0.2 b	234.35	92.85	210	117.15
w6 0.25 a	292.60	93.50	211	117.50
w6 0.25 b	292.71	93.44	211	117.56
w6 0.3 a	351.12	93.02	211	117.98
w6 0.3 b	351.06	93.49	210	116.51
w6 0.35 a	409.64	93.56	210	116.44
w6 0.35 b	409.63	93.12	211	117.88

w6 0.4 a	468.11	93.08	211	117.92
w6 0.4b	468.10	93.10	210	116.90
controll 1		93.03	211	117.97
controll 2		93.20	210	116.80

10.2 3rd adsorption experiment isotherms
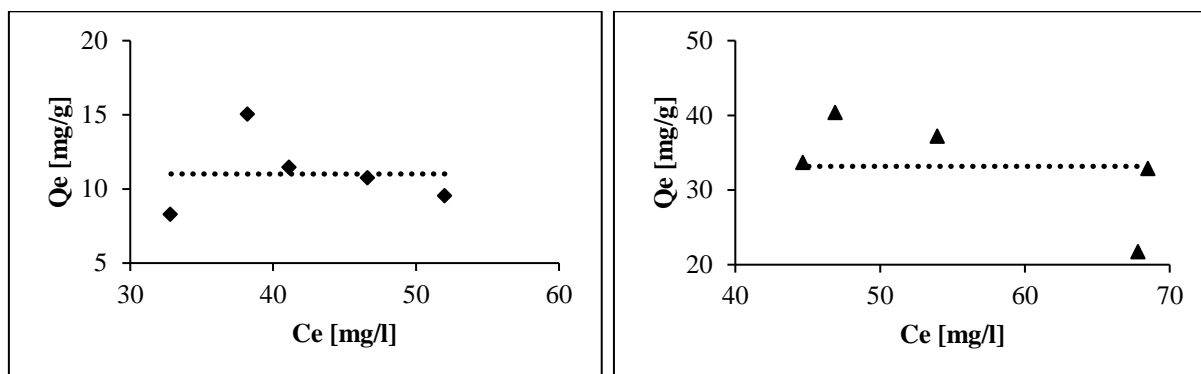
Figure 26: Freundlich Isotherm for A3 (♦ left) and S7 (▲ right) in the 3rd adsorption experiment.

Table 17: Freundlich constant KF [l/g]. Freundlich exponent n and R2 for A3 and S7.

Adsorbent	K_F [l/g]	1/n	R^2
A3	11.01	0.00004	>0
S7	33.17	0.000003	>0

10.3 **Basic characterization** *eurofins*

eurofins | **Umwelt**

Eurofins Umwelt Ost GmbH - Lindenstraße 11
Gewerbegebiet Freiberg Ost - D-09627 - Bobritzsch-Hilbersdorf

AIT Austrian Institute of Technology GmbH
Giefinggasse 4
1210 Wien
ÖSTERREICH

Titel:	**Prüfbericht zu Auftrag 12037075**
Prüfberichtsnummer:	**AR-20-FR-037535-01**
Auftragsbezeichnung:	**Biochar - Projekt 1.G2.00272, Deliv. 4510181562**
Anzahl Proben:	**11**
Probenart:	**Pflanzenkohle**
Probenehmer:	**Auftraggeber**
Probeneingangsdatum:	**15.10.2020**
Prüfzeitraum:	**15.10.2020 - 09.11.2020**

Die Prüfergebnisse beziehen sich ausschließlich auf die untersuchten Prüfgegenstände. Sofern die Probenahme nicht durch unser Labor oder in unserem Auftrag erfolgte, wird hierfür keine Gewähr übernommen. Die Ergebnisse beziehen sich in diesem Fall auf die Proben im Anlieferungszustand. Dieser Prüfbericht enthält eine qualifizierte elektronische Signatur und darf nur vollständig und unverändert weiterverbreitet werden. Auszüge oder Änderungen bedürfen in jedem Einzelfall der Genehmigung der EUROFINS UMWELT.

Es gelten die Allgemeinen Verkaufsbedingungen (AVB), sofern nicht andere Regelungen vereinbart sind. Die aktuellen AVB können Sie unter http://www.eurofins.de/umwelt/avb.aspx einsehen.

Das beauftragte Prüflaboratorium ist durch die DAkkS nach DIN EN ISO/IEC 17025:2018 DAkkS akkreditiert. Die Akkreditierung gilt nur für den in der Urkundenanlage (D-PL-14081-01-00) aufgeführten Umfang.

Dr. Sabine Bandemer
Prüfleitung
Tel. +49 37312076608

Digital signiert, 10.11.2020
Sabine Bandemer
Prüfleitung

DAkkS
Deutsche
Akkreditierungsstelle
D-PL-14081-01-00

eurofins | Umwelt

Parameter	Lab.	Akkr.	Methode	EBC-Feed Klasse I	EBC-AgroBio Klasse II	EBC-Agro Klasse III	EBC-Material Klasse IV	BG	Einheit	MCBC550 120139645 anl	MCBC550 120139645 wf	MCBC750 120139646 anl	MCBC750 120139646 wf	AKBC350 120139647 anl	AKBC350 120139647 wf
Eigenschaften der Pflanzenkohle															
spezifische Oberfläche (BET)	SND2/f		DIN ISO 9277						m²/g	-	215,62	-	453,32	-	0
Gesamtwassergehalt	FR	RE000 FY	DIN 51718: 2002-06					0,1	Ma.-%	4,0	-	3,4	-	2,8	-
Aschegehalt (550°C)	FR	RE000 FY	DIN 51719: 1997-07					0,1	Ma.-%	8,2	8,6	10,5	10,9	3,5	3,6
Kohlenstoff	FR	RE000 FY	DIN 51732: 2014-07					0,2	Ma.-%	81,2	84,6	81,5	84,3	71,7	73,8
Kohlenstoff, organisch	FR	RE000 FY	berechnet						Ma.-%	80,8	84,2	81,1	83,9	71,5	73,6
Wasserstoff	FR	RE000 FY	DIN 51732: 2014-07					0,1	Ma.-%	2,2	2,3	0,9	0,9	4,7	4,8
Stickstoff, gesamt	FR	RE000 FY	DIN 51732: 2014-07					0,05	Ma.-%	0,52	0,54	0,73	0,75	1,78	1,83
Schwefel, gesamt	FR	RE000 FY	DIN 51724-3: 2012-07					0,03	Ma.-%	0,17	0,18	0,23	0,24	0,05	0,05
Sauerstoff	FR	RE000 FY	DIN 51733: 2016-04						Ma.-%	4,4	4,5	3,3	3,4	15,7	16,1
TIC	FR	RE000 FY	DIN 51726: 2004-06					0,1	Ma.-%	0,4	0,4	0,4	0,4	0,2	0,2
Carbonate-CO2	FR	RE000 FY	DIN 51726: 2004-06					0,4	Ma.-%	1,4	1,4	1,3	1,4	0,6	0,6
H/C Verhältnis (molar)	FR	RE000 FY	berechnet							0,32	0,32	0,13	0,13	0,78	0,78
H/Corg Verhältnis (molar)	FR	RE000 FY	berechnet	< 0,7	< 0,7	< 0,7	< 0,7			0,32	0,32	0,13	0,13	0,78	0,78
O/C Verhältnis (molar)	FR	RE000 FY	berechnet	< 0,4	< 0,4	< 0,4	< 0,4			0,041	0,040	0,030	0,030	0,164	0,164
pH in CaCl2	FR		DIN ISO 10390: 2005-12							9,2	-	9,4	-	7,3	-
Leitfähigkeit	FR		BGK III. C2: 2006-09					5	µS/cm	2340	-	4240	-	188	-
Salzgehalt	FR		BGK III. C2: 2006-09					0,005	g/kg	12,3	-	22,4	-	0,994	-

Umwelt

Parameter	Lab.	Akkr.	Methode	EBC-Feed Klasse I	EBC-AgroBio Klasse II	EBC-Agro Klasse III	EBC-Material Klasse IV	BG	Einheit	MCBC550 120139645 anl	MCBC550 120139645 wf	MCBC750 120139646 anl	MCBC750 120139646 wf	AKBC350 120139647 anl	AKBC350 120139647 wf
					Vergleichswerte					Probenbezeichnung					
										Probennummer					
Bestimmung aus dem Mikrowellendruckaufschluss nach DIN 22022-1: 2014-07															
Arsen (As)	FR	RE000FY	DIN EN ISO 17294-2: 2005-02		13	13	15	0,8	mg/kg	-	< 0,8	-	< 0,8	-	< 0,8
Blei (Pb)	FR	RE000FY	DIN EN ISO 17294-2: 2005-02		45	150	250	2	mg/kg	-	< 2	-	< 2	-	< 2
Cadmium (Cd)	FR	RE000FY	DIN EN ISO 17294-2: 2005-02		0,7	1,5	5	0,2	mg/kg	-	< 0,2	-	< 0,2	-	< 0,2
Kupfer (Cu)	FR	RE000FY	DIN EN ISO 17294-2: 2005-02	100	70	100	250	1	mg/kg	-	8	-	11	-	19
Nickel (Ni)	FR	RE000FY	DIN EN ISO 17294-2: 2005-02	30	25	50	250	1	mg/kg	-	13	-	15	-	22
Quecksilber (Hg)	FR	RE000FY	DIN 22022-4: 2001-02		0,4	1	1	0,07	mg/kg	-	< 0,07	-	< 0,07	-	< 0,07
Zink (Zn)	FR	RE000FY	DIN EN ISO 17294-2: 2005-02	400	200	400	750	1	mg/kg	-	70	-	117	-	68
Chrom (Cr)	FR	RE000FY	DIN EN ISO 17294-2: 2005-02	80	70	90	250	1	mg/kg	-	20	-	34	-	27
Bor (B)	FR	RE000FY	DIN EN ISO 17294-2: 2005-02					1	mg/kg	-	5	-	6	-	26
Mangan (Mn)	FR	RE000FY	DIN EN ISO 17294-2: 2005-02					1	mg/kg	-	122	-	129	-	28

Umwelt

Parameter	Lab.	Akkr.	Methode	EBC-Feed Klasse I	EBC-AgroBio Klasse II	EBC-Agro Klasse III	EBC-Material Klasse IV	BG	Einheit	MCBC550 120139645 anl	MCBC550 120139645 wf	MCBC750 120139646 anl	MCBC750 120139646 wf	AKBC350 120139647 anl	AKBC350 120139647 wf
				Vergleichswerte				Probenbezeichnung		Probennummer					

Parameter	Lab.	Akkr.	Methode	EBC-Feed Klasse I	EBC-AgroBio Klasse II	EBC-Agro Klasse III	EBC-Material Klasse IV	BG	Einheit	MCBC550 / 120139645 anl	wf	MCBC750 / 120139646 anl	wf	AKBC350 / 120139647 anl	wf
Organ. Schadstoffe a. d. Toluolextrakt n. DIN EN 16181:2019-08(Extrakt.-verf. 2)															
Naphthalin	FR	RE000 FY	DIN EN 16181:2019-08					0,1	mg/kg	-	3,0	-	9,9	-	< 0,1
Acenaphthylen	FR	RE000 FY	DIN EN 16181:2019-08					0,1	mg/kg	-	< 0,1	-	0,6	-	< 0,1
Acenaphthen	FR	RE000 FY	DIN EN 16181:2019-08					0,1	mg/kg	-	< 0,1	-	< 0,1	-	< 0,1
Fluoren	FR	RE000 FY	DIN EN 16181:2019-08					0,1	mg/kg	-	< 0,1	-	< 0,1	-	< 0,1
Phenanthren	FR	RE000 FY	DIN EN 16181:2019-08					0,1	mg/kg	-	1,5	-	7,5	-	0,1
Anthracen	FR	RE000 FY	DIN EN 16181:2019-08					0,1	mg/kg	-	< 0,1	-	2,1	-	< 0,1
Fluoranthen	FR	RE000 FY	DIN EN 16181:2019-08					0,1	mg/kg	-	0,3	-	1,5	-	< 0,1
Pyren	FR	RE000 FY	DIN EN 16181:2019-08					0,1	mg/kg	-	< 0,1	-	1,5	-	< 0,1
Benzo[a]anthracen	FR	RE000 FY	DIN EN 16181:2019-08					0,1	mg/kg	-	< 0,1	-	0,7	-	< 0,1
Chrysen	FR	RE000 FY	DIN EN 16181:2019-08					0,1	mg/kg	-	< 0,1	-	0,8	-	< 0,1
Benzo[b]fluoranthen	FR	RE000 FY	DIN EN 16181:2019-08					0,1	mg/kg	-	< 0,1	-	0,6	-	< 0,1
Benzo[k]fluoranthen	FR	RE000 FY	DIN EN 16181:2019-08					0,1	mg/kg	-	< 0,1	-	0,5	-	< 0,1
Benzo[a]pyren	FR	RE000 FY	DIN EN 16181:2019-08					0,1	mg/kg	-	< 0,1	-	0,5	-	< 0,1
Indeno[1,2,3-cd]pyren	FR	RE000 FY	DIN EN 16181:2019-08					0,1	mg/kg	-	< 0,1	-	< 0,1	-	< 0,1
Dibenzo[a,h]anthracen	FR	RE000 FY	DIN EN 16181:2019-08					0,1	mg/kg	-	< 0,1	-	< 0,1	-	< 0,1
Benzo[ghi]perylen	FR	RE000 FY	DIN EN 16181:2019-08					0,1	mg/kg	-	< 0,1	-	< 0,1	-	< 0,1
Summe 16 EPA-PAK exkl.BG	FR	RE000 FY	DIN EN 16181:2019-08	4	4	6	30		mg/kg	-	4,8	-	26,2	-	0,1

eurofins | **Umwelt**

| | | | | Vergleichswerte | | | | | | **Probenbezeichnung** | | MCBC550 | | MCBC750 | | AKBC350 | |
| | | | | | | | | | | **Probennummer** | | 120139645 | | 120139646 | | 120139647 | |
Parameter	**Lab.**	**Akkr.**	**Methode**	EBC-Feed Klasse I	EBC-AgroBio Klasse II	EBC-Agro Klasse III	EBC-Material Klasse IV	**BG**	**Einheit**	**anl**	**wf**	**anl**	**wf**	**anl**	**wf**

Elemente a. d. Borataufschluss d. Asche 550°C nach DIN 51729-11: 1998-11 (AS)

Parameter	Lab.	Akkr.	Methode					BG	Einheit	anl	wf	anl	wf	anl	wf
Calcium als CaO	FR	RE000 FY	DIN EN ISO 11885 (E22): 2009-09					0,1	Ma.-%	-	-	-	-	-	11,9
Eisen als Fe2O3	FR	RE000 FY	DIN EN ISO 11885 (E22): 2009-09					0,1	Ma.-%	-	-	-	-	-	1,5
Kalium als K2O	FR	RE000 FY	DIN EN ISO 11885 (E22): 2009-09					0,1	Ma.-%	-	-	-	-	-	30,8
Magnesium als MgO	FR	RE000 FY	DIN EN ISO 11885 (E22): 2009-09					0,1	Ma.-%	-	-	-	-	-	13,3
Natrium als Na2O	FR	RE000 FY	DIN EN ISO 11885 (E22): 2009-09					0,1	Ma.-%	-	-	-	-	-	0,3
Phosphor als P2O5	FR	RE000 FY	DIN EN ISO 11885 (E22): 2009-09					0,1	Ma.-%	-	-	-	-	-	28,1
Schwefel als SO3	FR	RE000 FY	DIN EN ISO 11885 (E22): 2009-09					0,1	Ma.-%	-	-	-	-	-	2,3
Silicium als SiO2	FR	RE000 FY	DIN EN ISO 11885 (E22): 2009-09					0,1	Ma.-%	-	-	-	-	-	5,5

Elemente a. d. Borataufschluss d. Asche 550°C nach DIN 51729-11: 1998-11 (OS)

Parameter	Lab.	Akkr.	Methode					BG	Einheit	anl	wf	anl	wf	anl	wf
Calcium (Ca)	FR	RE000 FY	DIN EN ISO 11885 (E22): 2009-09					0,1	Ma.-%	-	-	-	-	-	0,3
Eisen (Fe)	FR	RE000 FY	DIN EN ISO 11885 (E22): 2009-09					0,1	Ma.-%	-	-	-	-	-	< 0,1
Kalium (K)	FR	RE000 FY	DIN EN ISO 11885 (E22): 2009-09					0,1	Ma.-%	-	-	-	-	-	0,9
Magnesium (Mg)	FR	RE000 FY	DIN EN ISO 11885 (E22): 2009-09					0,1	Ma.-%	-	-	-	-	-	0,3
Natrium (Na)	FR	RE000 FY	DIN EN ISO 11885 (E22): 2009-09					0,1	Ma.-%	-	-	-	-	-	< 0,1
Phosphor (P)	FR	RE000 FY	DIN EN ISO 11885 (E22): 2009-09					0,1	Ma.-%	-	-	-	-	-	0,4
Schwefel	FR	RE000 FY	DIN EN ISO 11885 (E22): 2009-09					0,1	Ma.-%	-	-	-	-	-	< 0,1
Silicium (Si)	FR	RE000 FY	DIN EN ISO 11885 (E22): 2009-09					0,1	Ma.-%	-	-	-	-	-	< 0,1

Umwelt

| | | | | Vergleichswerte | | | Probenbezeichnung | | AKBC550 | | AKBC750 | | SSBC350 | |
| | | | | | | | Probennummer | | 120139648 | | 120139649 | | 120139650 | |
Parameter	Lab.	Akkr.	Methode	EBC-Feed Klasse I	EBC-AgroBio Klasse II	EBC-Agro Klasse III	EBC-Material Klasse IV	BG	Einheit	anl	wf	anl	wf	anl	wf
Eigenschaften der Pflanzenkohle															
spezifische Oberfläche (BET)	SND2/f		DIN ISO 9277						m²/g	-	178,17	-	362,62	-	7,54
Gesamtwassergehalt	FR	RE000 FY	DIN 51718: 2002-06					0,1	Ma.-%	4,3	-	4,2	-	6,5	-
Aschegehalt (550°C)	FR	RE000 FY	DIN 51719: 1997-07					0,1	Ma.-%	4,7	4,9	6,1	6,4	8,0	8,6
Kohlenstoff	FR	RE000 FY	DIN 51732: 2014-07					0,2	Ma.-%	79,4	82,9	84,7	88,5	71,3	76,3
Kohlenstoff, organisch	FR	RE000 FY	berechnet						Ma.-%	79,1	82,6	84,4	88,2	71,0	75,9
Wasserstoff	FR	RE000 FY	DIN 51732: 2014-07					0,1	Ma.-%	2,7	2,8	1,1	1,1	3,1	3,4
Stickstoff, gesamt	FR	RE000 FY	DIN 51732: 2014-07					0,05	Ma.-%	1,56	1,63	1,41	1,47	1,42	1,51
Schwefel, gesamt	FR	RE000 FY	DIN 51724-3: 2012-07					0,03	Ma.-%	0,04	0,04	0,05	0,06	0,25	0,26
Sauerstoff	FR	RE000 FY	DIN 51733: 2016-04						Ma.-%	7,7	8,0	2,9	3,0	10,9	11,7
TIC	FR	RE000 FY	DIN 51726: 2004-06					0,1	Ma.-%	0,3	0,3	0,3	0,3	0,3	0,4
Carbonate-CO2	FR	RE000 FY	DIN 51726: 2004-06					0,4	Ma.-%	1,0	1,0	1,0	1,1	1,2	1,3
H/C Verhältnis (molar)	FR	RE000 FY	berechnet							0,40	0,40	0,15	0,15	0,52	0,52
H/Corg Verhältnis (molar)	FR	RE000 FY	berechnet	< 0,7	< 0,7	< 0,7	< 0,7			0,40	0,40	0,15	0,15	0,53	0,53
O/C Verhältnis (molar)	FR	RE000 FY	berechnet	< 0,4	< 0,4	< 0,4	< 0,4			0,073	0,072	0,026	0,025	0,115	0,115
pH in CaCl2	FR		DIN ISO 10390: 2005-12							8,1	-	8,9	-	10,0	-
Leitfähigkeit	FR		BGK III. C2: 2006-09					5	µS/cm	387	-	1190	-	3150	-
Salzgehalt	FR		BGK III. C2: 2006-09					0,005	g/kg	2,05	-	6,28	-	16,6	-

Umwelt

| | | | | Vergleichswerte | | | | Probenbezeichnung | | AKBC550 | | AKBC750 | | SSBC350 | |
| | | | | | | | | Probennummer | | 120139648 | | 120139649 | | 120139650 | |
Parameter	Lab.	Akkr.	Methode	EBC-Feed Klasse I	EBC-AgroBio Klasse II	EBC-Agro Klasse III	EBC-Material Klasse IV	BG	Einheit	anl	wf	anl	wf	anl	wf
Bestimmung aus dem Mikrowellendruckaufschluss nach DIN 22022-1: 2014-07															
Arsen (As)	FR	RE000 FY	DIN EN ISO 17294-2: 2005-02		13	13	15	0,8	mg/kg	-	< 0,8	-	< 0,8	-	< 0,8
Blei (Pb)	FR	RE000 FY	DIN EN ISO 17294-2: 2005-02		45	150	250	2	mg/kg	-	< 2	-	< 2	-	< 2
Cadmium (Cd)	FR	RE000 FY	DIN EN ISO 17294-2: 2005-02		0,7	1,5	5	0,2	mg/kg	-	< 0,2	-	< 0,2	-	< 0,2
Kupfer (Cu)	FR	RE000 FY	DIN EN ISO 17294-2: 2005-02	100	70	100	250	1	mg/kg	-	26	-	36	-	28
Nickel (Ni)	FR	RE000 FY	DIN EN ISO 17294-2: 2005-02	30	25	50	250	1	mg/kg	-	5	-	16	-	9
Quecksilber (Hg)	FR	RE000 FY	DIN 22022-4: 2001-02		0,4	1	1	0,07	mg/kg	-	< 0,07	-	< 0,07	-	< 0,07
Zink (Zn)	FR	RE000 FY	DIN EN ISO 17294-2: 2005-02	400	200	400	750	1	mg/kg	-	88	-	129	-	43
Chrom (Cr)	FR	RE000 FY	DIN EN ISO 17294-2: 2005-02	80	70	90	250	1	mg/kg	-	6	-	17	-	13
Bor (B)	FR	RE000 FY	DIN EN ISO 17294-2: 2005-02					1	mg/kg	-	35	-	38	-	48
Mangan (Mn)	FR	RE000 FY	DIN EN ISO 17294-2: 2005-02					1	mg/kg	-	29	-	43	-	22

Umwelt

Parameter	Lab.	Akkr.	Methode	EBC-Feed Klasse I	EBC-AgroBio Klasse II	EBC-Agro Klasse III	EBC-Material Klasse IV	BG	Einheit	AKBC550 anl	AKBC750 wf	AKBC750 anl	SSBC350 wf	SSBC350 anl	wf
										120139648		**120139649**		**120139650**	

Note: header structure — Probenbezeichnung / AKBC550 / AKBC750 / SSBC350; Probennummer / 120139648 / 120139649 / 120139650; Vergleichswerte columns and anl/wf sub-columns

Parameter	Lab.	Akkr.	Methode	EBC-Feed Klasse I	EBC-AgroBio Klasse II	EBC-Agro Klasse III	EBC-Material Klasse IV	BG	Einheit	anl	wf	anl	wf	anl	wf
Organ. Schadstoffe a. d. Toluolextrakt n. DIN EN 16181:2019-08(Extrakt.-verf. 2)															
Naphthalin	FR	RE000FY	DIN EN 16181:2019-08					0,1	mg/kg	-	1,2	-	0,5	-	3,2
Acenaphthylen	FR	RE000FY	DIN EN 16181:2019-08					0,1	mg/kg	-	< 0,1	-	< 0,1	-	< 0,1
Acenaphthen	FR	RE000FY	DIN EN 16181:2019-08					0,1	mg/kg	-	< 0,1	-	< 0,1	-	< 0,1
Fluoren	FR	RE000FY	DIN EN 16181:2019-08					0,1	mg/kg	-	< 0,1	-	< 0,1	-	0,3
Phenanthren	FR	RE000FY	DIN EN 16181:2019-08					0,1	mg/kg	-	0,7	-	0,2	-	2,3
Anthracen	FR	RE000FY	DIN EN 16181:2019-08					0,1	mg/kg	-	< 0,1	-	< 0,1	-	0,3
Fluoranthen	FR	RE000FY	DIN EN 16181:2019-08					0,1	mg/kg	-	0,1	-	< 0,1	-	0,4
Pyren	FR	RE000FY	DIN EN 16181:2019-08					0,1	mg/kg	-	0,1	-	< 0,1	-	0,4
Benzo[a]anthracen	FR	RE000FY	DIN EN 16181:2019-08					0,1	mg/kg	-	< 0,1	-	< 0,1	-	0,1
Chrysen	FR	RE000FY	DIN EN 16181:2019-08					0,1	mg/kg	-	< 0,1	-	< 0,1	-	0,1
Benzo[b]fluoranthen	FR	RE000FY	DIN EN 16181:2019-08					0,1	mg/kg	-	< 0,1	-	< 0,1	-	< 0,1
Benzo[k]fluoranthen	FR	RE000FY	DIN EN 16181:2019-08					0,1	mg/kg	-	< 0,1	-	< 0,1	-	< 0,1
Benzo[a]pyren	FR	RE000FY	DIN EN 16181:2019-08					0,1	mg/kg	-	< 0,1	-	< 0,1	-	< 0,1
Indeno[1,2,3-cd]pyren	FR	RE000FY	DIN EN 16181:2019-08					0,1	mg/kg	-	< 0,1	-	< 0,1	-	< 0,1
Dibenzo[a,h]anthracen	FR	RE000FY	DIN EN 16181:2019-08					0,1	mg/kg	-	< 0,1	-	< 0,1	-	< 0,1
Benzo[ghi]perylen	FR	RE000FY	DIN EN 16181:2019-08					0,1	mg/kg	-	< 0,1	-	< 0,1	-	0,3
Summe 16 EPA-PAK exkl.BG	FR	RE000FY	DIN EN 16181:2019-08	4	4	6	30		mg/kg	-	2,1	-	0,7	-	7,4

Umwelt

| | | | | Vergleichswerte | | | | Probenbezeichnung | | AKBC550 | | AKBC750 | | SSBC350 | |
| | | | | | | | | Probennummer | | 120139648 | | 120139649 | | 120139650 | |
Parameter	Lab.	Akkr.	Methode	EBC-Feed Klasse I	EBC-AgroBio Klasse II	EBC-Agro Klasse III	EBC-Material Klasse IV	BG	Einheit	anl	wf	anl	wf	anl	wf
Elemente a. d. Borataufschluss d. Asche 550°C nach DIN 51729-11: 1998-11 (AS)															
Calcium als CaO	FR	RE000 FY	DIN EN ISO 11885 (E22): 2009-09					0,1	Ma.-%	-	10,7	-	9,6	-	17,4
Eisen als Fe2O3	FR	RE000 FY	DIN EN ISO 11885 (E22): 2009-09					0,1	Ma.-%	-	0,7	-	1,2	-	0,3
Kalium als K2O	FR	RE000 FY	DIN EN ISO 11885 (E22): 2009-09					0,1	Ma.-%	-	31,6	-	30,1	-	32,9
Magnesium als MgO	FR	RE000 FY	DIN EN ISO 11885 (E22): 2009-09					0,1	Ma.-%	-	13,8	-	12,1	-	11,8
Natrium als Na2O	FR	RE000 FY	DIN EN ISO 11885 (E22): 2009-09					0,1	Ma.-%	-	0,7	-	0,3	-	0,3
Phosphor als P2O5	FR	RE000 FY	DIN EN ISO 11885 (E22): 2009-09					0,1	Ma.-%	-	29,9	-	26,1	-	7,7
Schwefel als SO3	FR	RE000 FY	DIN EN ISO 11885 (E22): 2009-09					0,1	Ma.-%	-	1,4	-	1,8	-	6,8
Silicium als SiO2	FR	RE000 FY	DIN EN ISO 11885 (E22): 2009-09					0,1	Ma.-%	-	5,5	-	3,3	-	1,6
Elemente a. d. Borataufschluss d. Asche 550°C nach DIN 51729-11: 1998-11 (OS)															
Calcium (Ca)	FR	RE000 FY	DIN EN ISO 11885 (E22): 2009-09					0,1	Ma.-%	-	0,4	-	0,4	-	1,1
Eisen (Fe)	FR	RE000 FY	DIN EN ISO 11885 (E22): 2009-09					0,1	Ma.-%	-	< 0,1	-	< 0,1	-	< 0,1
Kalium (K)	FR	RE000 FY	DIN EN ISO 11885 (E22): 2009-09					0,1	Ma.-%	-	1,3	-	1,6	-	2,3
Magnesium (Mg)	FR	RE000 FY	DIN EN ISO 11885 (E22): 2009-09					0,1	Ma.-%	-	0,4	-	0,5	-	0,6
Natrium (Na)	FR	RE000 FY	DIN EN ISO 11885 (E22): 2009-09					0,1	Ma.-%	-	< 0,1	-	< 0,1	-	< 0,1
Phosphor (P)	FR	RE000 FY	DIN EN ISO 11885 (E22): 2009-09					0,1	Ma.-%	-	0,6	-	0,7	-	0,3
Schwefel	FR	RE000 FY	DIN EN ISO 11885 (E22): 2009-09					0,1	Ma.-%	-	< 0,1	-	< 0,1	-	0,2
Silicium (Si)	FR	RE000 FY	DIN EN ISO 11885 (E22): 2009-09					0,1	Ma.-%	-	0,1	-	< 0,1	-	< 0,1

eurofins | Umwelt

| | | | | Vergleichswerte | | | | Probenbezeichnung | | SSBC550 | | SSBC750 | | WCBC350 | |
| | | | | | | | | Probennummer | | 120139651 | | 120139652 | | 120139653 | |
Parameter	Lab.	Akkr.	Methode	EBC-Feed Klasse I	EBC-AgroBio Klasse II	EBC-Agro Klasse III	EBC-Material Klasse IV	BG	Einheit	anl	wf	anl	wf	anl	wf
Eigenschaften der Pflanzenkohle															
spezifische Oberfläche (BET)	SND2/f		DIN ISO 9277						m²/g	-	82,97	-	361,83	-	5,16
Gesamtwassergehalt	FR	RE000 FY	DIN 51718: 2002-06					0,1	Ma.-%	4,9	-	4,6	-	3,8	-
Aschegehalt (550°C)	FR	RE000 FY	DIN 51719: 1997-07					0,1	Ma.-%	10,1	10,6	12,0	12,6	1,8	1,9
Kohlenstoff	FR	RE000 FY	DIN 51732: 2014-07					0,2	Ma.-%	78,9	83,0	79,3	83,1	73,6	76,5
Kohlenstoff, organisch	FR	RE000 FY	berechnet						Ma.-%	78,7	82,8	78,5	82,2	73,6	76,5
Wasserstoff	FR	RE000 FY	DIN 51732: 2014-07					0,1	Ma.-%	2,0	2,1	0,8	0,9	3,7	3,9
Stickstoff, gesamt	FR	RE000 FY	DIN 51732: 2014-07					0,05	Ma.-%	1,15	1,21	1,11	1,17	0,21	0,22
Schwefel, gesamt	FR	RE000 FY	DIN 51724-3: 2012-07					0,03	Ma.-%	0,20	0,21	0,27	0,28	0,03	0,03
Sauerstoff	FR	RE000 FY	DIN 51733: 2016-04						Ma.-%	4,5	4,7	3,9	4,1	17,2	17,9
TIC	FR	RE000 FY	DIN 51726: 2004-06					0,1	Ma.-%	0,2	0,2	0,8	0,9	< 0,1	< 0,1
Carbonate-CO2	FR	RE000 FY	DIN 51726: 2004-06					0,4	Ma.-%	0,8	0,9	3,0	3,2	< 0,4	< 0,4
H/C Verhältnis (molar)	FR	RE000 FY	berechnet							0,31	0,30	0,13	0,13	0,60	0,60
H/Corg Verhältnis (molar)	FR	RE000 FY	berechnet	< 0,7	< 0,7	< 0,7	< 0,7			0,31	0,31	0,13	0,13	0,60	0,60
O/C Verhältnis (molar)	FR	RE000 FY	berechnet	< 0,4	< 0,4	< 0,4	< 0,4			0,043	0,043	0,037	0,037	0,175	0,176
pH in CaCl2	FR		DIN ISO 10390: 2005-12							9,1	-	10,9	-	8,9	-
Leitfähigkeit	FR		BGK III. C2: 2006-09					5	µS/cm	3320	-	7790	-	284	-
Salzgehalt	FR		BGK III. C2: 2006-09					0,005	g/kg	17,5	-	41,1	-	1,50	-

Umwelt

Parameter	Lab.	Akkr.	Methode	EBC-Feed Klasse I	EBC-AgroBio Klasse II	EBC-Agro Klasse III	EBC-Material Klasse IV	BG	Einheit	SSBC550 120139651 anl	SSBC550 120139651 wf	SSBC750 120139652 anl	SSBC750 120139652 wf	WCBC350 120139653 anl	WCBC350 120139653 wf
					Vergleichswerte					Probenbezeichnung					
										Probennummer					

Bestimmung aus dem Mikrowellendruckaufschluss nach DIN 22022-1: 2014-07

Parameter	Lab.	Akkr.	Methode	EBC-Feed Klasse I	EBC-AgroBio Klasse II	EBC-Agro Klasse III	EBC-Material Klasse IV	BG	Einheit	anl	wf	anl	wf	anl	wf
Arsen (As)	FR	RE000 FY	DIN EN ISO 17294-2: 2005-02		13	13	15	0,8	mg/kg	-	< 0,8	-	< 0,8	-	< 0,8
Blei (Pb)	FR	RE000 FY	DIN EN ISO 17294-2: 2005-02		45	150	250	2	mg/kg	-	< 2	-	< 2	-	< 2
Cadmium (Cd)	FR	RE000 FY	DIN EN ISO 17294-2: 2005-02		0,7	1,5	5	0,2	mg/kg	-	< 0,2	-	< 0,2	-	0,4
Kupfer (Cu)	FR	RE000 FY	DIN EN ISO 17294-2: 2005-02	100	70	100	250	1	mg/kg	-	34	-	40	-	4
Nickel (Ni)	FR	RE000 FY	DIN EN ISO 17294-2: 2005-02	30	25	50	250	1	mg/kg	-	15	-	9	-	4
Quecksilber (Hg)	FR	RE000 FY	DIN 22022-4: 2001-02		0,4	1	1	0,07	mg/kg	-	< 0,07	-	< 0,07	-	< 0,07
Zink (Zn)	FR	RE000 FY	DIN EN ISO 17294-2: 2005-02	400	200	400	750	1	mg/kg	-	42	-	54	-	24
Chrom (Cr)	FR	RE000 FY	DIN EN ISO 17294-2: 2005-02	80	70	90	250	1	mg/kg	-	23	-	10	-	9
Bor (B)	FR	RE000 FY	DIN EN ISO 17294-2: 2005-02					1	mg/kg	-	65	-	68	-	8
Mangan (Mn)	FR	RE000 FY	DIN EN ISO 17294-2: 2005-02					1	mg/kg	-	33	-	42	-	94

Umwelt

| | | | | Vergleichswerte | | | | Probenbezeichnung | | SSBC550 | | SSBC750 | | WCBC350 | |
| | | | | | | | | Probennummer | | 120139651 | | 120139652 | | 120139653 | |
Parameter	Lab.	Akkr.	Methode	EBC-Feed Klasse I	EBC-AgroBio Klasse II	EBC-Agro Klasse III	EBC-Material Klasse IV	BG	Einheit	anl	wf	anl	wf	anl	wf
Organ. Schadstoffe a. d. Toluolextrakt n. DIN EN 16181:2019-08(Extrakt.-verf. 2)															
Naphthalin	FR	RE000FY	DIN EN 16181:2019-08					0,1	mg/kg	-	1,4	-	11	-	0,4
Acenaphthylen	FR	RE000FY	DIN EN 16181:2019-08					0,1	mg/kg	-	< 0,1	-	1,0	-	< 0,1
Acenaphthen	FR	RE000FY	DIN EN 16181:2019-08					0,1	mg/kg	-	< 0,1	-	0,8	-	< 0,1
Fluoren	FR	RE000FY	DIN EN 16181:2019-08					0,1	mg/kg	-	< 0,1	-	< 0,1	-	< 0,1
Phenanthren	FR	RE000FY	DIN EN 16181:2019-08					0,1	mg/kg	-	0,5	-	13	-	0,3
Anthracen	FR	RE000FY	DIN EN 16181:2019-08					0,1	mg/kg	-	< 0,1	-	4,3	-	< 0,1
Fluoranthen	FR	RE000FY	DIN EN 16181:2019-08					0,1	mg/kg	-	0,1	-	3,6	-	< 0,1
Pyren	FR	RE000FY	DIN EN 16181:2019-08					0,1	mg/kg	-	< 0,1	-	4,8	-	< 0,1
Benzo[a]anthracen	FR	RE000FY	DIN EN 16181:2019-08					0,1	mg/kg	-	< 0,1	-	2,7	-	< 0,1
Chrysen	FR	RE000FY	DIN EN 16181:2019-08					0,1	mg/kg	-	< 0,1	-	1,7	-	< 0,1
Benzo[b]fluoranthen	FR	RE000FY	DIN EN 16181:2019-08					0,1	mg/kg	-	< 0,1	-	1,7	-	< 0,1
Benzo[k]fluoranthen	FR	RE000FY	DIN EN 16181:2019-08					0,1	mg/kg	-	< 0,1	-	1,4	-	< 0,1
Benzo[a]pyren	FR	RE000FY	DIN EN 16181:2019-08					0,1	mg/kg	-	< 0,1	-	1,7	-	< 0,1
Indeno[1,2,3-cd]pyren	FR	RE000FY	DIN EN 16181:2019-08					0,1	mg/kg	-	< 0,1	-	0,3	-	< 0,1
Dibenzo[a,h]anthracen	FR	RE000FY	DIN EN 16181:2019-08					0,1	mg/kg	-	< 0,1	-	< 0,1	-	< 0,1
Benzo[ghi]perylen	FR	RE000FY	DIN EN 16181:2019-08					0,1	mg/kg	-	< 0,1	-	0,4	-	< 0,1
Summe 16 EPA-PAK exkl.BG	FR	RE000FY	DIN EN 16181:2019-08	4	4	6	30		mg/kg	-	2,0	-	48,4	-	0,7

Umwelt

Parameter	Lab.	Akkr.	Methode	EBC-Feed Klasse I	EBC-AgroBio Klasse II	EBC-Agro Klasse III	EBC-Material Klasse IV	BG	Einheit	SSBC550 anl	SSBC550 wf	SSBC750 anl	SSBC750 wf	WCBC350 anl	WCBC350 wf
										120139651	120139651	120139652	120139652	120139653	120139653
Elemente a. d. Borataufschluss d. Asche 550°C nach DIN 51729-11: 1998-11 (AS)
Calcium als CaO	FR	RE000 FY	DIN EN ISO 11885 (E22): 2009-09					0,1	Ma.-%	-	18,9	-	17,9	-	33,3
Eisen als Fe2O3	FR	RE000 FY	DIN EN ISO 11885 (E22): 2009-09					0,1	Ma.-%	-	0,4	-	0,5	-	0,7
Kalium als K2O	FR	RE000 FY	DIN EN ISO 11885 (E22): 2009-09					0,1	Ma.-%	-	30,7	-	30,7	-	10,3
Magnesium als MgO	FR	RE000 FY	DIN EN ISO 11885 (E22): 2009-09					0,1	Ma.-%	-	11,8	-	11,7	-	11,1
Natrium als Na2O	FR	RE000 FY	DIN EN ISO 11885 (E22): 2009-09					0,1	Ma.-%	-	1,8	-	1,3	-	0,9
Phosphor als P2O5	FR	RE000 FY	DIN EN ISO 11885 (E22): 2009-09					0,1	Ma.-%	-	7,9	-	8,4	-	6,6
Schwefel als SO3	FR	RE000 FY	DIN EN ISO 11885 (E22): 2009-09					0,1	Ma.-%	-	5,2	-	6,2	-	3,3
Silicium als SiO2	FR	RE000 FY	DIN EN ISO 11885 (E22): 2009-09					0,1	Ma.-%	-	3,3	-	2,6	-	4,3
Elemente a. d. Borataufschluss d. Asche 550°C nach DIN 51729-11: 1998-11 (OS)
Calcium (Ca)	FR	RE000 FY	DIN EN ISO 11885 (E22): 2009-09					0,1	Ma.-%	-	1,4	-	1,6	-	0,5
Eisen (Fe)	FR	RE000 FY	DIN EN ISO 11885 (E22): 2009-09					0,1	Ma.-%	-	< 0,1	-	< 0,1	-	< 0,1
Kalium (K)	FR	RE000 FY	DIN EN ISO 11885 (E22): 2009-09					0,1	Ma.-%	-	2,7	-	3,2	-	0,2
Magnesium (Mg)	FR	RE000 FY	DIN EN ISO 11885 (E22): 2009-09					0,1	Ma.-%	-	0,8	-	0,9	-	0,1
Natrium (Na)	FR	RE000 FY	DIN EN ISO 11885 (E22): 2009-09					0,1	Ma.-%	-	0,1	-	0,1	-	< 0,1
Phosphor (P)	FR	RE000 FY	DIN EN ISO 11885 (E22): 2009-09					0,1	Ma.-%	-	0,4	-	0,5	-	< 0,1
Schwefel	FR	RE000 FY	DIN EN ISO 11885 (E22): 2009-09					0,1	Ma.-%	-	0,2	-	0,3	-	< 0,1
Silicium (Si)	FR	RE000 FY	DIN EN ISO 11885 (E22): 2009-09					0,1	Ma.-%	-	0,2	-	0,2	-	< 0,1

Umwelt

Parameter	Lab.	Akkr.	Methode	EBC-Feed Klasse I	EBC-AgroBio Klasse II	EBC-Agro Klasse III	EBC-Material Klasse IV	BG	Einheit	WCBC550 120139654 anl	WCBC550 120139654 wf	WCBC750 120139655 anl	WCBC750 120139655 wf
Eigenschaften der Pflanzenkohle													
spezifische Oberfläche (BET)	SND2/f		DIN ISO 9277						m²/g	-	263,8	-	423,54
Gesamtwassergehalt	FR	RE000 FY	DIN 51718: 2002-06					0,1	Ma.-%	2,7	-	2,7	-
Aschegehalt (550°C)	FR	RE000 FY	DIN 51719: 1997-07					0,1	Ma.-%	2,2	2,3	2,9	3,0
Kohlenstoff	FR	RE000 FY	DIN 51732: 2014-07					0,2	Ma.-%	87,3	89,8	92,2	94,7
Kohlenstoff, organisch	FR	RE000 FY	berechnet						Ma.-%	87,1	89,6	91,9	94,3
Wasserstoff	FR	RE000 FY	DIN 51732: 2014-07					0,1	Ma.-%	2,7	2,8	1,0	1,1
Stickstoff, gesamt	FR	RE000 FY	DIN 51732: 2014-07					0,05	Ma.-%	0,53	0,55	0,75	0,77
Schwefel, gesamt	FR	RE000 FY	DIN 51724-3: 2012-07					0,03	Ma.-%	< 0,03	< 0,03	0,03	0,04
Sauerstoff	FR	RE000 FY	DIN 51733: 2016-04						Ma.-%	5,0	5,1	1,2	1,2
TIC	FR	RE000 FY	DIN 51726: 2004-06					0,1	Ma.-%	0,2	0,2	0,3	0,4
Carbonate-CO2	FR	RE000 FY	DIN 51726: 2004-06					0,4	Ma.-%	0,6	0,6	1,2	1,3
H/C Verhältnis (molar)	FR	RE000 FY	berechnet							0,37	0,37	0,13	0,13
H/Corg Verhältnis (molar)	FR	RE000 FY	berechnet	< 0,7	< 0,7	< 0,7	< 0,7			0,37	0,37	0,13	0,13
O/C Verhältnis (molar)	FR	RE000 FY	berechnet	< 0,4	< 0,4	< 0,4	< 0,4			0,043	0,043	0,010	0,010
pH in CaCl2	FR		DIN ISO 10390: 2005-12							8,3	-	9,3	-
Leitfähigkeit	FR		BGK III. C2: 2006-09					5	µS/cm	183	-	849	-
Salzgehalt	FR		BGK III. C2: 2006-09					0,005	g/kg	0,968	-	4,48	-

eurofins | Umwelt

| | | | | Vergleichswerte | | | | Probenbezeichnung | | | WCBC550 | | WCBC750 | |
| | | | | | | | | Probennummer | | | 120139654 | | 120139655 | |
Parameter	Lab.	Akkr.	Methode	EBC-Feed Klasse I	EBC-AgroBio Klasse II	EBC-Agro Klasse III	EBC-Material Klasse IV	BG	Einheit	anl	wf	anl	wf
Bestimmung aus dem Mikrowellendruckaufschluss nach DIN 22022-1: 2014-07													
Arsen (As)	FR	RE000FY	DIN EN ISO 17294-2: 2005-02		13	13	15	0,8	mg/kg	-	< 0,8	-	< 0,8
Blei (Pb)	FR	RE000FY	DIN EN ISO 17294-2: 2005-02		45	150	250	2	mg/kg	-	< 2	-	< 2
Cadmium (Cd)	FR	RE000FY	DIN EN ISO 17294-2: 2005-02		0,7	1,5	5	0,2	mg/kg	-	< 0,2	-	< 0,2
Kupfer (Cu)	FR	RE000FY	DIN EN ISO 17294-2: 2005-02	100	70	100	250	1	mg/kg	-	3	-	4
Nickel (Ni)	FR	RE000FY	DIN EN ISO 17294-2: 2005-02	30	25	50	250	1	mg/kg	-	8	-	4
Quecksilber (Hg)	FR	RE000FY	DIN 22022-4: 2001-02		0,4	1	1	0,07	mg/kg	-	< 0,07	-	< 0,07
Zink (Zn)	FR	RE000FY	DIN EN ISO 17294-2: 2005-02	400	200	400	750	1	mg/kg	-	17	-	13
Chrom (Cr)	FR	RE000FY	DIN EN ISO 17294-2: 2005-02	80	70	90	250	1	mg/kg	-	9	-	8
Bor (B)	FR	RE000FY	DIN EN ISO 17294-2: 2005-02					1	mg/kg	-	7	-	10
Mangan (Mn)	FR	RE000FY	DIN EN ISO 17294-2: 2005-02					1	mg/kg	-	139	-	173

Umwelt

Parameter	Lab.	Akkr.	Methode	EBC-Feed Klasse I	EBC-AgroBio Klasse II	EBC-Agro Klasse III	EBC-Material Klasse IV	BG	Einheit	WCBC550 120139654 anl	WCBC550 120139654 wf	WCBC750 120139655 anl	WCBC750 120139655 wf
Organ. Schadstoffe a. d. Toluolextrakt n. DIN EN 16181:2019-08(Extrakt.-verf. 2)													
Naphthalin	FR	RE000FY	DIN EN 16181:2019-08					0,1	mg/kg	-	3,2	-	7,5
Acenaphthylen	FR	RE000FY	DIN EN 16181:2019-08					0,1	mg/kg	-	< 0,1	-	0,5
Acenaphthen	FR	RE000FY	DIN EN 16181:2019-08					0,1	mg/kg	-	< 0,1	-	0,2
Fluoren	FR	RE000FY	DIN EN 16181:2019-08					0,1	mg/kg	-	< 0,1	-	0,3
Phenanthren	FR	RE000FY	DIN EN 16181:2019-08					0,1	mg/kg	-	1,5	-	10
Anthracen	FR	RE000FY	DIN EN 16181:2019-08					0,1	mg/kg	-	0,3	-	2,5
Fluoranthen	FR	RE000FY	DIN EN 16181:2019-08					0,1	mg/kg	-	0,2	-	3,2
Pyren	FR	RE000FY	DIN EN 16181:2019-08					0,1	mg/kg	-	0,2	-	4,0
Benzo[a]anthracen	FR	RE000FY	DIN EN 16181:2019-08					0,1	mg/kg	-	0,1	-	1,3
Chrysen	FR	RE000FY	DIN EN 16181:2019-08					0,1	mg/kg	-	0,1	-	0,9
Benzo[b]fluoranthen	FR	RE000FY	DIN EN 16181:2019-08					0,1	mg/kg	-	< 0,1	-	0,6
Benzo[k]fluoranthen	FR	RE000FY	DIN EN 16181:2019-08					0,1	mg/kg	-	< 0,1	-	0,5
Benzo[a]pyren	FR	RE000FY	DIN EN 16181:2019-08					0,1	mg/kg	-	< 0,1	-	0,6
Indeno[1,2,3-cd]pyren	FR	RE000FY	DIN EN 16181:2019-08					0,1	mg/kg	-	< 0,1	-	0,2
Dibenzo[a,h]anthracen	FR	RE000FY	DIN EN 16181:2019-08					0,1	mg/kg	-	< 0,1	-	< 0,1
Benzo[ghi]perylen	FR	RE000FY	DIN EN 16181:2019-08					0,1	mg/kg	-	< 0,1	-	0,1
Summe 16 EPA-PAK exkl.BG	FR	RE000FY	DIN EN 16181:2019-08	4	4	6	30		mg/kg	-	5,6	-	32,4

eurofins | **Umwelt**

Parameter	Lab.	Akkr.	Methode	EBC-Feed Klasse I	EBC-AgroBio Klasse II	EBC-Agro Klasse III	EBC-Material Klasse IV	BG	Einheit	WCBC550 / 120139654 anl	WCBC550 / 120139654 wf	WCBC750 / 120139655 anl	WCBC750 / 120139655 wf
Probenbezeichnung				*Vergleichswerte*						**WCBC550**		**WCBC750**	
Probennummer										**120139654**		**120139655**	
Elemente a. d. Borataufschluss d. Asche 550°C nach DIN 51729-11: 1998-11 (AS)													
Calcium als CaO	FR	RE000 FY	DIN EN ISO 11885 (E22): 2009-09					0,1	Ma.-%	-	37,7	-	30,8
Eisen als Fe2O3	FR	RE000 FY	DIN EN ISO 11885 (E22): 2009-09					0,1	Ma.-%	-	0,7	-	0,6
Kalium als K2O	FR	RE000 FY	DIN EN ISO 11885 (E22): 2009-09					0,1	Ma.-%	-	7,1	-	13,2
Magnesium als MgO	FR	RE000 FY	DIN EN ISO 11885 (E22): 2009-09					0,1	Ma.-%	-	9,5	-	8,5
Natrium als Na2O	FR	RE000 FY	DIN EN ISO 11885 (E22): 2009-09					0,1	Ma.-%	-	0,8	-	1,7
Phosphor als P2O5	FR	RE000 FY	DIN EN ISO 11885 (E22): 2009-09					0,1	Ma.-%	-	3,8	-	3,2
Schwefel als SO3	FR	RE000 FY	DIN EN ISO 11885 (E22): 2009-09					0,1	Ma.-%	-	2,1	-	2,8
Silicium als SiO2	FR	RE000 FY	DIN EN ISO 11885 (E22): 2009-09					0,1	Ma.-%	-	4,0	-	10,6
Elemente a. d. Borataufschluss d. Asche 550°C nach DIN 51729-11: 1998-11 (OS)													
Calcium (Ca)	FR	RE000 FY	DIN EN ISO 11885 (E22): 2009-09					0,1	Ma.-%	-	0,6	-	0,7
Eisen (Fe)	FR	RE000 FY	DIN EN ISO 11885 (E22): 2009-09					0,1	Ma.-%	-	< 0,1	-	< 0,1
Kalium (K)	FR	RE000 FY	DIN EN ISO 11885 (E22): 2009-09					0,1	Ma.-%	-	0,1	-	0,3
Magnesium (Mg)	FR	RE000 FY	DIN EN ISO 11885 (E22): 2009-09					0,1	Ma.-%	-	0,1	-	0,2
Natrium (Na)	FR	RE000 FY	DIN EN ISO 11885 (E22): 2009-09					0,1	Ma.-%	-	< 0,1	-	< 0,1
Phosphor (P)	FR	RE000 FY	DIN EN ISO 11885 (E22): 2009-09					0,1	Ma.-%	-	< 0,1	-	< 0,1
Schwefel	FR	RE000 FY	DIN EN ISO 11885 (E22): 2009-09					0,1	Ma.-%	-	< 0,1	-	< 0,1
Silicium (Si)	FR	RE000 FY	DIN EN ISO 11885 (E22): 2009-09					0,1	Ma.-%	-	< 0,1	-	0,1

Umwelt

Erläuterungen

BG - Bestimmungsgrenze

anl - Anlieferungszustand

wf - wasserfreier Zustand

Lab. - Kürzel des durchführenden Labors

Akkr. - Akkreditierungskürzel des Prüflabors

Die mit FR gekennzeichneten Parameter wurden von der Eurofins Umwelt Ost GmbH (Bobritzsch-Hilbersdorf) analysiert. Die Bestimmung der mit RE000FY gekennzeichneten Parameter ist nach DIN EN ISO/IEC 17025:2018 DAkkS D-PL-14081-01-00 akkreditiert.

Die mit SND2 gekennzeichneten Parameter wurden von der Ruhr Lab GmbH (Gelsenkirchen) analysiert.

/f - Die Analyse des Parameters erfolgte in Fremdvergabe.

Erläuterungen zu Vergleichswerten

Untersuchung nach Richtlinie für die nachhaltige Produktion von Pflanzenkohle - EBC, Version 9.0G – Stand 01.06.2020.

Ho,V / Hu,p: Brenn. bzw. Heizwert bei konstantem Volumen / Druck

AS: bezogen auf die Asche

OS: bezogen auf die Originalsubstanz

Bei der Darstellung von Grenz- bzw. Richtwerten im Prüfbericht handelt es sich ausschließlich um eine Serviceleistung der EUROFINS UMWELT. Eine rechtsverbindliche Zuordnung der Prüfberichtsergebnisse im Sinne der zitierten Regularien wird ausdrücklich ausgeschlossen. Diese liegt alleinig im Verantwortungsbereich des Auftraggebers. Die zitierten Grenz- und Richtwerte sind teilweise vereinfacht dargestellt und berücksichtigen nicht alle Kommentare, Nebenbestimmungen und/oder Ausnahmeregelungen des entsprechenden Regelwerkes.